Characterisation of the pulmonary vascular response to hypoxia in mitochondrial uncoupling protein 2 deficient mice

Inauguraldissertation

zur Erlangung des Grades eines Doktors der Medizin

des Fachbereichs Medizin

der Justus-Liebig-Universität Gießen

vorgelegt von

Timm Höres

aus Gießen

Gießen 2013

Aus dem Zentrum für Innere Medizin

Medizinische Klinik II

Direktor: Prof. Dr. Werner Seeger

der Universitätsklinikum Gießen und Marburg GmbH

Standort Gießen

Gutachter: Prof. Dr. Norbert Weißmann

Gutachter: Prof. Dr. Michael Henrich

Tag der Disputation: 11.12.2013

Meinen Eltern

Table of contents

1 Introduction

1.1 Hypoxic pulmonary vasoconstriction (HPV) – definition

HPV is a specific physiological mechanism regulating the lungs' vascular resistance in relation to alveolar oxygen availability. Although an increase in pulmonary artery pressure (PAP) following hypoxic stimuli has been reported earlier [25,142], it is mostly referred to as the `Euler-Liljestrand-mechanism´. The nomenclature gives credit to the authors who studied PAP changes during hypoxic ventilation in cats and suggested that this is caused by an intrinsic action of the lungs' vasculature. They also concluded that this mechanism is of significance for the regulation of blood flow in relation to the alveolar oxygen distribution throughout the lung [183].

1.1.1 HPV – physiological significance

Following the detailed characterisation by von Euler and Liljestrand in 1946 HPV has been described in a wide variety of animals and models, using different physiological techniques and preparations. Even though certain discrepancies concerning its characteristics have been reported, the fundamental rise in PAP following a hypoxic stimulus could be demonstrated in the majority of study subjects. This includes, but is not restricted to, humans [121], dogs [14], rats [73], mice [202], rabbits [206], cattle [163], birds [32] and reptiles [166]. Variability of the HPV response between species, gender, the level of maturity and the different experimental designs have influenced research on the underlying functional principle which is considered to be evolutionary conserved [137]. Physiological significance and efficiency of the HPV mechanism, especially compared to other factors impacting lung perfusion (e.g. gravity and the body position), have been extensively debated following its characterisation [57]. After all it is now widely accepted that HPV is an important intrinsic regulatory response that optimises gas exchange in a variety of situations. Basically it reduces blood flow through areas of low alveolar oxygen content, preventing shunt flow and preserving highest possible oxygen saturation [209]. Additionally, an elevated flow resistance throughout the non-aerated lungs is maintained during foetal circulation [119]. After birth, when ventilation begins, lungs are inflated and pulmonary vessels subsequently dilate [39]. Interestingly from this point of view lungs' vascular

adaptation to changing oxygen content can as well be understood as normoxic pulmonary vasodilatation [199].

1.1.2 HPV – physiological characteristics

Data from animal models with a detached nervous system and/or an exogenously controlled or simplified humoral system (e.g. the isolated buffer-perfused and ventilated lung), supported the idea that HPV is a intrinsic mechanism of the lung [57]. Nevertheless researchers identified a multitude of factors, from the autonomic nervous system and its transmitters [92,178], to histamines [74] to the acid-base status [153], which are modulating the vasoconstrictor response to hypoxia, without being essential for the reaction [56]. Following Ohm's- law, PAP depends directly on the lungs' total vascular resistance. HPV can only usefully function as a mechanism of local ventilation to perfusion (V/Q) matching, as the efficiency of blood-flow diversion is inversely proportional to the size of the affected segment [112,170]. Acute HPV (also referred to as phase 1 or early phase) occurs within seconds after alveolar oxygen concentration is lowered under a threshold of very roughly 10% [88,206] and reaches its maximum mostly within 5 and unlikely more than 15 minutes [21,189,202,206]. The kinetics and limits may vary among species and experimental setups, as additionally discussed in chapter 1.2, but generally exhibit a positive dependency between the degree of hypoxia and the resulting increase in PAP. In many reports continuous hypoxic exposure leads to a biphasic vasoconstrictor response, as in separated pulmonary arteries (PA) [19,148], isolated lungs [206,213] and in vivo [184]. It has been suggested that this more protracted rise in PAP (referred to as sustained HPV or phase 2) is regulated through a distinct pathway and is more closely connected to the structural changes observed under chronic hypoxia [146,209].

1.1.3 HPV – associated pathophysiology and clinical relevance

Considering the impact of the HPV linked mechanisms on pathological processes one can identify conditions of impaired vasomotor function, as well as diseases which are based on, or accompanied by, an increased or generalised pulmonary vasoconstriction and pulmonary vascular remodelling. For example during the acute respiratory distress syndrome, a life threatening condition that can be triggered by multiple processes [67], or in case of the hepatopulmonary syndrome, the diversion of blood flow away from

poorly ventilated areas becomes impaired [78,125]. Therefore desaturated blood is allowed to perfuse areas of low oxygenation, increase shunt flow and cause hypoxemia in the systemic circulation. Treatment of these conditions is complicated by the fact that a systemic oxygen deficit based on pulmonary shunt flow responds less to a therapeutic increase in fraction of inspired oxygen (FiO_2). On the contrary the process of generalised pulmonary vasoconstriction and pulmonary vascular remodelling connects HPV and several other diseases. Elevated PAP is considered to be an important pathogenetic factor during high-altitude pulmonary edema and also to be a susceptible therapeutic target in this condition [16]. Several morphological changes, for example an increased media thickness or enhanced muscularization of the small pulmonary vessels, occur during chronic exposure to hypoxia as well as during idiopathic pulmonary arterial hypertension (IPAH) and the different and heterogeneous forms of pulmonary arterial hypertension (PAH) with identified causes [55,164,165]. In lung fibrosis and other severe respiratory diseases, pulmonary hypertension (PH) is at least a concomitant factor [61]. In chronic obstructive pulmonary disease unregulated or generalised vasoconstriction conjoins with V/Q- mismatch [135]. Increased pulmonary vascular resistance and elevated PAP of different etiology may lead to restricted blood flow, right ventricular hypertrophy and eventually to right heart failure [11,61]. Finally a functional HPV is of significance for support of oxygenation during anaesthesia especially in thoracic surgery and its affiliated ventilation strategies [125,127].

1.1.4 HPV – site of action

It is now widely accepted that HPV is predominantly a function of the small precapillary pulmonary arterioles [56,170]. Increase of the pulmonary vascular resistance during hypoxia has been repeatedly shown for vessels above 30µm and up to 600µm [3,162,170]. Some authors reported that the strength of HPV is modified by the mixed venous oxygen tension (PvO_2) [20,73] while others demonstrated its independence conclusively [84,206]. Hypoxia leads to contraction of pulmonary arteries [110] even in absence of vascular endothelial cells [224]. However it was suggested that endothelial cells are particularly important during sustained HPV [147]. Isolated pulmonary artery smooth muscle cells (PASMC) exhibit membrane depolarization, show increased intracellular calcium (Ca^{2+}) levels and shorten during hypoxic conditions [110,111,155,225]. It is therefore plausible that at least for

acute HPV, both the essential oxygen sensor and the effector mechanisms are located within these cells [168]. Additionally it has been demonstrated that this characteristic is specific for PASMC, as it is not shared by tissue extracted from systemic vasculature [111,224].

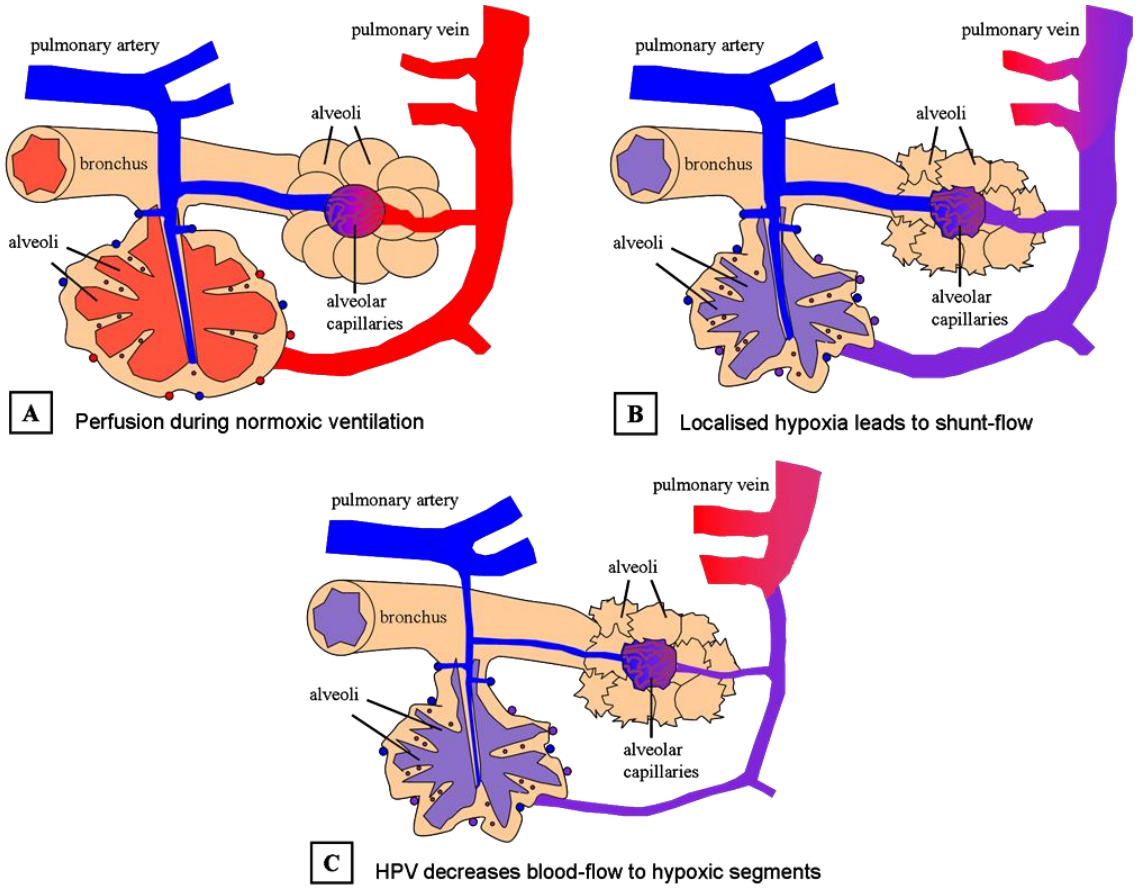

Fig. 1-1: HPV- mechanism of ventilation perfusion matching. This schematic shows important physiological characteristics of HPV. In each picture (A,B and C) the two depicted alveolar regions supplied by the bronchus represent a shared segment of ventilation and perfusion, while the upper two pulmonary arteries –depicted as truncated branches– lead to separate pulmonary segments. Blue colour indicates hypoxic/desaturated while red represents normoxic/saturated conditions. A) Normally ventilated and perfused terminal lung segment. B) Hypoventilation or hypoxic ventilation leads to shunt-flow of desaturated blood and causes systemic hypoxemia. C) Due to vasoconstriction of the pulmonary arteries in close relation to the hypoxic area, shunt-flow is reduced and systemic oxygenation improved. Schematic is based on the illustrations by Staub [170] and Budowick [30].

1.2 Models and physiological techniques

Isolated lung techniques have been widely used to study pulmonary vascular responses to hypoxia [137]. Especially artificially buffer-perfused setups offer the advantages of a

reduced system complexity compared to the in vivo experiments, combined with benefits of an intact organ and the potency to control many physiological and environmental variables [206]. On the other hand it has been noted before that the threshold for hypoxic stimulation may increase or the response become blunted under simplified and artificial conditions [56]. During in vivo studies, HPV can be elicited applying a FiO_2 of 0,12-0,15 at normal atmospheric pressure [57,69,126], in isolated lung experiments reduction to a FiO_2 of roughly 0,07-0,10 under atmospheric pressure is required [137,206]. In general tissue oxygen content decreases as a function of the diffusion distance to the oxygen source, and is particularly low in the surrounding area of oxygen consumption. Experiments with isolated cells or mitochondria are therefore usually conducted under very low oxygen concentration, sometimes even in anoxia. The upper and lower limits of oxygen serving as physiological stimulus are currently not uniformly established. This topic is of certain interest if results from studies using different degrees of hypoxia are compared, especially under increasingly artificial conditions. The terms “mild”, “moderate” or “physiological hypoxia” are not exactly defined but represent the attempt to incorporate physiologically graduated amounts of oxygen into the respective method. Using extremely low levels of oxygen may still lead to a similar reaction but can also mislead the interpretation of the results, as proposed for the use of anoxia as a most likely non-physiological HPV trigger [18,57].

1.3 Cellular mechanisms of HPV – sensor, mediator and effector pathway

The cellular mechanisms underlying oxygen sensing, signal transduction and the effector pathway in HPV are not fully elucidated yet. Current theories are partly opposing each other and obviously rely on contradicting results. These controversies may, to some extend, be explained by the use of incomparable methodology or models. Variability in the size or the extraction site of the studied vessels [38], in the extent and duration of the applied hypoxia [95], as well as in the strength of priming [174] and pretone [1] could lead to some of the controversial observations. Furthermore the complexity of the mechanism itself needs to be taken into account, as adaptation to hypoxia likely consists of more than one uniform phase and therefore also distinct but overlapping signalling pathways may contribute to it.

1.3.1 Cellular mechanism – effector pathway

1.3.1.1 Role of calcium

All muscular contraction is highly dependent on an increase in cytosolic Ca^{2+} concentration ($[Ca^{2+}]_c$) and its interaction with the contractile apparatus [140]. The necessary influx may either arise from the extracellular space or from intracellular calcium stores [23]. It is known that membrane depolarization, activation of voltage-operated calcium channels (VOCC) and calcium influx from the extracellular space play an important role in the smooth muscle cells' (SMC) calcium uptake [140]. This may also be true for the PASMC during acute HPV, as suggested by early inhibitor and facilitator studies [40,71,116,117]. Still calcium entry through other channels or from intracellular stores may represent essential sources of calcium in the effector pathway of HPV [43]. This is primarily supported by observations that during L-type calcium channel inhibition HPV remains functional to some extend [150,227]. The usage of Ca^{2+} depleted medium to study the overall dependency on extracellular calcium provided partly conflicting results [43,185,203]. Mitochondria and the sarcoplasmic reticulum (SR) are major intracellular calcium stores in SMC and contribute to calcium release and buffering [43,91]. Especially a role for inositol 1,4,5-trisphosphate (IP_3) and ryanodine-sensitive channels in intracellular calcium release has found supporting evidence [43,120,215,228]. Additionally store operated calcium channels (SOCC) may allow calcium influx through the plasma membrane via so called capacitative calcium entry (CCE) in an voltage independent manner [185,190]. For example Ca^{2+} could be released from the SR by endogenous mediators from ryanodine-sensitive stores or via Ca^{2+}-induced-Ca^{2+}-release (CICR) [120,214]. It is likely that proteins functioning as non-specific cation channels (NSCC) are centrally involved in the effector mechanism, as antagonist of certain NSCC inhibit CCE through SOCC and completely abolish HPV [190,198]. Calcium influx may also be triggered by another class of NSCC, the specific receptor operated calcium channels (ROCC), or be the result of a multi-factorial event involving different calcium sources [188]. One study demonstrated an essential and specific role for a member of the transient receptor potential channel family (TRPC) in acute HPV. During hypoxia PASMC isolated from TRPC6 knock-out ($TRPC6^{-/-}$) mice lacked $[Ca^{2+}]_c$ increase as well as these mice did not depict acute PAP rise following hypoxic ventilation in isolated buffer-perfused lung experiments [203]. It is known that

TRPC form NSCC [79] and may function as ROCCs, SOCCs or both [17]. It was suggested that during hypoxia TRPC may increase intracellular calcium by depolarising membrane potential or by effecting L-type calcium channels [168,176]. There is considerable evidence for distinct pathways and mechanisms underlying acute and sustained HPV. Prolonged contraction seems to depend less on voltage-operated calcium entry (VOCE) and calcium levels but more on the process of calcium sensitization [148,150]. For example in the TRPC6$^{-/-}$ mice sustained HPV was unchanged while acute phase was abolished [203]. The process of calcium sensitization may be reinforced by the endothelium and base upon protein kinase mediated changes in the phosphorylation status of the contractile apparatus [148]. It was found that Rho-kinase, activated by the G protein RhoA, inhibits myosin light chain (MLC) phosphatase and enhances PASMC contraction during hypoxia [146,187.]

1.3.1.2 Role of potassium

The resting cellular membrane potential (E_M) is mainly built up by the ion gradient of the potassium concentrations ($[K^+]$) between the extracellular and the intracellular space and depends on the relatively high potassium conductance (I_K) [140]. In PASMC depolarisation of E_M following potassium (K^+) channel inhibition may lead to calcium influx through VOCE as outlined before. Several functional classes of variably composed K^+ channels are expressed in PASMC and some might be involved in the effector pathway of HPV [38]. There is evidence that K^+ channels are influenced by oxygen directly or maybe controlled by specific mediators which are generated depending on oxygen [38,122]. An alternative hypothesis suggests K^+ channel inhibition due to release of Ca^{2+} from intracellular Ca^{2+} stores [143]. It could be demonstrated that hypoxia inhibits I_K and depolarizes E_M in PASMC and that certain K^+ channel antagonists mimic reactions to hypoxia [144,222]. Voltage-gated K^+ channels (Kv channels), especially those composed of Kv1.2, Kv1.5, Kv2.1 and Kv9.3 alpha-subunits, play an important role in support of resting E_M in PASMC, exhibit reduced permeability and lead to depolarization in response to hypoxia [10,83,221]. Even though these channels are somehow directly susceptible to oxygen, as suggested by patch clamp preparations with isolated Kv- channels, it was found unlikely that this characteristic is essential for the HPV sensor system [10,38]. Furthermore studies in knock-out mice suggested an important but likely a non-essential

role for the investigated Kv channels regarding the effector mechanism of acute HPV [8,201]. Other potassium channel classes are expressed in PASMC as well and might additionally contribute to the mechanism: 1) calcium activated 2) adenosine triphosphate (ATP) -sensitive and 3) two-pore domain K^+ channels [201]. Recently an important contribution of the large conductance calcium activated potassium channel (BKα) to the oxygen sensor mechanism in HPV has been widely excluded using BKα deficient mice [152].

1.3.2 Cellular mechanism – mediators

There are several potential mediators which may connect the oxygen sensors with the effector pathway that induces calcium influx and contraction. Major importance has been ascribed to mediators connected to cellular energy utilization (e.g. ATP), to reactive oxygen species (ROS) and the cytosolic redox state. Additional potentially important mediator candidates include the arachidonic acid metabolites hydroxyeicosatetraenoic acid and epoxyeicosatrienoic acid [85], as well as carbon monoxide [80].

1.3.2.1 Reactive oxygen species (ROS) and redox state

There is great support for the hypothesis that ROS and/or the cellular redox-state, represented by cytosolic redox couples [e.g. oxidised/reduced nicotinamide adenine dinucleotide (NAD/NADH) or glutathione (GSSG/GSH)], are involved in the signalling pathway responding to hypoxia. Two opposing theories regarding the role of these substances are currently established. One is suggesting a decrease in ROS and a more reduced state, the other one is favouring an increase as important HPV mediator. The first theory proposes that during hypoxia the level of ROS decreases and the intracellular compartment is shifted to a more reduced state. Redox-sensitive Kv channels may therefore close and lead to calcium influx via VOCC [200]. In line with these theories oxidants were able to reverse HPV, while reducing agents elicited vasoconstriction [131,200]. Important data promoting the latter theory is that hydrogen-peroxide (H_2O_2) is able to induce vasoconstriction and added antioxidants, superoxide (O_2^-) scavengers, as well as overexpressed catalase and glutathione peroxidase are capable of inhibiting HPV or HPV equivalent reactions in isolated cells [160,186,193,195,205]. A possible pathway that involves a rise in ROS and especially H_2O_2 as a calcium trigger might work via activation of phospholipase C (PLC), which metabolizes phosphatidyl-inositol 4,5-bisphosphate to IP_3

and diacylglycerol (DAG) [195]. Calcium might then be released from IP_3 –sensitive intracellular stores [195] or via DAG activating TRPC6 channels as recently suggested [60,203]. Furthermore it was reported that H_2O_2 is able to stimulate Ca^{2+} release from mitochondria and activate VOCC [159,196]. Monitoring of ROS and the cellular redox-state during hypoxia has lead to contradicting observations depending on the applied method [9,118,186,192,193]. The controversy might at least partially be based on problems in reliably detecting ROS [182], or be explained by the influence of HPV kinetics, pretone or sub-cellular localization of differentially acting ROS sources and targets [168,194].

1.3.2.2 Nucleoside phosphates and nitric oxide signalling

Other theories focus on signal transduction via mediators linked to the cellular energy state. It was found unlikely that an overall cellular decrease in ATP concentration is a specific signal in HPV as the overall energy state seems well conserved during moderate hypoxia [103]. It has been suggested that energy production during hypoxia is maintained by activation of glycolysis and glucose uptake but this shift may lead to alteration in cellular distribution of ATP production and its utilization [102]. ATP might therefore work as a signal molecule in a sub-cellular context. The adenosine monophosphate (AMP) - activated protein kinase (AMPK) was found regulated by increasing AMP/ATP ratio during hypoxia and activate cyclic adenosine diphosphate ribose (cADPR) dependent SR- calcium release [51]. Pharmacological stimulation of the AMPK pathway leads to increase in cADPR and $[Ca^{2+}]_c$, as does hypoxia [52]. There may also be a link between ROS and the cADPR pathways as it was shown that increased ROS stimulates cADPR synthesis [130,191] and found necessary for AMPK activation [50]. Nitric oxide (NO) is a vasodilator of systemic and pulmonary vessels that is generated by isoforms of the nitric oxide synthase family (NOS) from L-arginine, oxygen (O_2), and NADH [41,100]. Endothelial NO reaches proximal SMC via diffusion and induces the production of cyclic guanosine monophosphate (cGMP) which directly or indirectly leads to dephosphorylation of the MLC and muscular relaxation [41,167]. The effect of NO on the different phases of HPV is incompletely understood but inhibitor studies in isolated lungs and in vivo studies in humans found amplification of both acute and sustained vasoconstrictor responses [22,210] while NO inhalation attenuated HPV [59]. Conversely basal pulmonary vascular tone was sometimes found unaffected by the interruption of NO signalling and

does not mimic HPV [2,64,156]. Therefore inhibition of NO production via hypoxia (e.g. via substrate deficiency) is unlikely a major HPV triggering mechanism but NO signalling pathways are likely regulating the strength of the vasoconstrictor responses.

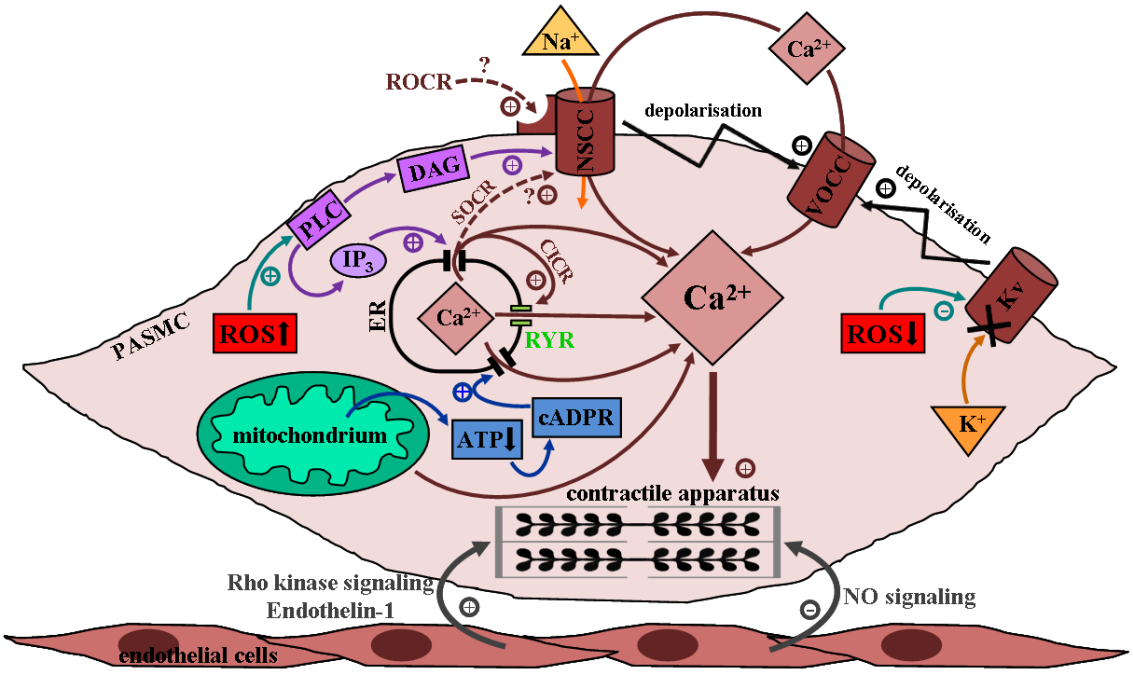

Fig. 1-2: Model of potential effector and mediator pathways in HPV. ATP: adenosine triphosphate, cADPR: cyclic-adenosine-diphosphate-ribose, CICR: calcium-induced calcium release, DAG: diacylglylycerol, ER: endoplasmic reticulum, IP_3: inositol-1,4,5-trisphosphate, Kv: voltage-gated potassium channel, NO: nitric oxide, NSCC: non-specific cation channel, PASMC: pulmonary artery smooth muscle cell, PLC: phospholipase C, ROCR: receptor-operated calcium release, ROS: reactive oxygen species, RYR: ryanodine receptor, SOCR: store operated calcium release, VOCC: voltage-gated L-type calcium channel.

1.3.2.3 Mediators in sustained HPV

There are several observations regarding the mentioned mediators that underline differences, but also point out overlaps in the pathways and mechanisms of acute and sustained HPV. For example ROS seems to be involved in both phases as reducing agents and O_2^- scavengers can affect sustained and acute HPV [45]. Interestingly inhibitors of AMPK were only capable of preventing sustained pulmonary vasoconstriction but not acute HPV [151]. Also only phase 2 was found to directly depended on the uptake of exogenous glucose [101,102]. Despite some controversial reports [12,89,113] it has been suggested that the sustained phase of HPV is dependent on the pulmonary vascular endothelium [2,147] and maybe on calcium sensitization via the Rho kinase signalling pathway [149]. It is

known that the endothelium is able to control vascular tone via production and release of vasoactive substances like NO [64] and endothelin-1 (ET-1) [94,175] and that this function can be altered by hypoxia. Even though the role of these substances in HPV has not been fully elucidated, they do not seem to have an essential, but rather an important modulatory and facilitatory effect on HPV [106,189].

1.3.3 Cellular mechanism – oxygen sensor

Mitochondria are the major oxygen consumers in vital cells [15] and it is therefore plausible to suspect their direct involvement in regulation of oxygen dependent pathways. Furthermore they are important regulators of putative HPV signals via production and detoxification of ROS, control of energy state and Ca^{2+} handling. The list of potential primary oxygen sensors in HPV further includes certain nicotinamide adenine dinucleotide phosphate oxidase (NADPH- oxidase) isoforms and cytochrome P450 containing enzymes.

1.3.3.1 Oxygen sensor – mitochondria

Mitochondria are important oxygen sensor candidates as they interact with the established signal pathways of HPV, and experimental manipulation of mitochondrial functions alters HPV responses. By depleting mitochondrial deoxyribonucleic acid (DNA) it was demonstrated that a functional electron transport chain (ETC or respiratory chain) is necessary to maintain the HPV linked responses of PASMC to hypoxia [35,192]. The ETC enables the process of oxidative phosphorylation for ATP production using energy derived from reducing equivalents, themselves generated in upstream metabolic processes [27]. The respiratory chain is composed of four main protein complexes, embedded in the inner mitochondrial membrane (complex I-IV) [27]. Coenzyme NADH is oxidized at complex I, reduced flavin adenine dinucleotide (FADH) at complex II and their electrons are transferred down the ETC to be finally accepted by oxygen at complex IV [27]. The mobile molecules cytochrome c and ubiquinone/ubiquinol (Q/QH_2) allow electron flow between the individual complexes and cytochromes. While transferring electrons, the complexes I, III and IV pump protons into the intermembrane space, thereby building up the electrochemical gradient that drives ATP synthesis at the mitochondrial enzyme ATP synthase [27]. It is reasonable to suggest that a deficiency in oxygen as a sub-

strate may cause inhibition of ETC functions and act as the primary trigger of HPV. In general the affinity of complex IV, which transfers electrons to molecular oxygen, is considered to be very high during mild hypoxia [18,27]. Nevertheless there is considerable change in mitochondrial function due to hypoxia and PASMC might be equipped with a structurally modified complex IV or its oxygen affinity might be mediator modulated [123,182]. Recently oxygen affinity of mitochondrial respiration was determined in PASMC by respirometry and in isolated lungs by remission spectrophotometry and a small but significant decrease of respiration and reduction of mitochondrial cytochromes under hypoxic conditions that may increase [Ca^{2+}] and elicit HPV could be demonstrated [169]. Data from pharmacological blockade, for example using cyanide (CN^-) compounds, seems particular dose and/or preparation dependent and has not been overall consistent with a role as an oxygen sensor for this complex [7,192]. It has been suggested that, presuming oxidative phosphorylation is somehow impaired during hypoxia, an increasing AMP/ATP ratio may serve as a signal mediating HPV even in absence of marked ATP depletion [52].

1.3.3.1.1 Mitochondrial ROS production

Current hypothetical pathways of HPV often involve the metabolism of ROS although the source and regulation of these molecules during hypoxia is highly controversial. Several mitochondrial elements have been identified as putative ROS generators, and depending on the production site, ROS can be emitted to the mitochondrial matrix, the intermembrane space or the cytoplasm [4]. Location and mode of ROS production must be taken into account, as detoxifying systems are unequally distributed and lifetime, diffusion range and interaction vary between different types of ROS. [36]. There is considerable variation of ROS production depending on tissue type and the state of respiration, but complex I and III might be the most important mitochondrial ROS sources [15,182]. Primary mechanism of ROS production is single electron (e^-) donation to oxygen resulting in O_2^- [29,123]. O_2^- may react with nearby partners, transferring an e^- back into the ETC via cytochrome c as well as being converted spontaneously or enzymatically to more stable and less diffusion restricted forms of ROS (e.g. H_2O_2) [182]. Assumptions regarding mitochondrial functions in HPV pathways are in many cases derived from studies using ETC inhibitors and combinations of substrates under different conditions and the speci-

ficity of these substances, the comparability and physiological relevance of the experiments is therefore an additional matter of debate [204]. It has been suggested that ROS increases during hypoxia and is mainly derived from complex III [192]. Especially the quinol oxidase site located at the cytosolic side of the inner membrane (Qo) of this complex releases O_2^- directly into the intermembrane space what might serve as an important cellular signal [36]. This is supported by observations in which substances blocking electron flow upstream of the assumed production site (e.g. rotenone – complex I or myxothiazol – proximal complex III) inhibited O_2^- production as well as HPV [204], while blockers acting downstream did not [101]. The use of exogenous succinate to bypass the proximal blockade of rotenone then again restored ETC functions and was interpreted as a confirmatory result which should underpin specificity of this experimental intervention [101]. In other experiments, even though not performed in PASMC, compounds acting distal from the proposed production site could increase ROS generation. This was likely by slowing down the e^- flow and elevating the concentration of single e^- donors, especially ubisemiquinone (Q•) [182]. In HPV a similar mechanism might cause reduction of proximal ETC and prolong lifetime of Q• and therefore increase ROS production at complex III [192]. According to the authors who conversely propose a decrease in ROS production during hypoxia, the ETC complexes exhibit a relatively high baseline production of ROS [118]. In line with this theory they found proximal ETC inhibitors (e.g. rotenone and antimycin A) to mimic effects of hypoxia and to prevent subsequent HPV [7]. In favour of this hypothesis is the fact that decrease of ROS could be easily explained by the fact that ROS formation is proportional to available oxygen as well as the potential e^- donors [123,182]. It is understandable that during hypoxia at least one of these variables will decrease and lead to decline in ROS formation. Variables known to generally modify ROS production are among others: a) the mitochondrial protonmotive force (Δp), b) the intra-mitochondrial calcium concentration ($[Ca^{2+}]_m$) [29] and c) K^+ influx into the mitochondrial matrix [5]. Additionally efflux of certain ROS types may be regulated via membrane channels [e.g. inner membrane anion channels (IMAC) [192] or voltage-dependent anion channels (VDAC) [70]].

1.3.3.1.2 Mitochondrial protonmotive force

The energy stored in the electrochemical gradient over the inner mitochondrial membrane is generated by the ETC complexes and called the Δp [27]. It consists of a chemical/osmotic gradient (ΔpH) and an electrical gradient, the mitochondrial membrane potential (ΔΨm) [27]. Δp is an highly important mitochondrial parameter as it drives ATP synthesis, supports transport processes over the inner mitochondrial membrane [29] and was found to determine ROS generation [93,99]. Studies in isolated mitochondria demonstrate that complex I produces high amounts of O_2^- under conditions of elevated Δp, either by reversed electron transfer from QH_2 or under an increased NADH/NAD ratio [123]. This may occur when ATP synthesis and respiration are low and there is no proton leakage (coupled state). It was also suggested that elevated Δp might be able to stabilize Q• and thereby promote ROS production at complex III [123]. Measurement of ΔΨm in isolated PASMC using fluorescent dyes suggested hyperpolarisation during hypoxia [118,169]. Experimental uncoupling of ATP synthesis from electron transport can be provoked using the protonophores 2,4-dinitrophenol (DNP) or carbonyl–cyanide-p–triflouromethoxyphenylhydrazone (FCCP) [177] and results in decrease of Δp and likely decreased ROS production as outlined above. The impact of the chemical uncoupler DNP on pulmonary circulation was investigated early in intact animals [20] and an isolated lung model [108]. Although the effect was initially attributed to a change in metabolic rate and through a reduction in PvO_2 [20], these results are consistent with a newer study in isolated organs [204]. According to these authors DNP increases PAP during normoxia and/or augments the effect of hypoxia when applied at lower concentrations [20,108,204] but decreases HPV and baseline pressure at higher concentrations [204]. The value of chemical uncouplers in isolated lung models is limited for they can induce severe edema [204]. Additionally in isolated PASMC, FCCP induced an increase in $[Ca^{2+}]_c$ attributed to a release from intracellular Ca^{2+} stores [223].

1.3.3.1.3 Mitochondrial calcium metabolism

Mitochondria are able to increase $[Ca^{2+}]_c$ by Ca^{2+} release and maybe via participation in CCE processes [91] or in connection with the endoplasmic reticulum (ER) [66], as well as they are able to buffer cytosolic Ca^{2+} rises due to Ca^{2+} uptake. Additionally many mitochondrial functions themselves are $[Ca^{2+}]_m$ dependent or regulated. Ca^{2+} transport

through the mitochondrial membranes is achieved by several channels with distinct characteristics and functions [66]. It was found that the major part of Ca^{2+} uptake is driven by $\Delta\Psi m$ via a selective mitochondrial Ca^{2+} uniporter (MCU) and the main efflux accomplished via Ca^{2+}/Na^{+} antiport which in turn relies on Na^{+}/H^{+} exchange [29]. It was suggested that rise in $[Ca^{2+}]_c$ during HPV is augmented or triggered by inhibition of mitochondrial calcium uptake [196]. Yet, the process and importance of mitochondrial calcium uptake in smooth muscle cells, especially under hypoxia is not known. It was demonstrated that increase in $[Ca^{2+}]_c$ due to release from SR is followed by a rise of $[Ca^{2+}]_m$ in rat PASMC [44]. FCCP amplifies this increase in $[Ca^{2+}]_c$, but diminishes the rise in $[Ca^{2+}]_m$ suggesting a possible $\Delta\Psi m$ dependent modulation of $[Ca^{2+}]_c$ and contraction via mitochondrial calcium uptake [44]. Mitochondrial Ca^{2+} is an activator of ATP synthesis and thereby able to couple energy consuming processes (e.g. muscular contraction) to energy production [66]. It has been suggested that rise in $[Ca^{2+}]_m$ increases ROS generation, for example by enhancing metabolic turnover and inhibition of complex III and IV, but experimental data is not consistent in this regard [29,66,191].

1.3.3.2 Additional oxygen sensor candidates

The commonly proposed oxygen sensor candidates of HPV share the capability to bind and react with oxygen using heme-based proteins. Some of these proposed sensor concepts of HPV are underpinned by findings and observations in other oxygen responsive tissues like the carotid body cells. Furthermore the principle of iron-containing proteins acting as oxygen responsive element is encountered in bacteria, yeast and multicellular organisms [31]. One hypothesis involves the activity of a NADPH oxidase isoform that may function as oxygen sensor and enable signal transduction via ROS up- or down-regulation [209]. Other concepts propose a role for cytochrome P450 containing monooxygenases as well as for certain hemoxygenase (HO) isoforms and their metabolites [209]. Recently a study using hemeoxygenase-2 (HO-2) - knock-out mice widely excluded HO-2 as putative oxygen sensor in HPV [152].

1.4 Hypoxia-induced pulmonary hypertension (PH)

Chronic hypoxia induces substantial changes in physiological functions which are in part appropriate to improve oxygen uptake, transport and to adjust systemic homeosta-

sis. Beside the increase of hematocrit, hypoxia induces structural changes in pulmonary circulation [207], causes metabolic changes and weight loss [220]. In regard to the pulmonary circulation, reduced alveolar oxygen availability leads to remodelling of pulmonary vessels, PH and right ventricular hypertrophy [48,87]. Contrary to the mechanisms of acute HPV, the long-term reactions to generalised hypoxia in the lung and the secondary response to increased PAP, like right ventricular hypertrophy, are inadequate to improve organisms' oxygen uptake and become harmful with increasing extent [65].

1.4.1 Pathophysiology and morphology of PH

The morphology of vascular remodelling in PH of different types and etiology has general hallmarks, but also depicts specific variations. A common feature is the thickening of the entire arterial wall by cellular hypertrophy and hyperplasia and especially the formation of a smooth muscle layer in the smaller and usually non-muscularized PA [87]. Remodelling processes under chronic hypoxia are of extended clinical significance when applied as a model of PH. It has to be considered that these processes do not completely mimic the findings in the various types of severe pulmonary vascular diseases. However, PH also arises from chronic hypoxia in humans and thus the model of chronic hypoxia-induced PH particularly represents the pathogenesis of PH in this condition. In the process of hypoxia-induced remodelling medial hypertrophy occurs and characteristic strands of longitudinally oriented intimal SMC develop [171]. Wall thickening, narrowing of the lumen and muscularization are further enhanced by recruitment of fibroblasts and pericytes, as well as an increased matrix protein deposition [87,171]. In contrast to different clinically relevant forms of severe PAH in humans (e.g. IPAH), changes in the hypoxia animal model are mainly reversible and do not include the formation of a neointima or plexiform lesions [87,171].

1.4.2 Molecular basis of adaptation to chronic hypoxia

There is good evidence that hypoxia stimulates proliferation of PASMC, endothelial cells and fibroblasts via regulation of mitogenic factors like ET-1, vascular endothelial growth factor (VEGF) and inflammatory mediators as well as of antimitogenic factors like NO and prostacyclin [133]. The hypoxia-inducible factor-1 (HIF-1) is established as an important, maybe universal oxygen dependent transcription factor triggering effects

of chronic hypoxia via gene regulation [31]. The subunit HIF-1α is defining the biological activity of HIF-1 [158] and is an essential factor for embryonic development of the cardiovascular system. Furthermore it affects the adaption of the pulmonary circulation to hypoxia, which was shown in a mouse model [220]. Among other functions, HIF-1 can induce production of proteins that are relevant for PH like erythropoietin, VEGF or ET-1, and might regulate glucose transport and glycolysis [34,87,158]. ROS may arise from different sources and represent important signal molecules during hypoxia. Matching this concept, ROS were found to stabilize HIF and therefore suggested as mediator of both acute and long-term adaptation to hypoxia [34,196]. The NO signalling pathway is additionally involved, or at least altered, in the processes of chronic hypoxic PH as well as those of IPAH [100,217]. NO can inhibit vascular remodelling and might play a antagonistic role during PH, as pharmacological inhibition of NOS and knock-out of endothelial NOS (eNOS) function aggravated PH in hypoxic animal models [42,100,172]. Additionally long-term inhalation of NO could attenuate remodelling [208].

1.5 Mitochondrial uncoupling protein 2 (UCP-2)

1.5.1 UCP-2 – structure and classification

UCP-2 is part of the UCP protein family which is encoded by the genomic DNA of mammals, fish, birds, plants and likely also of fungi and protozoa [104]. UCPs in turn belong to a superfamily of mitochondrial anion-carriers whose members share structural and functional characteristics [96,104]. Mammals express UCP-1 to UCP-5. The calculated sequence similarities are high between UCP-2, UCP-3 and UCP-1, but lower between UCP-4 and UCP-5 [96]. UCP-1, 2 and 3 are alkaline proteins with a molecular mass of 31 – 34 kDa and six α-helical regions spanning the inner mitochondrial membrane. A functional unit is probably formed by a homodimer of the individual UCP proteins [96].

1.5.2 UCP-2's more popular relative

The first member of the UCP family, UCP-1 or thermogenin, was discovered in 1978 [75] and is now relatively well characterised. It primarily enables heat generation in specialized brown adipose tissue (BAT) of mammals by uncoupling the e^- flow along the ETC from ATP production. Activity of UCP-1 is inhibited by nucleotides but can be restored

and enhanced by increasing concentrations of fatty acids (FA) arising from lipolysis triggered by noradrenalin via β_3-adrenoceptors [33]. UCP-1 is thereby functioning as a regulator of body temperature through non-shivering heat production, but also modifies energy balance and body weight, all under control of the sympathetic nervous system [33]. The amount of functional UCP-1 protein can be increased for example during cold acclimation and hibernation, and the quantity and distribution of BAT generally varies between species, age/size and the living conditions of animals [33]. Distribution, physiological function and regulation of the protein UCP-2 is currently less clear. As UCP-2 and UCP-1 are structurally related it is plausible to assume overlaps in function and regulation, especially considering the conserved amino-acid sequences in key regions linked to proton transport and at substrate binding sites.

1.5.3 UCP-2 – distribution, function and physiological role

First described in 1997, as a 59% amino-acid identical homologue of UCP-1 in humans, UCP-2 was found capable of lowering the $\Delta\Psi m$, when expressed in yeast, and initially suggested as a regulator of body weight, thermogenesis and immunity [58]. In contrast to the exclusive occurrence of UCP-1 in BAT, UCP-2 is expressed in a variety of tissues. Unfortunately most of the studies on localization are performed on messenger- ribonucleic acid (mRNA) level only, and it has been reported that expression levels do not actually predict UCP-2 protein abundance [138]. Due to difficulties with immunodetection reliable studies are rare, nevertheless highest UCP-2 protein levels can be expected in spleen, lung, stomach, kidney, pancreatic β-cells and immune cells [138]. Even in tissues with a relatively high UCP-2 abundance the calculated protein concentration is likely only a small fraction, maybe around 1/500, of the concentration of UCP-1 in BAT [26]. The generally low mitochondrial UCP-2 amount, together with preserved adaptation to cold temperatures and a normal body weight in UCP-2 deficient (UCP-$2^{-/-}$) mice, is pointing toward functions other then thermogenesis [13]. Uncoupling activity under physiological conditions in intact cells is fairly established for UCP-2 [49,97] and there is evidence for a role in the multifaceted metabolism of ROS [128]. By controlling Δp, UCP-2 might change ROS production and intracellular signalling in different cells. Furthermore O_2^- is able to activate uncoupling activity via UCPs under certain conditions and this might enable a feedback loop to control mitochondrial ROS generation [49,124]. Nu-

cleotides and FA do impact UCP-2 activity in vitro but whether or not they are important mediators in vivo has not been decided yet [96]. Regarding the physiological or pathological significance of UCP-2, it was published that macrophages, isolated from UCP-2 deficient (UCP-$2^{-/-}$) mice, produce more ROS than those of wild type (WT) mice and this fact was considered to be responsible for an increased resistance against infectious agents, observed in these animals [13]. Additionally UCP-2 can negatively influence insulin secretion and was found upregulated in a type 2 diabetes mellitus animal model [226]. Additional UCP-2 gene knock-out in these animals improved blood glucose control by increasing ATP signalling [226]. Under physiological conditions UCP-2 might decrease oxidative damage or fine tune the magnitude of different cellular responses [26]. Later a physiological significant uncoupling activity was questioned again and new functions were suggested for the UCP-1 homologues. In an intensely debated publication Trenker et al. proposed a fundamental function for UCP-2/3 in enabling mitochondrial Ca^{2+} uptake via the MCU [28,179,180]. Intriguingly UCP mediated calcium flux could also be able to mimic a protonophoric uncoupling activity by additional involving Ca^{2+}/Na^{+} and Na^{+}/H^{+} exchangers [63]. Recently another theory suggested involvement of UCPs in glucose and pyruvate metabolism. According to this hypothesis UCP-2/3, themselves regulated by FA and glutamine, decrease mitochondrial pyruvate affinity under certain conditions and influence the composition of fuel for ATP production [24].

1.6 Aim of the study

HPV is an important, but especially regarding its sub-cellular processes, incompletely understood physiological mechanism. The oxygen sensor and signal transduction systems may involve ROS, Ca^{2+} as well as ATP and may be regulated or triggered via alterations of the mitochondrial metabolism. Understanding of these processes is of general scientific interest and furthermore, elucidation of the underlying principle may help to understand pathological conditions like PH and can be a prerequisite to establish new therapies to prevent hypoxemia due to disturbed HPV.

UCP-2 is a mitochondrial protein whose physiological role and biochemical activity has not been finally determined but is proposed to regulate ROS, Ca^{2+} and ATP and therefore could be particularly important for regulation of HPV. Thus the aim of this study

was to investigate the role of UCP-2 in acute and sustained HPV as well as in chronic hypoxia-induced PH.

To achieve this aim, physiological responses of UCP-$2^{-/-}$ mice were compared to matched WT mice in experiments of:

1. Exposure to acute and sustained hypoxia in an artificially ventilated, buffer-perfused mouse lung system by determining the changes in the pulmonary arterial pressure (Δ-PAP).

2. Exposure to chronic hypoxia by evaluating the in vivo right ventricular systolic pressure (RVSP) as well as performing lung vessel morphometry and measurement of heart ratio.

The hypothesis was that UCP-2 negatively regulates mitochondrial ROS production and that an increasing levels of ROS acts as a mediator of HPV and vascular remodelling. Therefore the extend of vasoconstriction in acute and sustained HPV as well as the changes due to long term exposure to hypoxia were expected to be found enhanced in UCP-$2^{-/-}$ mice compared to WT mice.

2 Materials and methods

2.1 Animals

Homozygous UCP-2$^{-/-}$ mice (B6.129S4-*Ucp2*^{tm1Lowl}/J) were purchased from Jackson Laboratories (Bar Harbor, USA). WT mice (C57BL/6J) bought from Charles River Laboratory (Sulzfeld, Germany) served as control animals. The UCP-2$^{-/-}$ strain was created by Lowell et al. as described [226]. Briefly their procedures involved replacing part of the UCP-2 gene sequence between the introns 2 and 7 with a PGK-NEO-Poly(A) expression cassette and transferring the DNA by electroporation into J1 embryonic stem cells. Subsequently these were injected into C57BL/6 blastocytes generating chimeric mice which were mated with C57BL/6J animals. Finally heterozygous offspring were backcrossed to obtain homozygous study objects. UCP-2$^{-/-}$ offspring used for the described experiments were generated by inbreeding of offspring of two pairs of animals. After delivery from Jackson and Charles River Laboratories the mice were supplied by animal caretakers under equal conditions and had ad libitum access to food and water. All animal studies were approved by the local authority for animal research - Regierungspräsidium Giessen - reference number: “GI 20/10 Nr. 105/2010” and the permit for isolated lung experiments “Pathomechanismen der respiratorischen Insuffizienz am Mausmodell”. All interventions before the time of death of the animals by circulatory arrest, especially the conduction of anaesthesia, were supervised by Prof. Dr. Norbert Weißmann or another approved researcher. UCP-2$^{-/-}$ and WT-mice used for the experiments were of either sex with a body weight between 18 and 35g.

2.2 Materials

2.2.1 Equipment and devices

2.2.1.1 Isolated lung, chronic hypoxia and in vivo measurement

Bubble trap made of 1.5ml Eppendorf cup	Eppendorf Hamburg, Germany
Flow meter Model “P”	Aalborg Instruments and Controlls; Orangeburg, USA
Gas pre-mixtures -	Air Liquide GmbH

Normoxic gas (5.3% CO_2 / 21% O_2 / rest N_2) Hypoxic gas (5.3% CO_2 / 1.0% O_2 / rest N_2) O_2 and N_2	Ludwigshafen, Germany
Infusion pump Model “Secura FT”	Braun Melsungen AG Melsungen, Germany
Isometric force transducer and base amplifier	Kent Scientific Litchfield, USA
Magnetic valve Model “SV 04”	Rausch & Pausch GmbH Selb, Germany
O_2 controller Model “4010”	Labotect Göttingen, Germany
Personal computer (PC)	Siemens Nixdorf AG Paderborn, Germany
Positive end-expiratory pressure (PEEP) valve made of 15ml centrifuge tube	Bio-Rad Laboratories GmbH München, Germany
Positive pressure respirator Model “Minivent, Type 845”	Hugo Sachs Elektronik March-Hugstetten, Germany
Pressure transducers Model “Combitrans”	Braun Melsungen AG Melsungen, Germany
Refrigeration/ Heating circulator Model “F32-MC”	Julabo Labortechnik GmbH Seelbach, Germany
Reservoir and continuous flow heat exchanger	Glassblowing factory University Giessen, Germany
Surgical instruments Forceps and fine scissors	Martin Medizintechnik Tuttlingen, Germany
Surgical threads non-absorbable, different sizes	Ethicon GmbH Norderstedt, Germany
Threads	Coats GmbH Kenzingen, Germany
Time switch programmable, 4 channels	Grässlin GmbH St. Georgen, Germany
Transducer- amplifier module “Type 705/1”in “PLUGSYS Type 601”	Hugo Sachs Elektronik March-Hugstetten, Germany
Tracheal tube made of a “Microlance 20G”	Becton Dickinson Heidelberg, Germany
Tubes- air-tight Model “Tygon”	Cole-Parmer Instruments Vernon Hills, USA
Tubing pump Model “Reglo Digital MS-4/8”	Ismatec SA Glattbrugg, Switzerland

2.2.1.2 Lung vessel morphometry, heart ratio and hematocrit

Autocrit centrifuge	Clay Adams Parsippany, USA
Digital camera Model “DC 300F”	Leica Microsystems Wetzlar, Germany
Hematocrit capillaries	Hirschmann Laborgeräte Eberstadt, Germany
Microtome Model “RM 2165”	Leica Microsystems Wetzlar, Germany
Stereo light microscope Model “DMLA”	Leica Microsystems Wetzlar, Germany
Tissue processor Model “TP1050”	Leica Microsystems Wetzlar, Germany

2.2.2 Chemicals, reagents and antibodys

Anti-α-smooth muscle actin (anti-α-SMA) Mouse anti-human antibody diluted 1:900 with Bovine serum albumin (BSA) 10%	Sigma-Aldrich Saint Louis, USA
Anti-von Willebrand factor (anti-vWF) Rabbit anti-human diluted 1:900 with BSA 10%	Dako Hamburg, Germany
Aqua ad iniectabilia	Baxter Unterschleißheim, Germany
Avidin/ Biotin blocking kit	Vector/ Linaris Wertheim-Bettingen, Germany
BSA 10% prepared with 20g BSA powder and 0.26g NaN_3 ad 200ml phosphate buffered saline (PBS)	Sigma-Aldrich Saint Louis, USA
DAB (3,3-diaminobenzidine) substrate kit	Vector/ Linaris Wertheim-Bettingen, Germany
Disodium hydrogen phosphate (Na_2HPO_4 x $2H_2O$)	Merck Darmstadt, Germany
Ethanol - 99.6%, 96% and 70%	Fischer Saarbrücken, Germany
Formaldehyde (CH_2O) - 37%	Roth Karlsruhe, Germany
Goat serum	Alexis Biochemicals Grünberg, Germany

H_2O_2 - 30%	Merck Darmstadt, Germany
Ketamin (Ketavet) 100mg/ml	Pfizer Berlin, Germany
Krebs– Henseleit buffer (II/N) containing 120mM NaCl, 4.3mM KCl, 1.1mM KH_2PO_4, 2.4mM $CaCl_2$, 1.3 mM $MgCl_2$, 13.32mM Glucose and 5% Hydroxyethylamylopectin	Serag-Wiessner Naila, Germany
Methanol and Isopropyl alcohol 99.8%	Fluka Chemie Buchs, Switzerland
Methyl green	Vector/ Linaris Wertheim-Bettingen, Germany
Mouse on Mouse (M.O.M) and Vectastain Elite Avidin/Biotinylated Enzyme Complex (ABC) immunodetection kit	Vector/ Linaris Wertheim-Bettingen, Germany
Na-Heparin (Liquemin) 5000IU/ml	Roche Basel, Switzerland
PBS prepared with 8g NaCl, 2g KCl, 11.5g Na_2HPO_4 x $2H_2O$, 2g KH_2PO_4 ad 1l Aqua destillata	Prepared in lab
Pertex mounting media	Medite GmbH Burgdorf, Germany
Picric acid	Fluka Chemie Buchs, Switzerland
Potassium chloride (KCl)	Roth Karlsruhe, Germany
Potassium dihydrogen phosphate (KH_2PO_4)	Merck Darmstadt, Germany
Rotihistol	Roth Karlsruhe, Germany
Saline solution	Baxter Unterschleißheim, Germany
Sodium bicarbonate ($NaHCO_3$) 8.4%	Braun Melsungen AG Melsungen, Germany
Sodium chloride (NaCl)	Roth Karlsruhe, Germany
Thromboxane A_2 mimetic - U46619	Paesel and Lorei, Frankfurt am Main, Germany

Trypsin Digest All 2	Zymed San Francisco, USA
Very intense purple (VIP), Chromogen substrate kit for peroxidase	Vector/ Linaris Wertheim-Bettingen, Germany
Xylazinhydrochlorid (Rompun) 20mg/ml	Bayer Vital GmbH Leverkusen, Germany
Xylol	Roth Karlsruhe, Germany
Zamboni's fixative prepared with 50ml CH_2O - 37%, 200ml 0.2M NaH_2PO_4, 300ml 0.2M Na_2HPO_4, 150ml picric acid ad 1l Aqua destillata	Prepared in lab

2.2.3 Software

GraphPad Prism 5	GraphPad Software, Inc. La Jolla, USA
Labtech Notebook Pro	Laboratory Technologies Corp. Wilmington, USA
Microsoft Office Word, Powerpoint and Excel 2003	Microsoft Corp. Unterschleißheim, Germany
QWin V3	Leica Microsystems Wetzlar, Germany

2.3 Methods

2.3.1 Isolated buffer-perfused and ventilated mouse lung

A system for isolated buffer-perfused and ventilated mouse lung experiments was set up with small modifications as described [202]. Functionally the system can be divided into three parts: The ventilation unit (Fig. 2-1), the perfusion unit (Fig. 2-2) and the measurement unit (Fig. 2-3). Gas flow was adjusted to 50ml/min by the flow meter for both normoxic and hypoxic gas mixtures. Buffer fluid was prepared by adding $NaHCO_3$ and introducing normoxic gas mixture to the Krebs-Henseleit solution resulting in a pH of 7.30 – 7.40. The perfusion system was flushed multiple times with Aqua ad iniectabilia and cooled down to 4°C before being filled with buffer fluid. Mice were deeply anesthetised with intraperitoneal (i.p.) injection of ketamin [100mg/kg body weight (body wt.)] and xylazine [10mg/kg body wt.]. If necessary the injection was repeated with half of the above stated dosage until deep anesthesia was reached. Anticoagulation was per-

formed by i.p. injection of heparin [1000IU/kg body wt.]. Animals were mounted in an upright supine position on a rack and a longitudinal incision from the mandible to the upper abdomen was conducted. Salivary glands and muscle covering the trachea were cut, displaced and a ligature was loosely applied around the lower part of the airway.

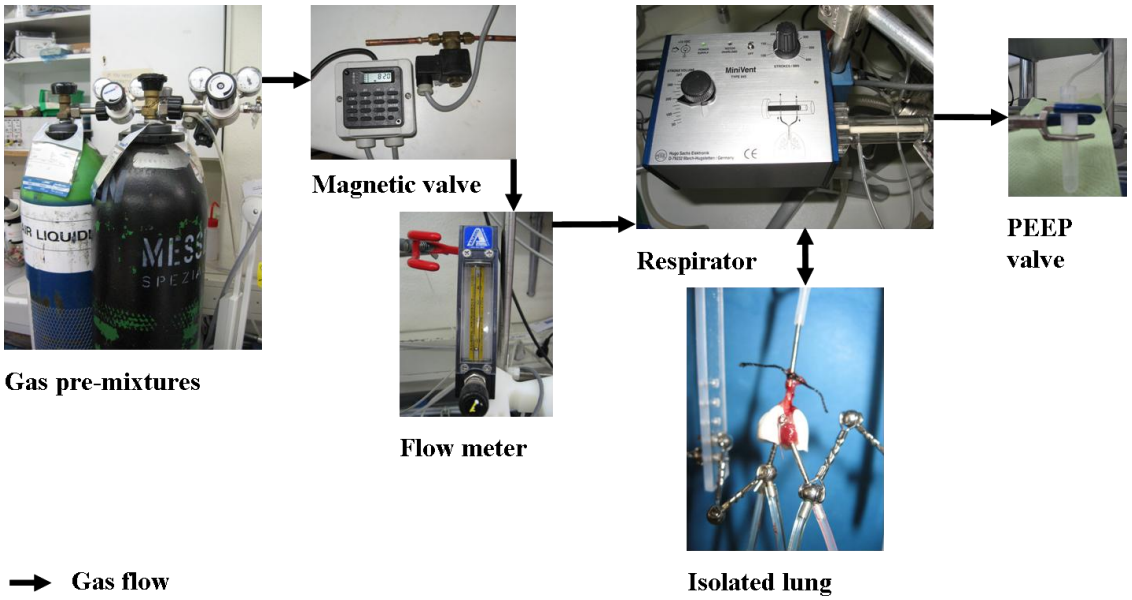

Fig. 2-1: Isolated buffer perfused mouse lung - Ventilation unit. After passing the pressure regulators, the normoxic, as well as the hypoxic gas stored in the gas pre-mixture tanks passes the magnetic valves, which allows the selection of the gas source, then the flow meter before reaching the respirator. The respirator delivers positive pressure ventilation to the isolated lung and leads the exhaled air over the positive end-expiratory pressure (PEEP) valve.

Subsequently a transverse incision was set in the mid-abdomen, organs were dislocated downwards to reach the diaphragm, where a small tear close to the sternum was made and caused a pneumothorax. Now a midsternal thoracotomy, wide opening and immobilizing of the ribcage became possible without injuring the sensitive lung tissue. Diaphragm and thymus were carefully removed and after placing a surgical thread around the root of the pulmonary artery (PA) the left ventricle (LV) was pierced and the right ventricle (RV) was longitudinally incised. The PA was catheterised via the open RV, the prepared ligature tied and the perfusion initiated with Krebs- Henseleit buffer at a flow rate of 0.2ml/min. The lungs and heart were then carefully detached en-block from the body by cutting behind and along the trachea and pulling the sensitive lung tissue away from the parietal pleura. The LV was catheterized and connected to the perfusion circuit after the lung was suspended freely. The isolated organ was held only by the airway

tube aligned to the isometric force transducer and was connected to the PA- and LV-catheters. The perfusion system's temperature was steadily increased via the heating circulator to a temperature of 37°C. During the next 30min the flow rate was stepwise elevated to 2.0ml/min, as was the tidal volume to 300µl. This allowed the lungs to get rinsed and adapt before switching the system to recirculation.

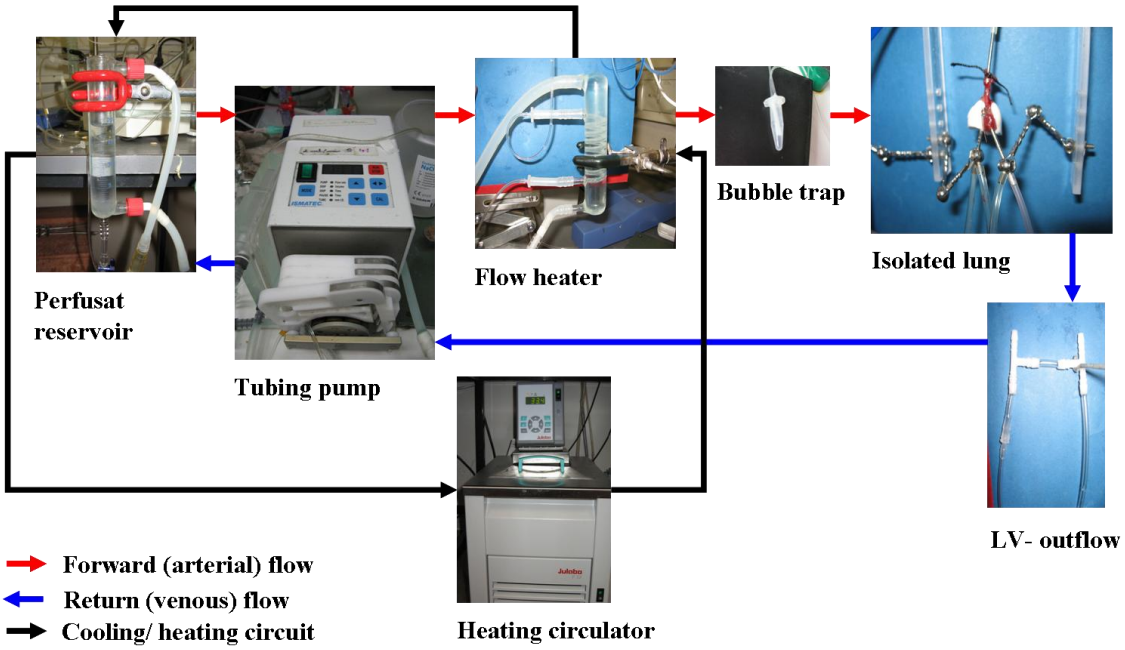

Fig. 2-2: Isolated buffer perfused mouse lung - Perfusion unit. The buffer fluid is pumped from the reservoir over the flow heater and the bubble trap to the PA catheter (red arrows) and drained back from the left ventricle over the tubing pump to the reservoir (blue arrows). The temperature of the buffer fluid is regulated by a reversely directed flow of tempered water over flow heater and reservoir (black arrows).

After onset of recirculation the system contained approximately 20ml of buffer fluid and was run for additional 15min to achieve a PAP steady-state before proceeding with the different experimental protocols. A deep inspiration with doubled tidal volume was delivered to reduce atelectasis. A one point calibration procedure was performed before the measurements. All pressure transducers were opened to allow equilibration with atmospheric pressure for calibration, the transducer- amplifier module was set to 0mmHg and the transducers were reconnected to the catheters. The left ventricular pressure (LVP) was adjusted to 1.2 - 1.3mmHg by elevating or lowering the LV- outflow tube before the start of the individual protocol. Weight force (WF) signals from the isometric force transducer during steady-state were used as reference point from which

weight gain could be registered. All data collected from homogenous white lungs without signs of edema or persistent atelectasis and an obtainable PAP and weight steady-state during the initial 15min of recirculation were included into the study.

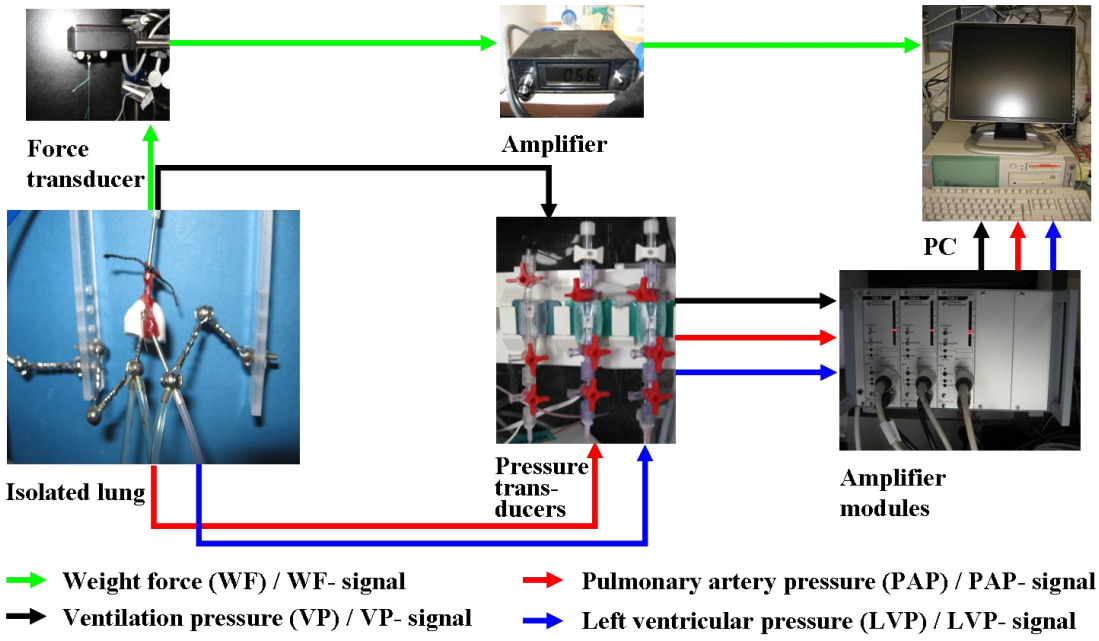

Fig. 2-3: Isolated buffer-perfused mouse lung - Measuring unit. Pressure transducers are attached to the tracheal tube (ventilation pressure), the PA- catheter (pulmonary artery pressure) and the LV- catheter (left ventricular pressure). The generated electrical signals of the pressure transducers as well as the signals of the isometric force transducer (weight force) are amplified and finally recorded on a PC.

2.3.1.1 Repetitive hypoxia

15min of normoxic ventilation were alternated with 10min of hypoxic ventilation as illustrated in figure 2-4. Δ-PAP of six cycles of alternating ventilation was compared. Δ-PAP was calculated by subtracting peak baseline PAP from peak PAP for each individual cycle.

2.3.1.2 Sustained hypoxia and normoxic control

After one cycle of normoxic (15min) and hypoxic ventilation (10min) three hours of sustained hypoxia were applied. The experiment was completed by another cycle of repetitive hypoxia (15min normoxic and 10min hypoxic ventilation) as shown in figure 2-5. The PAP levels during sustained hypoxia were compared. Additionally experiments with continuous normoxic ventilations were conducted.

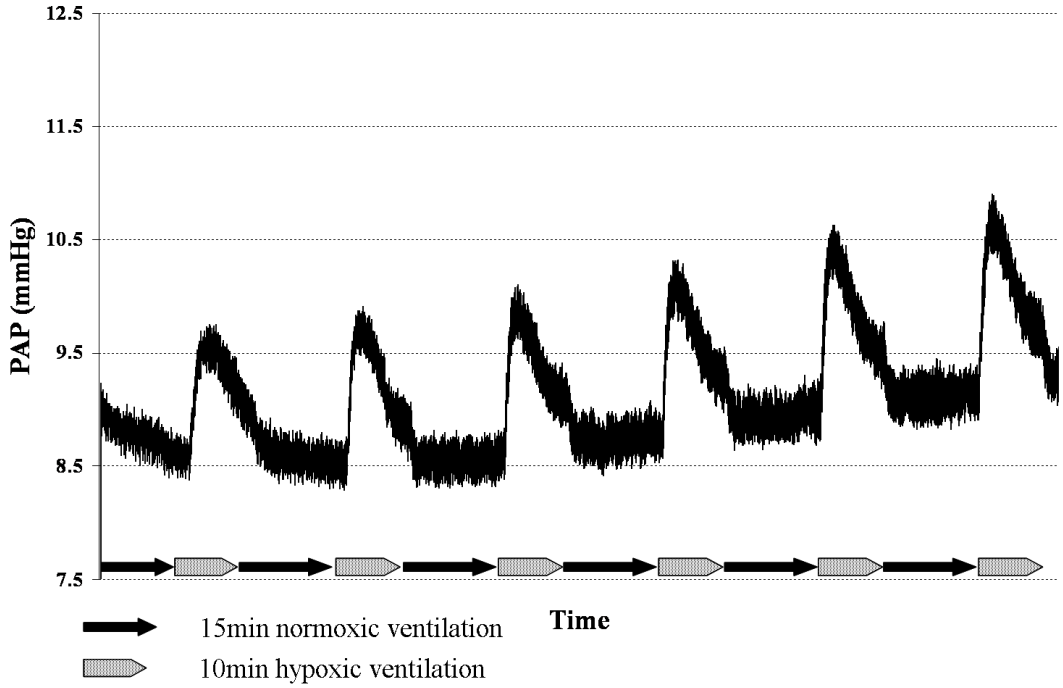

Fig. 2-4: Example of a PAP registration of a repetitive hypoxia experiment.

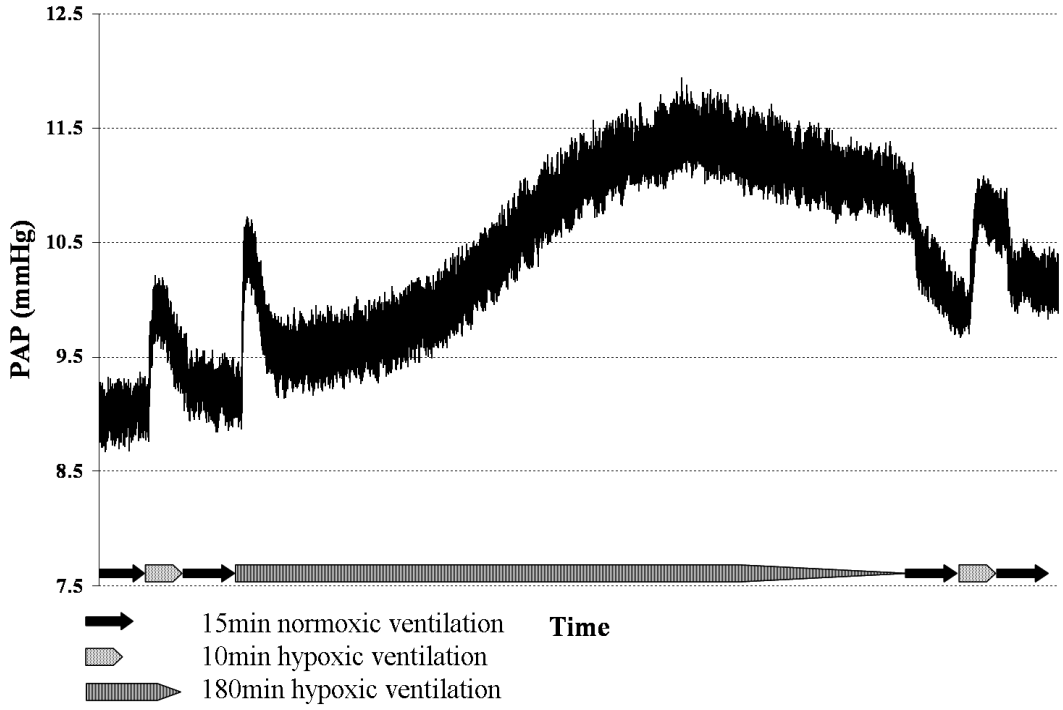

Fig. 2-5: Example of a PAP registration of a sustained hypoxia experiment.

2.3.1.3 Repetitive stimulation with U46619

An infusion pump loaded with the thromboxane A_2 mimetic U46619 [0.06µg/ml - solved in buffer fluid] was installed into the system at the arterial line leading from the buffer reservoir to the lung. Dose finding tests in control mice were conducted to determine an infusion speed and duration which caused an increase in PAP similar to that caused by HPV. A dosage of 15ng U46619 was applied over 1min and 30s [10ng/min] with an infusion speed of 10ml/h (Fig. 2-6).

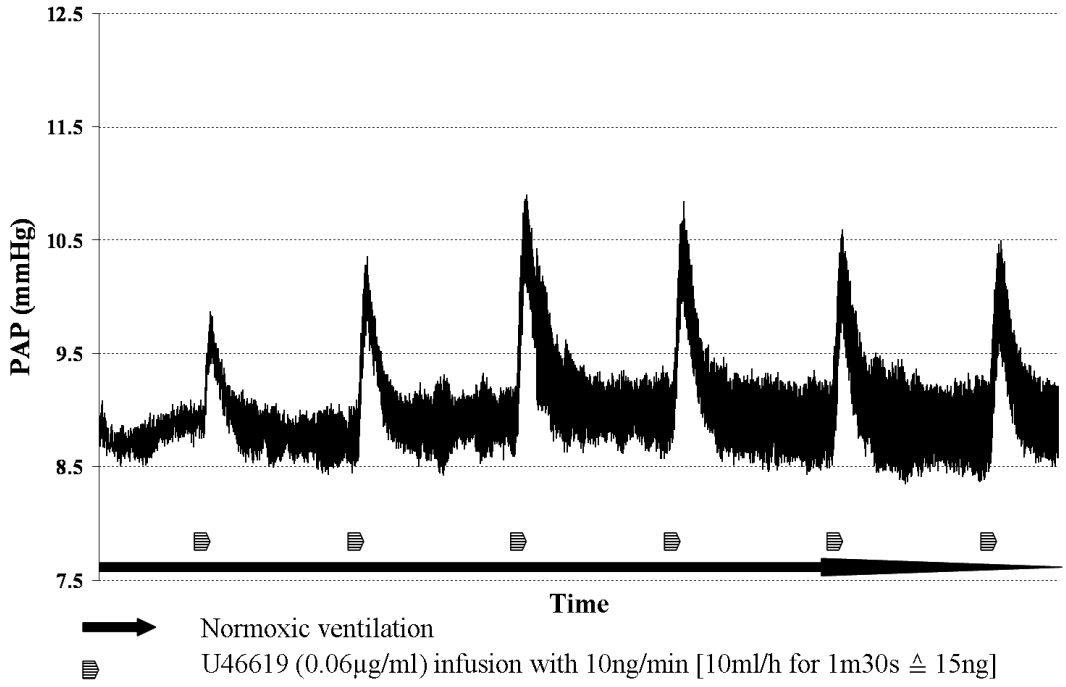

Fig. 2-6: Example of a PAP registration from an experiment with a repetitive stimulation by the thromboxane mimetic U46619.

2.3.1.4 Sustained stimulation with U46619

Similar to the prior protocol a sustained infusion of U46619 [0.06µg/ml] was used to generate an effect now resembling the changes in PAP caused by sustained hypoxic ventilation. A short term stimulation as described before was followed by an infusion of a total dose of 0.72µg U46619 over 3h [4.2ng/min] with an infusion speed of 4ml/h. Each experiment ended after another short term stimulation with 15ng U46619. The initial buffer load was reduced to 8ml in this protocol.

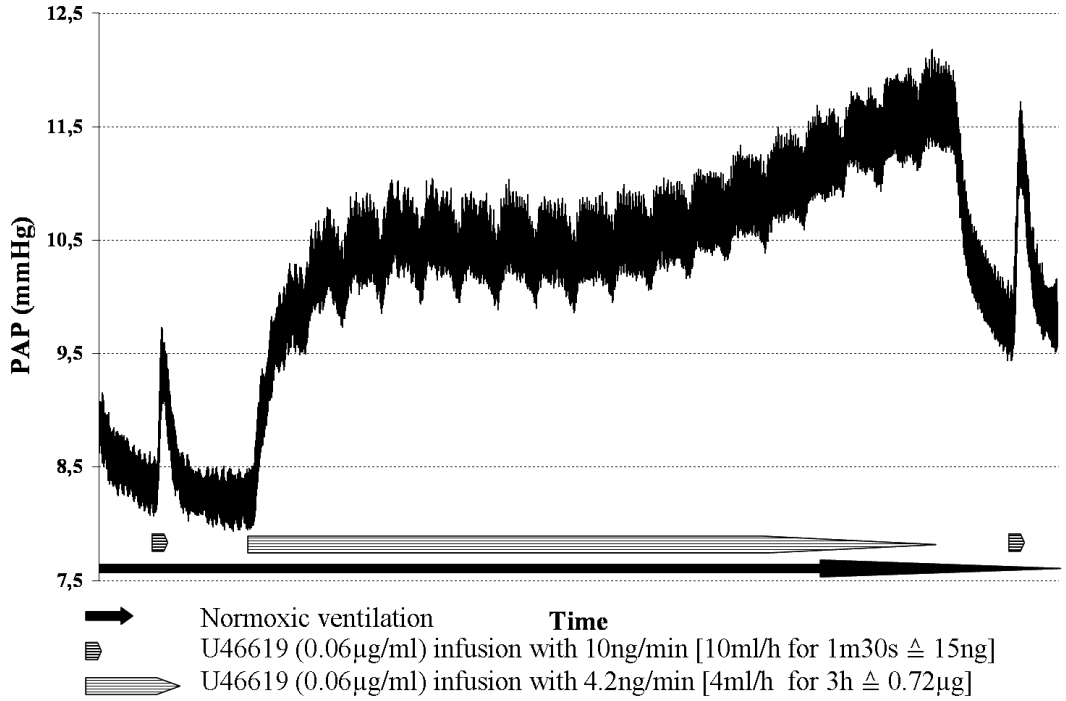

Fig. 2-7: Example of a PAP registration from an experiment with a sustained stimulation by the thromboxane mimetic U46619.

2.3.2 Chronic hypoxia

All WT and UCP-2$^{-/-}$ mice were randomly assigned either to the normoxic or the hypoxic group. Animals assigned to the hypoxic treatment / the hypoxic group (HOX) were exposed to a reduced, normobaric FiO_2 of 0.10 and those assigned to the normoxic treatment / the normoxic group (NOX) to atmospheric FiO_2 as described previously [54]. Both groups were held in chambers connected to an air circulating system to create an, apart from oxygen concentration, identical environment. Conditions were regulated by supplementing oxygen or nitrogen via an automated O_2-controller, a soda lime container that removed CO_2 and a cooling system to drain off humidity from the system. Mice were exposed for four weeks and subsequently used for the experiments described under 2.3.2.1 – 2.3.2.4. Mice were removed from their chambers and held at room air shortly before (5-15min) and during the individual measurements described below.

2.3.2.1 Right ventricular systolic pressure measurement

Measurement of right ventricular systolic pressure (RVSP) was accomplished in vivo as a slightly modified procedure of the techniques described before [47]. For this measure-

ment mice were anticoagulated with heparin [1000IU/kg body wt.] by i.p. injection. After a latency of approximately 30min mice were anesthetised with an i.p. injection of ketamin [100mg/kg body wt.] and xylazine [10mg/kg body wt.]. After onset of general anaesthesia mice were placed supine on a heating pad, tracheotomy tube inserted as described in chapter 2.3.1, but using a smaller incision at the neck. Positive pressure ventilation was performed with room air and a tidal volume of 200µl, respiratory rate of 120/min and a PEEP of 1cm H_2O. Using a stereo microscope the right internal jugular vein was located through the neck incision and secured with surgical threads at the proximal and distal part. A small incision into the vein was made, the fluid filled silicon catheter inserted and gently pushed towards the right ventricle. The proper location could be verified by real time pressure recordings resembling the typical pressure curve of the right ventricle (Fig. 2-8).

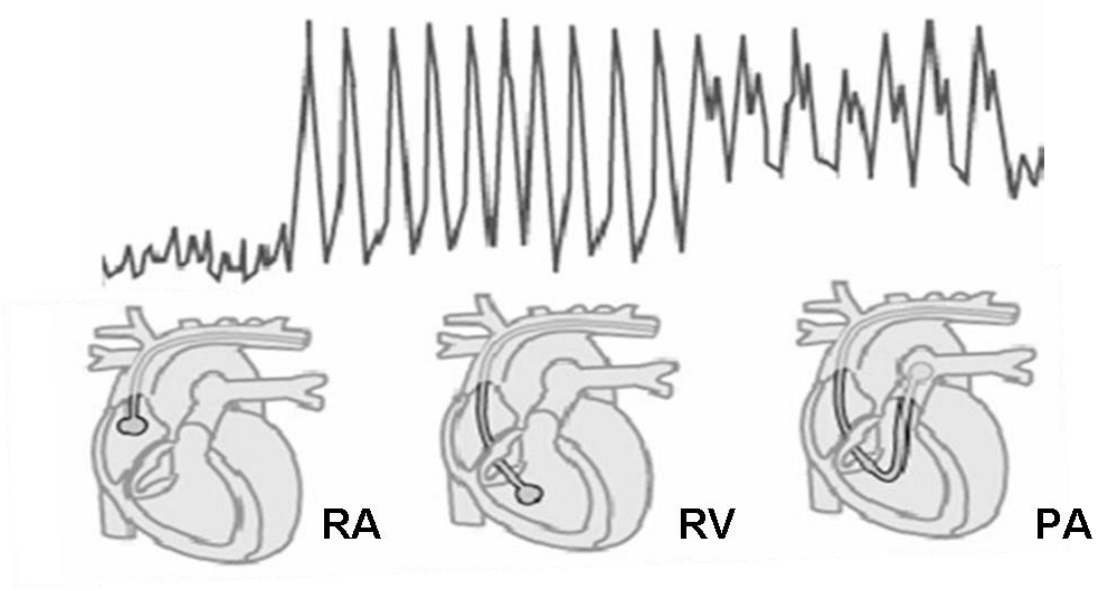

Fig. 2-8: Schematic illustrating the catheter location and the associated pressure waveform. RA: right atrium, RV: right ventricle, PA: pulmonary artery. Picture of human heart and typical hemodynamic tracing [115] adapted with kind permission of the author L. Mathews.

The pressure transducer was calibrated before each experiment. Inclusion criterion was a stable pressure registration with homogenous waveform for at least 5min. Pressure curves were then recorded for 15–30min and the highest, stable RVSP were utilized. The investigator was blinded with regard to the genotype of the mice (WT or UCP-$2^{-/-}$), and the treatment regimen (NOX or HOX). However, the NOX or HOX treatment could

be easily distinguished by intensity of blood and tissue colour of the mice during the preparation.

2.3.2.2 Hematocrit

A blood sample was collected in a hematocrit capillary directly from the right or left ventricle after completion of the RVSP measurement or during the procedure of lung fixation described in the following chapter. Capillary was closed, centrifuged and hematocrit read.

2.3.2.3 Immunohistochemistry and lung vessel morphometry

Lung fixation was performed after completing RVSP measurement. Thoracotomy and cannulation of the PA was done as described in chapter 2.3.1. The LV was opened widely, the PA- catheter was used to flush the lungs with normal saline until they were free of blood. Simultaneously ventilation was stopped, and the tracheal tubing connected to a saline filled reservoir which served as a hydrostatic counter pressure during fixation. Airway pressure was held at 12cm H_2O during the following perfusion with Zamboni's fixative with a pressure of 22cm H_2O through the pulmonary catheter for around 15min. Afterwards the heart was explanted, rinsed with saline and kept frozen until used for heart ratio determination as described in chapter 2.3.2.4. The lungs were removed and kept in Zamboni's fixative overnight, then transferred to PBS and preserved at 4°C. Finally the lungs were separated in lobes, dehydrated and embedded in paraffin with an automated tissue processor. A double immunohistochemical (IHC) staining of 3µm thick, microtome cut sections against α-smooth muscle actin (α-SMA) and von Willebrand factor (vWF) was used to evaluate the degree of muscularization in the lung vasculature. Similar staining techniques have been described previously [145,207,218]. Detailed staining protocol is given here:

Step	Procedure	Time
1	Heating sections at 58-60°C	20min
2	Rotihistol	3 x 10min
3	Ethanol 99,6%	2 x 5min
4	Ethanol 96%	5min
5	Ethanol 70%	5min
6	H_2O_2 3% in Methanol	15min
7	Aqua destillata	2 x 5min

8	Phosphate buffered saline (PBS)	2 x 5min
9	Trypsin at 37°C	10min
10	PBS	2 x 5min
11	Avidin Blocking	15min
12	PBS	5min
13	Biotin Blocking	15min
14	PBS	5min
15	10% BSA	15min
16	PBS	2 x 5min
17	Mouse on Mouse (M.O.M.) Ig Blocking	60min
18	PBS	2 x 5min
19	M.O.M. diluent	5min
20	Anti-α-SMA antibody	30min
21	PBS	4 x 5min
22	M.O.M. biotinylated IgG	10min
23	PBS	2 x 5min
24	M.O.M. ABC reagent	5min
25	PBS	2 x 5min
26	Very intense purple(VIP) substrate for peroxidase	3-4min
27	Tap water	5min
28	PBS	5min
29	Avidin Blocking	15min
30	PBS	5min
31	Biotin Blocking	15min
32	PBS	5min
33	10% BSA	15min
34	PBS	2 x 5min
35	Goat Serum	20min
36	Anti-vWF antibody at 37°C	30min
37	PBS	4 x 5min
38	Avidin Biotinylated Complex (ABC)- reagent	30min
39	PBS	2 x 5min
40	Diaminobenzidine (DAB) substrate	20s-25s
41	Tap water	5min
42	Methyl green on heating plate at 60°C	5min
43	Aqua destillata	1min
44	Ethanol 96%	2 x 2min
45	Isopropyl alcohol	2 x 5min
46	Rotihistol	2 x 5min
47	Xylol	5min
48	Coverslipping with Pertex mounting media	

Morphometric analysis of IHC stained sections from the upper left lobe for each animal was performed by an investigator blinded blinded with regard to the genotype of the mice as well as the treatment regimen and using a computer-aided procedure as described before [157]. Digital photos of the sections were analysed with Qwin software determining size and muscularization of the pulmonary vessel. Approximately 80 vessels

of different outer diameters were categorized in nonmuscularized, partially muscularized or fully muscularized depending on the amount of α-SMA labelled by IHC. Vessels were manually selected for evaluation based on their size thereby setting the ratio of small (outer diameter = 20-70µm), medium (outer diameter = 70-150µm) and large (outer diameter >150µm) vessels in every experiment to 85% small, 10% medium and 5% large ones. The categories of muscularization were defined as: 1. nonmuscularized with up to 4% of α-SMA positive staining in the tunica media, 2. partially muscularized with more then 4% and up to 75% and 3. fully muscularized with more than 75% positive staining. Coloration was detected and the associated category automatically assigned by the software. The distribution of the muscularization categories was expressed as percentage of the total vessel count including all sizes of vessels (small, medium and large).

2.3.2.4 Heart ratio

Procedures were carried out in a blinded fashion as described [157]. Hearts were thawed and cut under binocular loupe magnification to separate the RV from the associated septum and LV (LV+septum). Tissue was dried at 40°C for 1 week and all parts weighed separately. Heart ratio was calculated as percentage of weight of RV divided by the sum of the weight of LV and septum: Heart ratio = RV * 100 / [LV+ Septum]

2.4 Statistical analysis

All results, except for the hematocrit, are presented as means ± standard error of the mean (SEM). Hematocrit distribution is presented as box-and-whiskers plot. Two-way-analysis of variance (two-way-ANOVA) with Bonferroni post hoc test was performed for comparison of PAP responses to repetitive hypoxic challenges, as well as PAP and weight pattern during sustained hypoxic and normoxic ventilation and those following sustained thromboxane infusion. One-way-ANOVA with the Student-Newman-Keuls multiple comparison test was performed for analysis of RVSP, heart ratio, hematocrit, vessel morphometry, body weight and growth. A two-tailed Student t-test was performed for comparison of baseline PAP measured before the first and before the sixth cycle of repetitive hypoxia and repetitive thromboxane infusion, as well as for compari-

son of weight during these experiments. P-values < 0.05 were considered statistically significant.

3 Results

3.1 Isolated buffer-perfused and ventilated mouse lung

3.1.1 Response to repetitive hypoxic ventilation

PAP characteristics of WT [n=7] and UCP-2$^{-/-}$ [n=5] mice were analysed in an isolated buffer-perfused mouse lung system during six cycles of alternating positive pressure ventilation with a hypoxic (1.0% O_2 for 10min) or normoxic (21.0% O_2 for 15min) gas mixture.

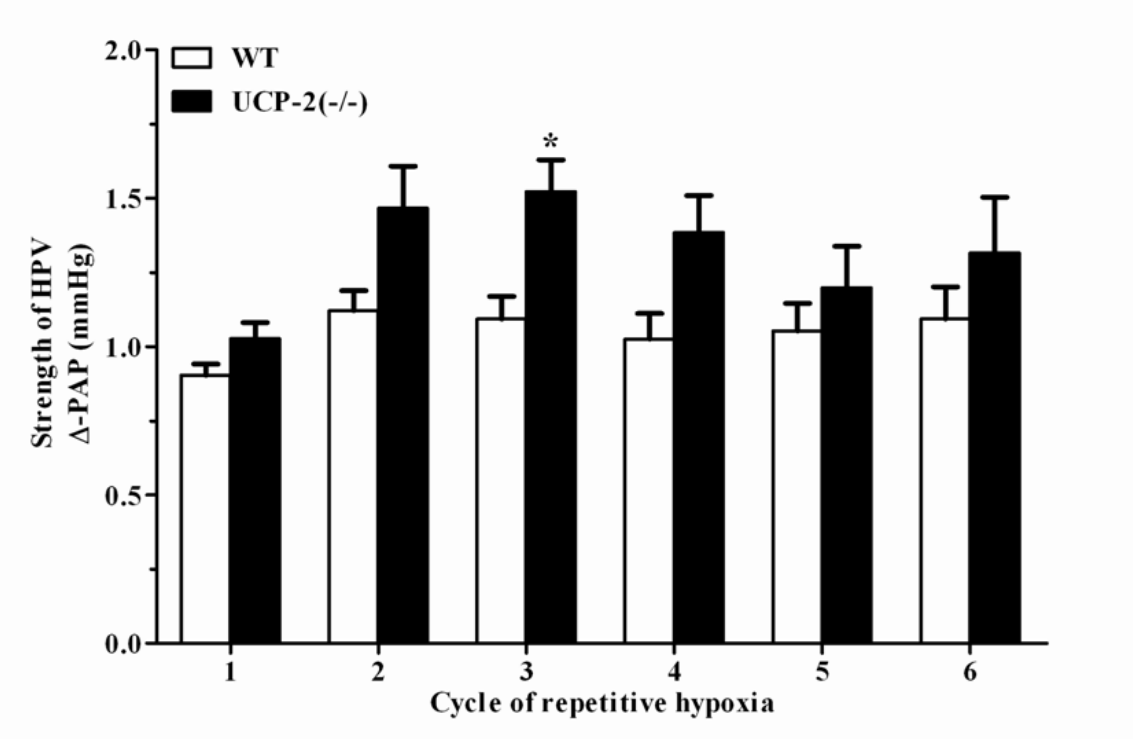

Fig. 3-1: PAP response to repetitive hypoxic ventilation in UCP-2$^{-/-}$ and WT mice. Six cycles of hypoxic ventilation, 10min each were alternated with 15min of normoxic ventilation in UCP-2$^{-/-}$ [n=5] and WT mice [n=7]. Maximum Δ-PAP (mmHg) from corresponding baseline is given for each cycle. Bars represent mean ± SEM, * = $p<0.05$.

As demonstrated in figure 3-1, UCP-2$^{-/-}$ mice had an overall tendency towards higher Δ-PAP (difference between highest PAP during hypoxic cycle and the normoxic baseline PAP). This difference was statistically significant during the third cycle (mean ± SEM for UCP-2$^{-/-}$: 1.5 ± 0.1mmHg and WT: 1.0 ± 0.1mmHg). As depicted in figure 3-2 A, no significant difference was found comparing baseline PAP during the phases of normoxic

ventilation of cycle 1 and 6. The isolated organs weight gain (difference between weight before the first and after the sixth cycle) were not significantly different as shown in figure 3-2 B.

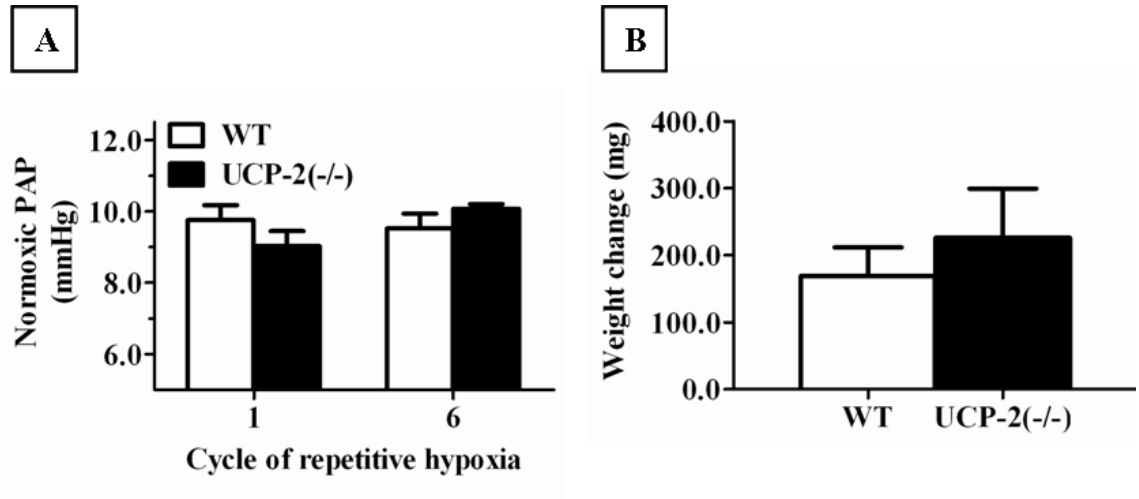

Fig. 3-2: Normoxic PAP and isolated organs' weight gain in UCP-2$^{-/-}$ and WT mice. Six cycles of hypoxic ventilation, 10min each were alternated with 15min of normoxic ventilation in UCP-2$^{-/-}$ [n=5] and WT mice [n=7]. Bars represent mean ± SEM (A) Baseline PAP (mmHg) recorded before the first (1) and last (6) hypoxic maneuver. (B) Change in isolated organs' weight (mg) during the experiment.

3.1.2 Response to repetitive stimulation with U46619

To further investigate the higher pressure response to hypoxia in UCP-2$^{-/-}$ animals, another vasoconstrictor stimulus was applied and the resulting pressure increase monitored. Repetitive short-time infusions (1min and 30s) of the thromboxane A_2 mimetic U46619 were tested in isolated lungs while ventilated with a normoxic gas mixture. Dosage was designed to trigger a pressure response similar to that caused by HPV in WT mice. As depicted in figure 3-3 A, B and C, the Δ-PAP, baseline PAP and weight gain, respectively, were measured in both UCP-2$^{-/-}$ [n=5] and WT mice [n=5] during six cycles of repetitive thromboxane infusion, each containing 15ng of U46619. In this experiment UCP-2$^{-/-}$ mice did not react significantly different from WT mice. Baseline PAP and isolated organs' weight gain during these experiments were not significantly distinct.

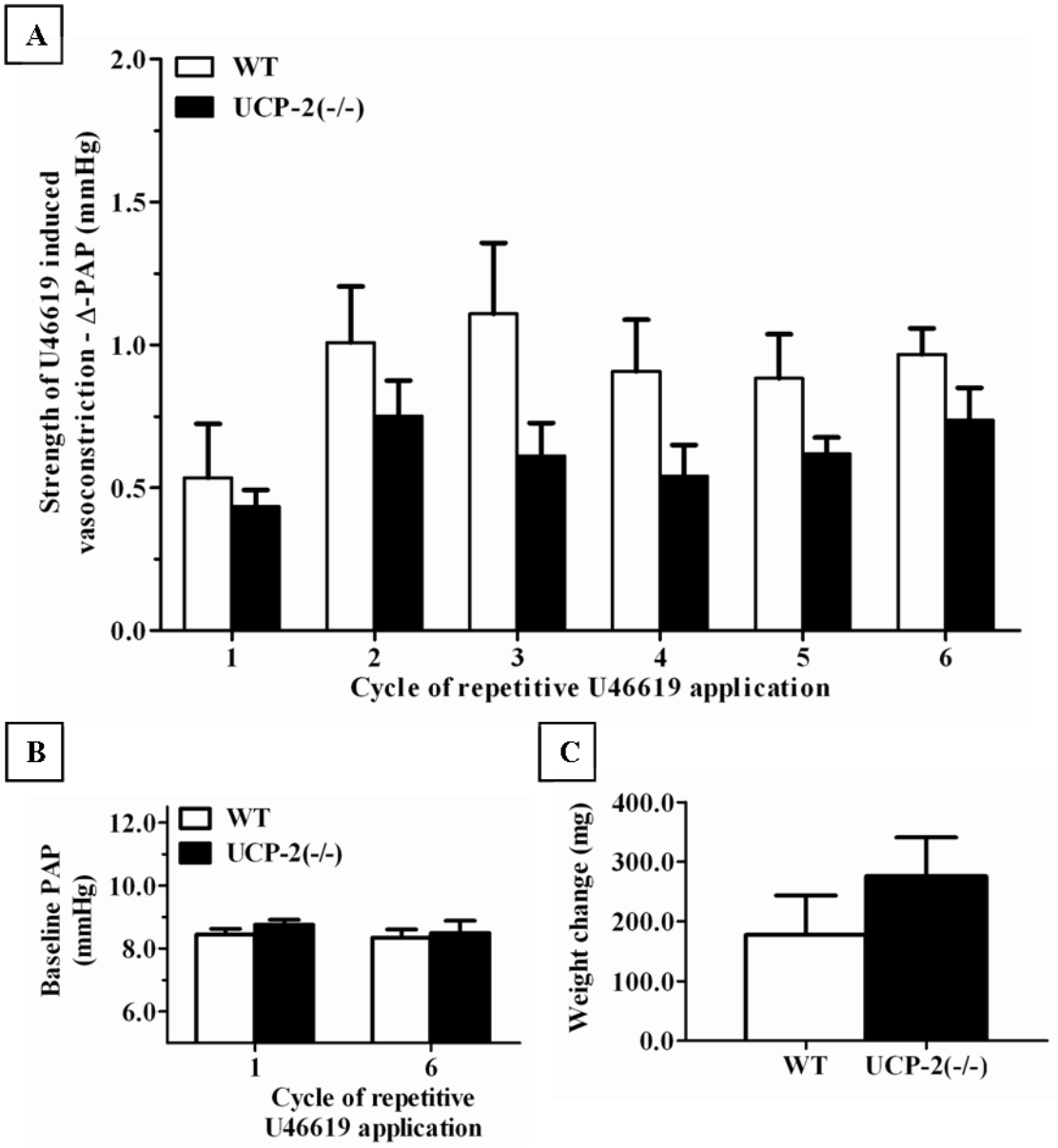

Fig. 3-3: PAP response to repetitive stimulation with the thromboxane mimetic U46619 in UCP-2$^{-/-}$ and WT mice. Six cycles of thromboxane infusion (10ng/min) each lasting 1min and 30s, equivalent to a dose of 15ng U46619, were applied to UCP-2$^{-/-}$ [n=5] and WT mice [n=5]. Bars represent mean ± SEM. (A) Maximum Δ-PAP from corresponding baseline for each application. (B) Baseline PAP recorded before the first (1) and the last (6) application of U46619. (C) Change in isolated organs' weight during the course of the experiment.

3.1.3 Response to sustained hypoxic and normoxic ventilation

Investigations in UCP-2$^{-/-}$ mice regarding their different HPV characteristics compared to WT mice were continued in an experimental setup applying prolonged hypoxia. Mice of both genotypes were assigned to hypoxic treatment (HOX) and normoxic treatment (NOX) groups: During HOX protocol one cycle of hypoxic / normoxic ventilation (cf.

chapter 3.1.1) was followed by three hours of sustained hypoxia. Experiments were completed by another cycle of normoxic / hypoxic ventilation. The members of NOX groups were ventilated with normoxic gas throughout the entire experiment lasting 200min.

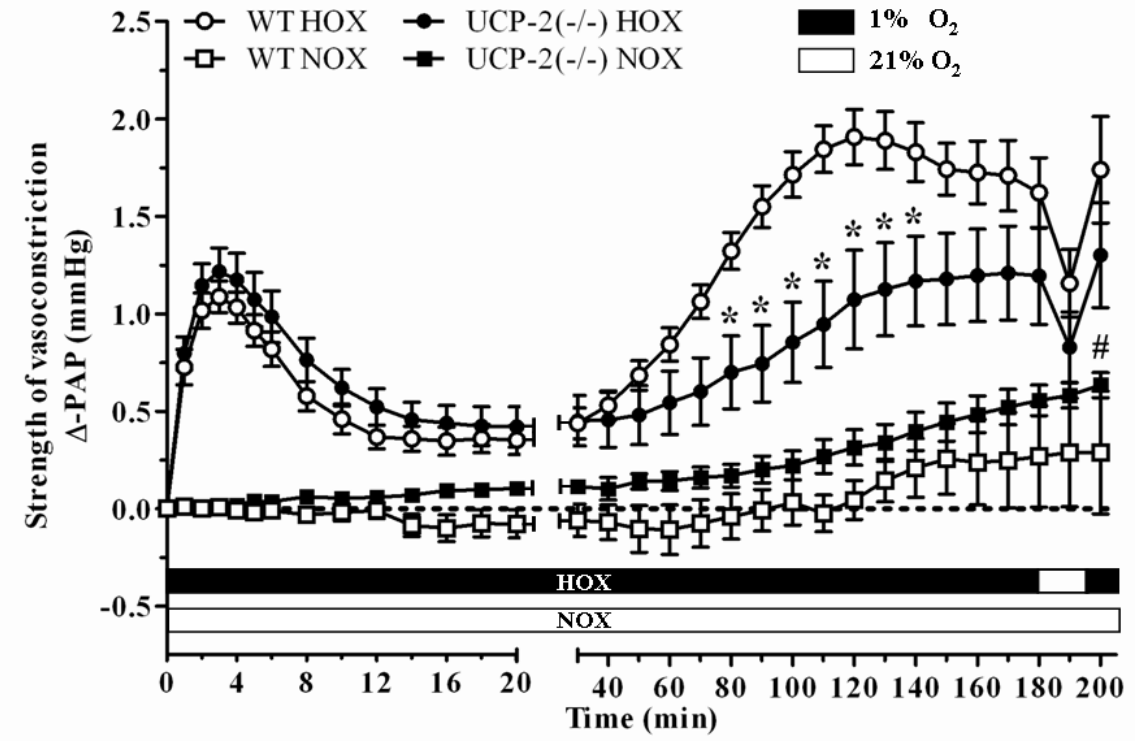

Fig. 3-4: Δ-PAP during sustained hypoxic and normoxic ventilation. Data are presented as changes in PAP from normoxic baseline at time point "zero" (Δ-PAP – mmHg) plotted against time. Curves labelled HOX reflect changes during three hours of sustained hypoxia and a following cycle of normoxic and hypoxic ventilation in both UCP-$2^{-/-}$ [n=9] and WT mice [n=9]. For the NOX group the changes during sustained normoxic ventilation in UCP-$2^{-/-}$ [n=6] and WT mice [n=5] are plotted similar. Data are shown as mean ± SEM, * = $p<0.05$ comparing WT HOX and UCP-$2^{-/-}$ HOX, # = $p<0.05$ comparing WT NOX and UCP-$2^{-/-}$ NOX. Significant differences comparing HOX and NOX treatment are not indicated.

Figure 3-4 illustrates the course of PAP changes during HOX and NOX ventilation after the first 40min of the experimental protocol, this time point is called time point "zero". The initial cycle of alternating hypoxic / normoxic (HOX –group) as well as the initial 40min of normoxic ventilation (NOX –group), respectively, are not shown for clarity reasons (cf. figure 2–5). WT HOX [n=9] and UCP-$2^{-/-}$ HOX [n=9] pressure registrations proceeded in a similar pattern with a fast increase and following decline in PAP during the initial 20min of sustained hypoxia. Pressure levels did not return to baseline under

hypoxic ventilation, but entered a phase of slow and steady increment referred to as sustained phase of HPV. When switched to normoxic ventilation at time point 180min, PAP decreased rapidly, but remained elevated compared to the PAP of the normoxic groups for the corresponding time points. UCP-2 deficient mice demonstrated similar characteristics, but the magnitude of the sustained HPV response was altered. UCP-$2^{-/-}$ mice demonstrated a significantly lower sustained HPV compared to WT mice between 80 and 140min of hypoxic ventilation. At 110min pressure values were 1.0 ± 0.2mmHg for UCP-$2^{-/-}$ and 1.8 ± 0.1mmHg for WT mice. PAP in mice ventilated with normoxia was significantly higher at time point 200min in UCP-$2^{-/-}$ mice (0.7 ± 0.1mmHg) compared to WT mice (0.3 ± 0.3mmHg). Comparing NOX and HOX treatment in the same genotype, PAP was significantly different from minute 1 to 8 for both WT and knock-out mice and again from minute 50 to 200 in WT, but only between 100 and 160min in UCP-$2^{-/-}$ animals. In respect to the figures' clarity this statistic is not included in figure 3-4.

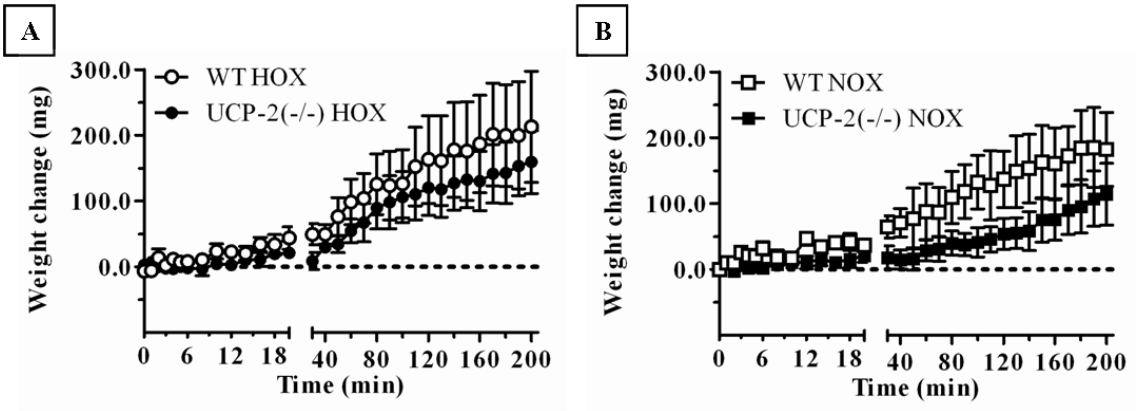

Fig. 3-5: Weight change during sustained hypoxic and normoxic ventilation. Isolated organs' changes in weight (mg) during sustained ventilation with (A) hypoxia in both UCP-$2^{-/-}$ [n=9] and WT mice [n=9] or (B) normoxia in UCP-$2^{-/-}$ [n=6] and WT mice [n=5]. Data is presented as mean ± SEM.

Figure 3-5 exhibits the change in weight during (A) hypoxic and (B) normoxic treatment. There was no significant difference in weight gain comparing UCP-$2^{-/-}$ and WT mice during HOX and NOX treatment as well as comparing weight gain between HOX and NOX treatment in the individual genotype .

3.1.4 Response to sustained stimulation with U44619

Analogous to the short term application of U46619 for comparison with acute HPV, this substance was used for induction of prolonged vasoconstriction, and the resulting PAP responses were monitored and compared between WT and UCP-2$^{-/-}$mice. Infusion dosage was determined in pre-tests using WT mice and was intended to generate a persistent increase in PAP in similar dimensions like sustained HPV. Figure 3-6 demonstrates PAP characteristics of WT [n=7] and UCP-2$^{-/-}$ [n=7] mice during the continuous infusion of U46619.

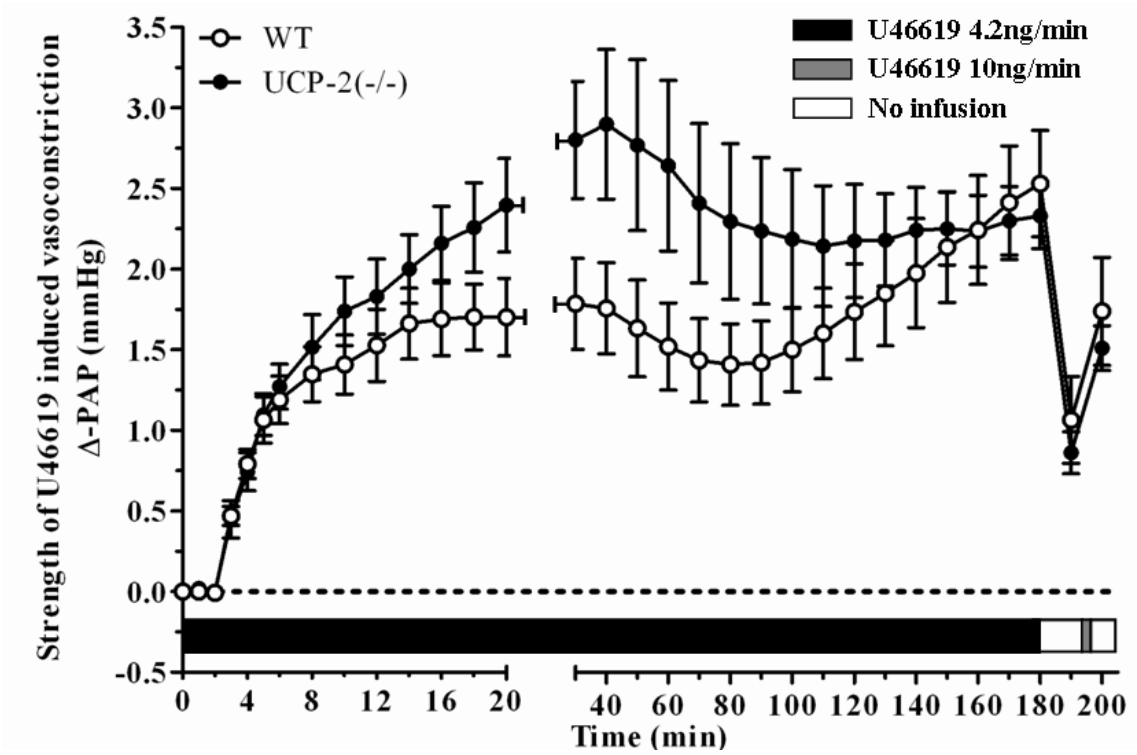

Fig. 3-6: PAP characteristics during sustained infusion of thromboxane mimetic U44619. Data are presented as changes in PAP from baseline (Δ-PAP in mmHg) plotted against time. Curves reflect changes during three hours infusion of the thromboxane mimetic U44619 (4.2ng/min), an infusion free interval of 15min and a final bolus of 15ng U46619 for 1min and 30s (10ng/min). Data of WT [n=7] and UCP-2$^{-/-}$ [n=7] mice are presented as mean ± SEM.

PAP course is plotted from the moment the sustained infusion was started, this time point was defined as "zero". A single bolus of 15ng was given during the initial 40 minutes before the sustained infusion was started (data not shown). Infusion was stopped after 180min and the experiment completed with another 15ng bolus of U46619 at time point 195min. PAP began to increase about 2min after the start of the infusion with

similar kinetics in both mouse strains. The pressure responses to U46619 showed a higher variability compared to the pressure characteristics in HPV and the difference between UCP-2$^{-/-}$ and WT mice did not reach a statistically significant level. Likewise weight gain did not differ significantly as depicted in figure 3-7.

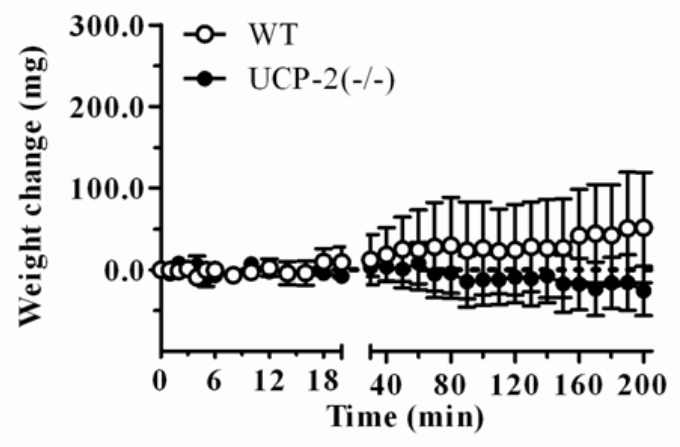

Fig. 3-7: Weight change during sustained infusion of thromboxane mimetic U44619. Isolated organs' changes in weight (mg) during infusion of thromboxane for both WT [n=7] and UCP-2$^{-/-}$ [n=7] mice presented as mean ± SEM.

3.2 Chronic hypoxia

Different parameters reflecting adaptation and remodelling of the cardiovascular system during prolonged exposure to normobaric hypoxia were compared in WT and UCP-2$^{-/-}$ mice.

3.2.1 Right ventricular systolic pressure

RVSP was measured under general anaesthesia using a closed chest catheter technique in both WT and UCP-2$^{-/-}$ mice which had been exposed to hypoxic or normoxic atmosphere. Randomly assigned mice of both genotypes were held either under a normobaric atmosphere with normoxic oxygen concentrations of 21% (NOX) or were exposed to a normobaric atmosphere containing 10% oxygen (HOX) over four weeks. As illustrated in figure 3-8 both mouse strains demonstrated a statistically significant increase of RVSP comparing exposure to hypoxia with exposure to normoxia. Examining the impact of genotypes a significant difference was found comparing animals exposed to hypoxic conditions but not after normoxic exposure. WT NOX [n=7]: 25.5 ± 1.0mmHg

and WT HOX [n=7]: 37.8 ± 1.2mmHg compared to UCP-2$^{-/-}$ NOX [n=7]: 26.4 ± 1.3mmHg and UCP-2$^{-/-}$ HOX [n=7]: 44.6 ± 2.0mmHg.

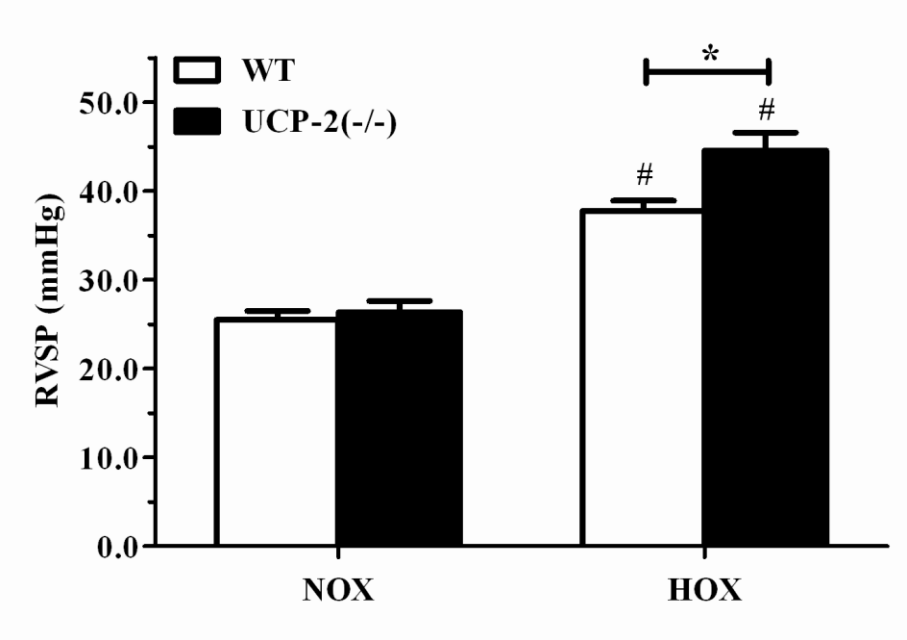

Fig. 3-8: RVSP after exposure to hypoxia and normoxia. Mice of different genotypes were exposed to a reduced, normobaric FiO_2 of 0.10 referred to as HOX group: WT [n=7] and UCP-2$^{-/-}$ [n=7] or held at a normal atmospheric, normobaric FiO_2 of 0.21 labelled NOX group: WT mice [n=7] and UCP-2$^{-/-}$ [n=7]. RVSP (mmHg) recorded after treatment using a closed chest catheter technique under general anesthesia and positive pressure ventilation with room air. Bars represent mean ± SEM, * = $p<0.05$ comparing WT and UCP-2$^{-/-}$, # = $p<0.05$ comparing HOX and NOX treatment in the same genotype. **RVSP measurements were performed in cooperation with Nirmal Parajuli.**

3.2.2 Heart ratio

Heart ratio, presented as weight proportion of the separated and dried animal organ (RV * 100 / [LV + ventricular septum]), can be used as a parameter to evaluate cardiac adaptation to changes in pulmonary vascular resistance and pressure. It was determined in WT and UCP-2$^{-/-}$ mice previously held under hypoxic as well as those held under normoxic conditions. As illustrated in figure 3-9 both strains of mice demonstrated statistically significant increase of heart ratio induced by hypoxia. WT NOX [n=7]: 27 ± 2% compared to WT HOX [n=7]: 37 ± 1% and UCP-2$^{-/-}$ NOX [n=7]: 29 ± 2% compared to UCP-2$^{-/-}$ HOX [n=7]: 37 ± 2%. Heart ratio in UCP-2$^{-/-}$ mice was not significantly different from WT mice under normoxic or hypoxic conditions. There was no significant difference in the absolute value of the LV weight in respect to genotype or exposure: WT

NOX [n=7]: 17.4 ± 0.5mg, WT HOX [n=7]: 17.4 ± 0.5mg, UCP-2$^{-/-}$ NOX [n=7]: 18.6 ± 0.6mg and UCP-2$^{-/-}$ HOX [n=7]: 17.8 ± 1.1mg (data not depicted).

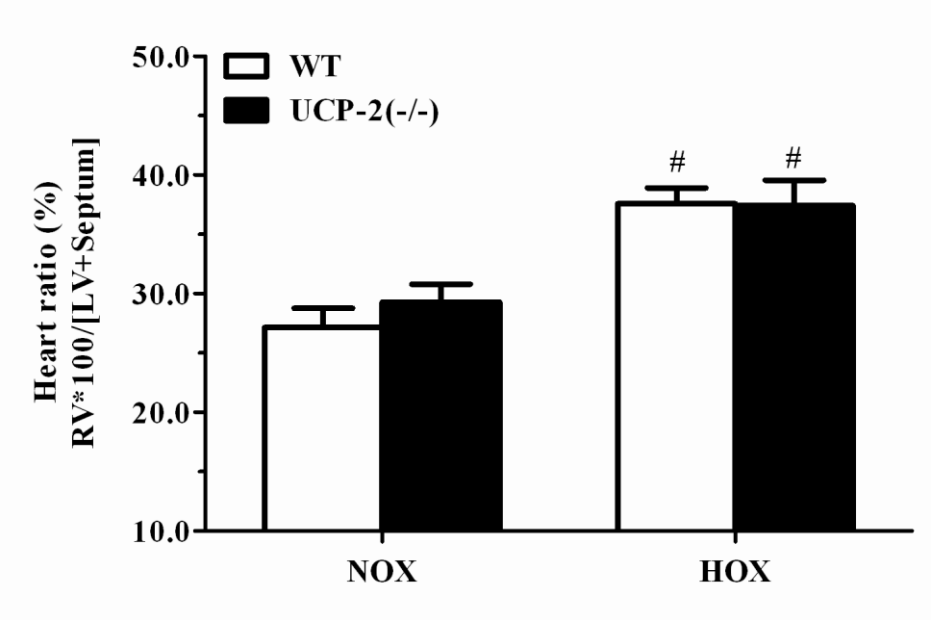

Fig. 3-9: Heart ratio after exposure to hypoxia and normoxia. Mice of different genotypes were exposed to a reduced, normobaric FiO_2 of 0.10 referred to as HOX group: WT [n=7] and UCP-2$^{-/-}$ [n=7] or held at a normal atmospheric, normobaric FiO_2 of 0.21 labelled NOX group: WT mice [n=7] and UCP-2$^{-/-}$ [n=7]. Heart ratio (%) determined after these treatments. Bars represent mean ± SEM, # = $p<0.05$ comparing HOX and NOX treatment in the same genotype.

3.2.3 Morphometric analysis of lung vasculature

Morphometric analysis of pulmonary vessels in immunohistochemically double stained lung tissue was conducted for both WT and UCP-2$^{-/-}$ mice held under normoxic and hypoxic conditions. Examples of the staining results are given in figure 3-10. For each animal approximately 80 vessels of different outer diameters (85% small [20 to 70µm], 10% medium [70-150µm] and 5% large [>150µm]) were categorized in nonmuscularized, partially muscularized or fully muscularized. The categories' fraction of total vessel count is shown in figure 3-11. Comparison of WT and UCP2$^{-/-}$ mice during NOX treatment revealed a statistical significant difference in vessel muscularization between WT and UCP-2$^{-/-}$ animals. Fraction of fully and partially muscularized vessels was higher in UCP-2$^{-/-}$ mice while the number of nonmuscularized vessels was reduced accordingly. UCP-2$^{-/-}$ NOX [n=7]: fully 12.6 ± 1.3%, partially 60.4 ± 0.5% and nonmus-

cularized 27.1 ± 1.2% compared to WT NOX [n=7]: fully 4.1 ± 0.8%, partially 46.5 ± 1.0% and nonmuscularized 49.4 ± 1.3%.

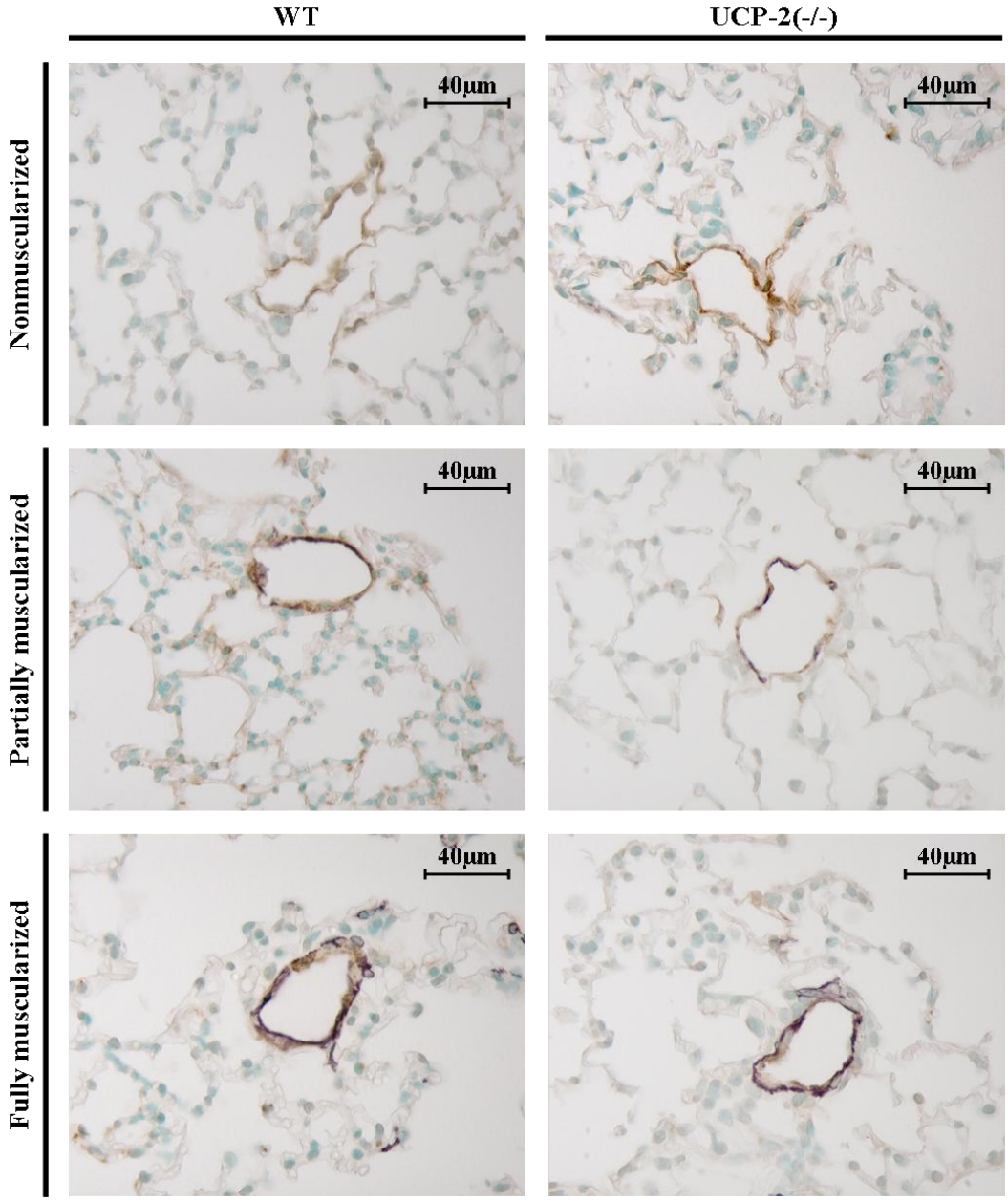

Fig. 3-10: Example of immunohistochemically double stained lung tissue. Endothelium of pulmonary arteries is positive for von Willebrand factor staining (brown), α- smooth muscle actin labelling (violet) depends on the amount of muscularization. As an example a single small vessel (outer diameter 20-70µm) from each class of muscularization is shown for both WT and UCP-$2^{-/-}$ mice.

There was no significant difference between WT and UCP-$2^{-/-}$ mice in the HOX group. Numbers of fully muscularized vessels were significantly increased and nonmuscular-

ized vessels significantly decreased in both mouse strains comparing hypoxic and normoxic exposure.

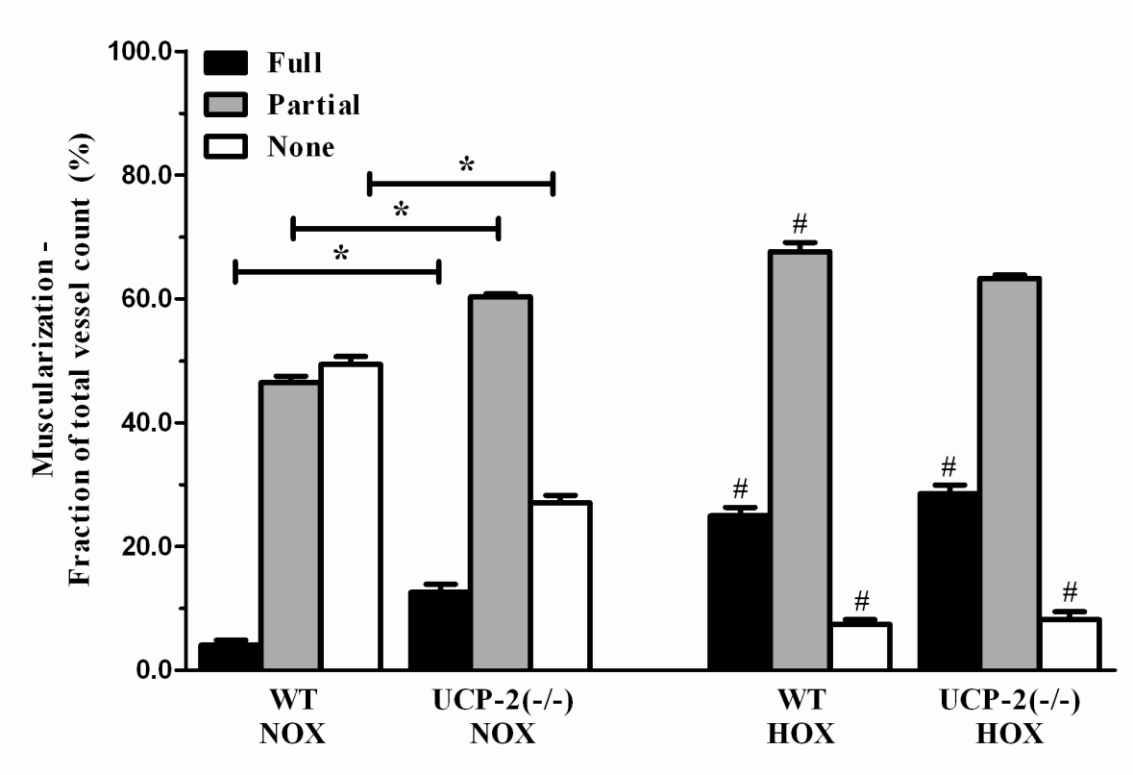

Fig. 3-11: Vessel morphometry after exposure to hypoxia or normoxia. Mice of different genotypes were exposed to a reduced, normobaric FiO_2 of 0.10 referred to as HOX group (WT [n=7] and UCP-$2^{-/-}$ [n=7]) or held at a normal atmospheric, normobaric FiO_2 of 0.21 labelled NOX group (WT mice [n=7] and UCP-$2^{-/-}$ [n=7]). Lung vessel morphometry determined after these treatments revealed the fraction of the three muscularization categories from total vessel count. Bars represent mean ± SEM, * = $p<0.05$ comparing WT and UCP-$2^{-/-}$, # = $p<0.05$ comparing HOX and NOX treatment in the same genotype. **Performance of vessel counting was supported by Adel Bakr.**

3.2.4 Body weight and growth

Measurement of body weight was conducted previous to and after the exposure period, before sacrificing the animals for the experiments specified in chapters 3.2.1 –3.2.3. Results (body weight in g) at the specified time points and the calculated growth or change in weight (g) are shown in figure 3-12. WT NOX [n=7]: before exposure 21.6 ± 1.3g / after exposure 24.5 ± 1.2g and WT HOX [n=7]: before exposure 21.1 ± 0.9g / after exposure 22.6 ± 0.6g compared to UCP-$2^{-/-}$ NOX [n=7]: before exposure 22.2 ± 0.9g / after exposure 26.2 ± 1.1g and UCP-$2^{-/-}$ HOX [n=7]: before exposure 22.4 ± 0.8g

/ after exposure 22.4 ± 1.1g. There was no statistically significant difference in body weight between mice assigned to any of the groups or any significant difference in growth during the experiment.

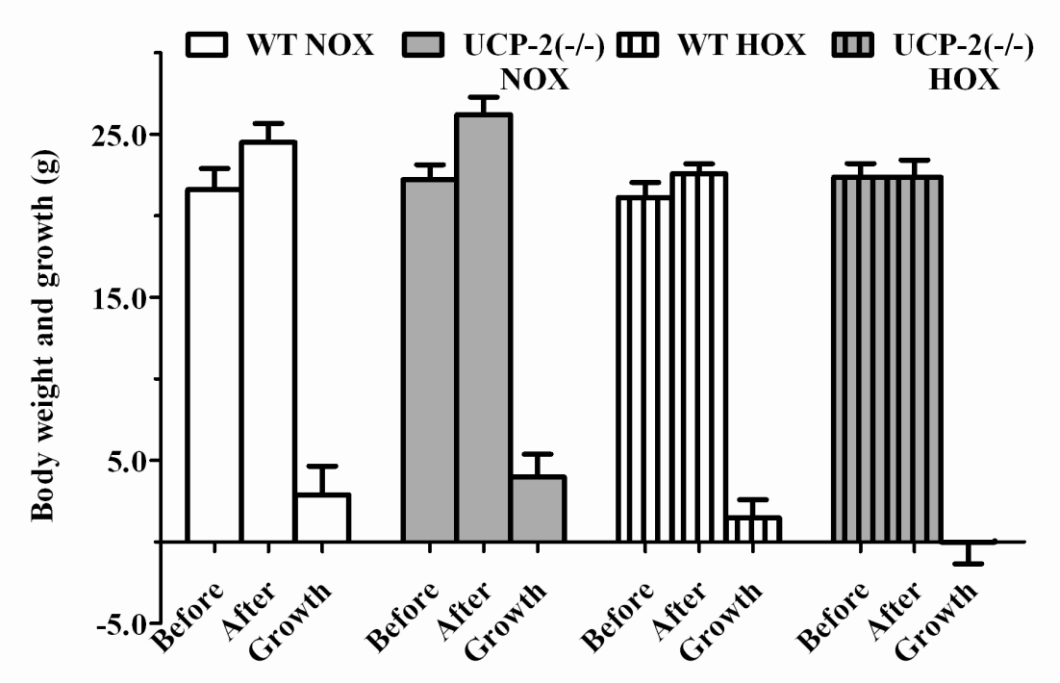

Fig. 3-12: Body weight of animals before and after exposure to hypoxia and normoxia. Mice of different genotypes were exposed to a reduced, normobaric FiO_2 of 0.10 referred to as HOX group (WT [n=7] and UCP-$2^{-/-}$ [n=7]) or held at a normal atmospheric, normobaric FiO_2 of 0.21 labelled NOX group (WT mice [n=7] and UCP-$2^{-/-}$ [n=7]). Mice were weighed before and after exposure and resulting growth calculated as difference between the weight after exposure minus the body weight before exposure. Bars represent mean ± SEM.

3.2.5 Hematocrit

Measurement of hematocrit was performed after completion of RVSP measurement or during the procedure of lung fixation for vessel morphometry. Results (hematocrit in %) are shown in figure 3-13 as a box-and-whiskers plot. Both WT and UCP-$2^{-/-}$ mice exposed to hypoxia had a statistically significant higher hematocrit: WT HOX [n=6]: 60 ± 3% and UCP-$2^{-/-}$ HOX [n=6]: 56 ± 4% compared to mice exposed to normoxia: WT NOX [n=5]: 37 ± 2% and UCP-$2^{-/-}$ NOX [n=5]: 39 ± 5% There was no statistically significant difference in hematocrit as a function of the genotype.

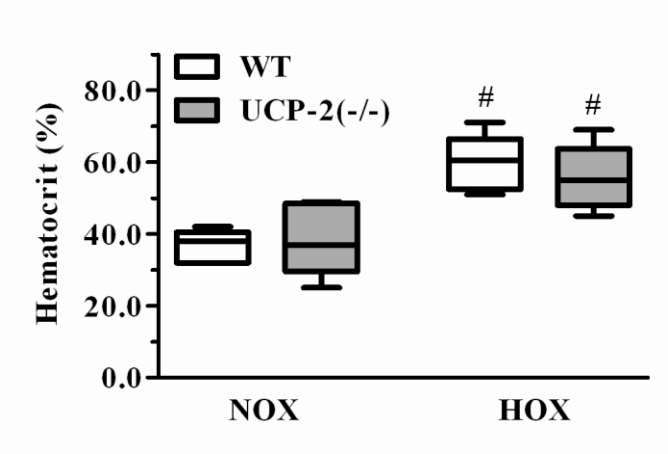

Fig. 3-13: Hematocrit of animals exposed to hypoxia and normoxia. Mice of different genotypes were exposed to a reduced, normobaric FiO_2 of 0.10 referred to as HOX group or held at a normal atmospheric, normobaric FiO_2 of 0.21 labelled NOX group. Hematocrit (%) distribution of HOX group (WT [n=6] and UCP-$2^{-/-}$ [n=6]) and NOX group (WT mice [n=5] and UCP-$2^{-/-}$ [n=5]) is shown as a box-and-whiskers plot.

4 Discussion

4.1 Discussion of the study limitations

The sub-cellular pathways underlying HPV, especially the mechanism of oxygen sensing but also the downstream processes leading to the lung's adaptation during hypoxia have not been sufficiently clarified yet. UCP-2 is a mitochondrial protein that is linked to some of the important mediators of HPV, but was, according to the best of my knowledge, never studied in regard to its function in this mechanism. The availability of UCP-$2^{-/-}$ mice and specific physiological techniques offered the chance to investigate the contribution of this protein to the processes of acute and sustained HPV as well as to pulmonary vascular remodelling and PH induced by chronic hypoxia. As this study is based on experiments with intact animals as well as isolated organs, it offers several advantages (cf. chapter 1.2 and 1.5), but also includes considerable limitations. Due to their "loss of function phenotype", studies using knock-out mice may avoid some of the major drawbacks that result from the usage of pharmacological inhibitor. Ideally these experiments demonstrate the impact of the UCP-2 gene on important physiological characteristics of HPV. This would imply that the difference between the genetically altered and WT mouse strain is restricted to the presence or absence of this individual target gene. This state can only be approximated in our experimental setups even though we applied the standard practice of using a knock-out mouse strain developed from blastocytes of the same strain of mice as the control animals (cf. chapter 2.1). For example it has been reported that the characteristic of improved glucose tolerance in UCP-$2^{-/-}$ mice depends on other strain related variables, as the original finding could not be reproduced in backcrossed UCP-$2^{-/-}$ mice [136].

As sensitive, interference-prone experiments were performed and small amplitudes of physiological parameters were compared, technical issues need to be addressed as well: It is known from studies conducted in the same laboratory as was this thesis and it has been reported for similar experiments, that the quality and time of the preparation as well as the presence of haemoglobin in the buffer fluid can affect the magnitude of the vasoconstrictor responses [107,206]. Furthermore the investigator was not blinded in regard to the genetic identity of the animals while performing the isolated buffer-perfused lung

experiments. To prevent systematic errors the experimental procedures were standardized and inclusion criteria were established (cf. chapter 2.3.1). To minimize effects arising from changes in the performance of the investigator, or factors like air pressure and room temperature, the timetable was outlined to alternate measurements of the genetically altered and wild type animals.

Finally it should be taken into account that UCP-2 is only a single member of the UCP family and there are marked local, structural and functional adjacencies especially to UCP-3 [104]. Even though we do not have any indications for this event, it remains conceivable that the deficit of UCP-2 is compensated by UCP-3 or other mechanisms as congenital UCP-$2^{-/-}$ mice were investigated.

4.2 Considerations regarding the interpretation of the results

The maybe most important issue regarding the interpretation and the integration of the results is, however, the incomplete characterization of the basic function of the UCP-2 protein itself. In an experimental setup measuring the reactivity of an intact organ or a complete animal, general difficulties in the act of interpretation occur. On account of the used methodology it is not overall possible to separate effects that act directly in the pulmonary vessels from indirect effects induced by systemic alterations by the knockout of UCP-2. In this regard the UCP-2 protein may exert its effects on the pulmonary vasculature by its local uncoupling activity, but could also influence pulmonary vasculature by its known property to regulate the plasma insulin level. The observed distinctive phenotype in the UCP-$2^{-/-}$ mouse strain might principally be based on a direct modification in mitochondrial metabolism in the PASMC, as well as on the changes in insulin secretion or the associated plasma glucose levels. This latter mechanism is however largely excluded in the isolated and buffer-perfused and ventilated lung preparation. However, an interpretation focusing solely on the initially stated uncoupling theory might be inappropriate, as this hypothesis was repeatedly challenged. At least two, more recent, hypothesis, one suggesting an important role for the UCPs in the mitochondrial calcium [180] and the other an impact on the cellular glucose metabolism [24] need to be addressed accordingly. This discussion is intended to offer an interpretation of the study results by demonstrating possible links between the best characterized UCP-2 functions

and the sensor, mediator and effector pathways in HPV. Additional studies are needed to support or falsify this hypothesis and to establish the relationships of cause and effect on the cellular and sub-cellular level as well as to reliably localize UCP-2.

4.3 Effect of UCP-2 on acute HPV

In this study the strength of acute HPV in WT and UCP-$2^{-/-}$ mice following repetitive hypoxic stimulation is compared using an isolated, artificially ventilated and buffer-perfused mouse lung model. UCP-$2^{-/-}$ mice depicted an intensified PAP increase, while baseline pressures during normoxic ventilation periods in these experiments were similar to those of WT mice. To evaluate the specificity of the increased pulmonary vasoconstriction of the UCP-$2^{-/-}$ mice to acute hypoxia, repetitive stimulations with the thromboxane A_2 mimetic - U46619 were conducted in an otherwise comparable procedure. These experiments showed a tendency towards lower PAP responses in UCP-$2^{-/-}$ mice, but overall without statistically significant differences. The hereby stimulated thromboxane A_2 (TXA_2)– receptors are G-protein-coupled receptors and have been suggested to enable cellular Ca^{2+} mobilization via activation of the second messenger systems IP_3 and DAG and through Ca^{2+} sensitization via regulation of myosin light chain kinase, Rho and Rho-kinase [82,86,114,154]. Furthermore in mesenteric arteries the effect of U46619 depends on the activity of VOCC as well as SOCC [68]. As UCP-2 deletion leads to different changes in PAP characteristics, depending on the applied trigger, acute hypoxia versus U46619, it can be concluded that the mechanism of acute HPV becomes altered in a specific manner and that these changes are not caused by a general increase in pulmonary vascular contractility. Additionally it suggests that, assumed the effector pathway in the TXA_2-mediated contraction relies on processes similar to those of HPV, e.g. the intracellular calcium increase, the UCP-2 protein influences the upstream signalling pathways and is therefore related to the processes of oxygen sensing or other HPV specific parts of the further upstream mediator system. Studies using different ETC inhibitors as well as PA myocytes lacking mitochondrial DNA, indicated the dependence of the HPV mechanism, but the independence of U46619-mediated contractions, on a properly functioning mitochondrial metabolism [192].

Weight change of the isolated organ is interpreted as a control value to estimate the extent of lung edema formation during the experiments, as it is known that fluid accumulation can alter the vasoconstrictor response [202]. UCP-2$^{-/-}$ mice showed no statistically significant difference regarding weight change in both, the repetitive hypoxia and the U46119 experiments. Thus an important difference in vascular permeability for the observed effects can be excluded.

There are several possible mechanisms of how UCP-2 might influence PAP under hypoxia: 1) UCP-2 increases vessel muscularization, (cf. chapter 3.2.3 and discussion in chapter 4.2) and increases unspecific pulmonary vasoconstriction. This possibility was excluded, as U46619-induced vasoconstriction was not increased in UCP-2$^{-/-}$ mice compared to WT mice. 2) UCP-2 is active under normoxic conditions and deletion causes generally increased pulmonary vascular tone. This view is supported by the fact that PAP was increased in sustained normoxic experiments at late time points when comparing UCP-2$^{-/-}$ and WT mice (cf. chapter 3.1.3). However, in acute HPV the normoxic baseline PAP values between repetitive hypoxic maneuvers did not differ, and in vivo there was no significantly higher RVSP in mice held under normoxic conditions, comparing UCP-2$^{-/-}$ and WT mice (cf. chapter 3.2.1). It needs to be added that in a just recently published study performed in the same laboratory as was this thesis, RVSP and heart ratio were found to be statistically elevated comparing UCP-2$^{-/-}$ and WT mice under normoxia [134]. 3) UCP-2 is active under normoxic conditions, but only a second hypoxia-induced stimulus, that is influenced by UCP-2, e.g. ROS, results in increased PAP. 4) UCP-2 function is directly activated by hypoxia and attenuates HPV. 5) UCP-2 function is activated indirectly by hypoxia. Hence, the following discussion will focus on factors that may be released in hypoxia and regulated by UCP-2, as well as mechanisms of direct or indirect modulation of UCP-2 function in acute hypoxia.

4.3.1 Uncoupling function of UCP-2

A reasonable interpretation of the current results connects the hypothesis of an increasing ROS production serving as trigger of HPV and the assumed uncoupling function of UCP-2. Through protonophoric activity the UCP-2 protein could be able to decrease Δp and also restrict the rise in ROS production during acute HPV [49]. A dependency between

Δp and ROS production is established under certain conditions [93,99]. A mild uncoupling mediated by the activity of UCP may decrease ROS production [128] and an elevated ROS production was already demonstrated in macrophages isolated from UCP-2$^{-/-}$ mice [13]. In previous studies, the chemical uncoupler DNP increased PAP during normoxia and/or augmented the effect of hypoxia when applied at lower concentrations [20,108,204] but inhibited HPV and decreased baseline PAP at higher concentrations [204]. One of the cited publications further addressed the dose-dependent effect of the substance and its relation to normoxic and hypoxic ventilation [204]. Normoxic PAP rose after administration of DNP at concentrations between 10 and 100µM, but declined at 200µM [204]. A following hypoxic stimulus was found - not significantly - elevated at 10µM but significantly attenuated at 70, 100 and 200µM [204]. It is interesting to note that pressure responses due to the application of U46619 were on the other hand significantly elevated under 70µM (and non- significantly under 10 and 100µM) of DNP [204]. It can be concluded that uncoupling induced by this substance, in a certain concentration range, had an opposite effect than the knock-out of UCP-2, supporting an uncoupling function for this protein.

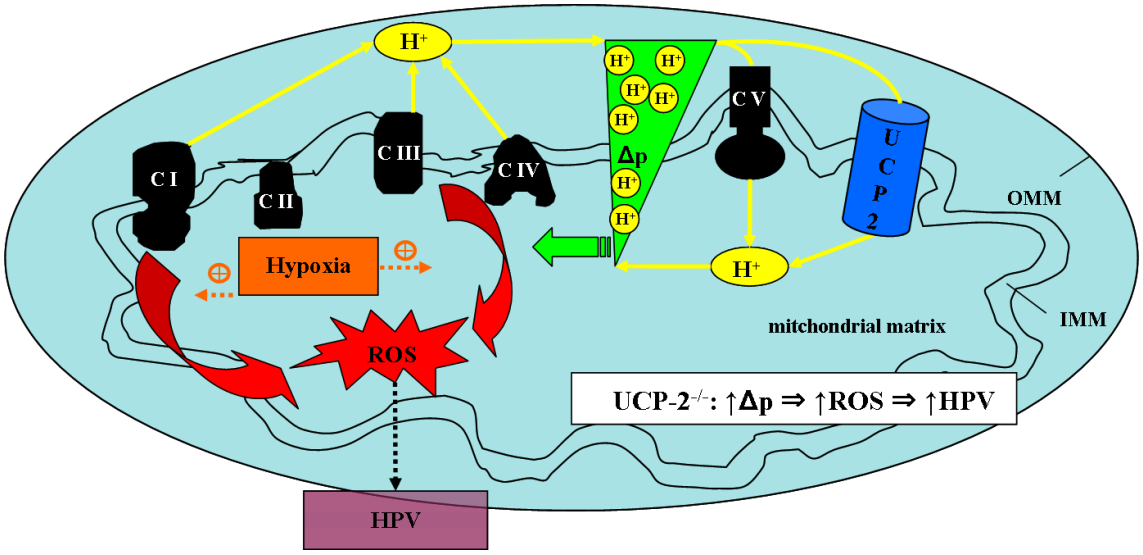

Fig. 4-1: Possible model of UCP-2 functioning as a protonophore. Absence of UCP-2 in UCP-2$^{-/-}$ mice reduces uncoupling, increases ROS production and HPV. CI – CIV: respiratory chain complexes I – IV, CV: ATP synthase, Δp: mitochondrial protonmotive force, H^+: hydrogen ion, HPV: hypoxic pulmonary vasoconstriction, IMM: inner mitochondrial membrane, OMM: outer mitochondrial membrane, ROS: reactive oxygen species.

In contrast to these results, another study described that the mitochondrial protonophore carbonyl cyanide m–chlorophenyl–hydrazone (CCCP) increased the hypoxia and also

the caffeine-induced rise in $[Ca^{2+}]_c$, what was interpreted as disruption of the mitochondrial Ca^{2+} buffering capacity due to uncoupling [90] (cf. chapter 4.3.2). The finding of contrary effects, depending on the applied dosage or the kind of uncoupling substance, might be caused by the complex influence of Δp on the mitochondrial metabolism. A direct and positive relationship between Δp and the generation of ROS might only exist in certain limits or under certain conditions, while outside these limits other effects for example the calcium handling could play a more important role. A recent study conducted in cardiomyocytes and isolated mitochondria addressed the complex interaction of Δp, redox potentials and oxidative stress and provided evidence that in intact cells uncoupling due to the chemical uncoupler FCCP leads to increase of ROS at particular low and particular high concentrations [6]. This hypothesis integrates both, the influence of high redox potentials and of cellular radical detoxification systems, on ROS balance and could therefore explain opposite effects of uncoupling [6]. In this regard it has also been noted that short mitochondrial depolarization mediated by the mitochondrial permeability transition pore (PTP) can lead to a burst of mitochondrial ROS through a yet unrevealed mechanism [66].

4.3.2 Mitochondrial calcium handling

Considering the suggested role for UCP-2 and UCP-3 in the mitochondrial calcium uniport [180], a UCP-2 deficient phenotype might have an impaired mitochondrial Ca^{2+} buffering capacity as well as an increased $[Ca^{2+}]_c$ and an amplified vasoconstrictor response following hypoxic stimulation, as observed in this study. UCP-$2^{-/-}$ mitochondria could also hypothetically exhibit an increased ROS production assuming that a reduced Δp, which might be based on a decreased mitochondrial Ca^{2+} uptake and a consecutive reduction in the dependent Ca^{2+}/Na^+ and Na^+/H^+ exchange over the inner mitochondrial membrane, is of greater importance compared to the described positive Ca^{2+} dependency of ROS production [29]. As mitochondria play an important role in calcium buffering [62], a reduced Ca^{2+} buffering capacity or slower buffering kinetics might explain the observation of an amplified acute HPV in UCP-$2^{-/-}$ mice. Unfortunately mitochondrial Ca^{2+} homeostasis in PASMC is not well characterized, especially its interaction with the $[Ca^{2+}]_c$ under hypoxia. Thus there is little evidence to suggest a different importance of the calcium buffering mechanism for hypoxia triggered vasoconstriction compared to

thromboxane-induced vasoconstriction that would be necessary to explain the findings of this thesis.

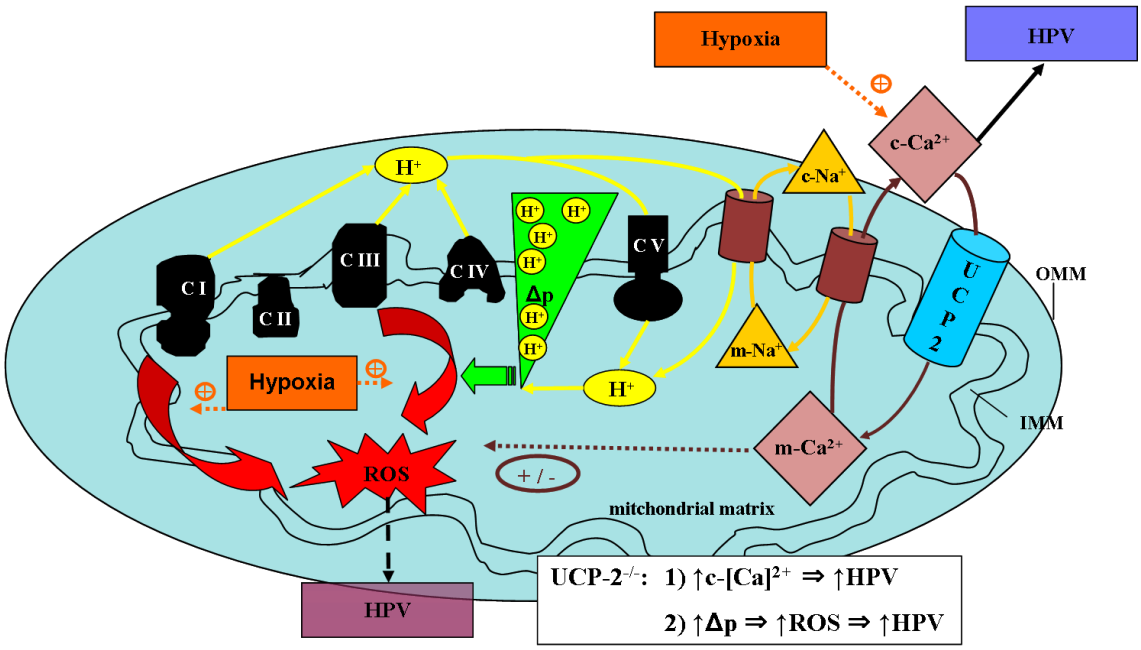

Fig. 4-2: Possible model of UCP-2 functioning as an essential part of the mitochondrial calcium uniporter. Absence of UCP-2 in UCP-$2^{-/-}$ mice leads to decreased calcium uptake into the mitochondria and a higher calcium concentration in the cytoplasm. Uncoupling is reduced and increases ROS production and HPV. CI – CIV: respiratory chain complexes I – IV, CV: ATP synthase, c-Ca^{2+}: cytoplasmic calcium, c-Na^{+}: cytoplasmic sodium, Δp: mitochondrial proton-motive force, H^{+}: hydrogen ion, HPV: hypoxic pulmonary vasoconstriction, IMM: inner mitochondrial membrane, m-Ca^{2+}: mitochondrial calcium, m-Na^{+}: mitochondrial sodium, OMM: outer mitochondrial membrane, ROS: reactive oxygen species.

4.3.3 UCP-2 functioning as a metabolic switch

The so called metabolic theory of UCP-2 is also well suited to explain the increased strength of acute HPV in UCP-$2^{-/-}$ mice. According to Bouillaud et al., UCP-2 and 3 might act as negative regulators of pyruvate uptake into the mitochondria and change the ratio of anaerobic and aerobic glucose utilization [24]. In absence of UCP-2 higher amounts of pyruvate might reach the mitochondrial matrix, become utilized in the tricarboxylic acid (TCA) cycle and lead to an increase in redox pressure on the ETC and subsequently enhanced ROS formation [24]. An increased ratio of NADH/NAD^{+} could also change the overall redox balance and increase ROS production from NAD(P)H oxidases, which have been suggested as sensors in acute HPV [211]. NADP is reduced to

NADPH along the pentose phosphate pathway (PPP), a degrading process that uses glucose-6-phosphat (G-6-P), thus runs in competition with glycolysis and may be influenced by UCP-2 functioning as a metabolic switch. The PPP might be enhanced as cytosolic pyruvate concentration rises due to reduced mitochondrial pyruvate import and slows down glycolysis via feedback inhibition. As NADPH is also needed to replenish GSH from GSSG and other ROS detoxifying systems, an highly reduced NADP pool could also decrease certain types of ROS [216]. Regarding the importance of these substances during hypoxia a study in isolated pulmonary arterial rings reported an increase in NAD(P)H/NAD(P)$^+$ ratio [101], while another one demonstrated that changes only affect NADH/NAD$^+$ but did not alter the content of NADPH or NADP$^+$ during hypoxia [161].

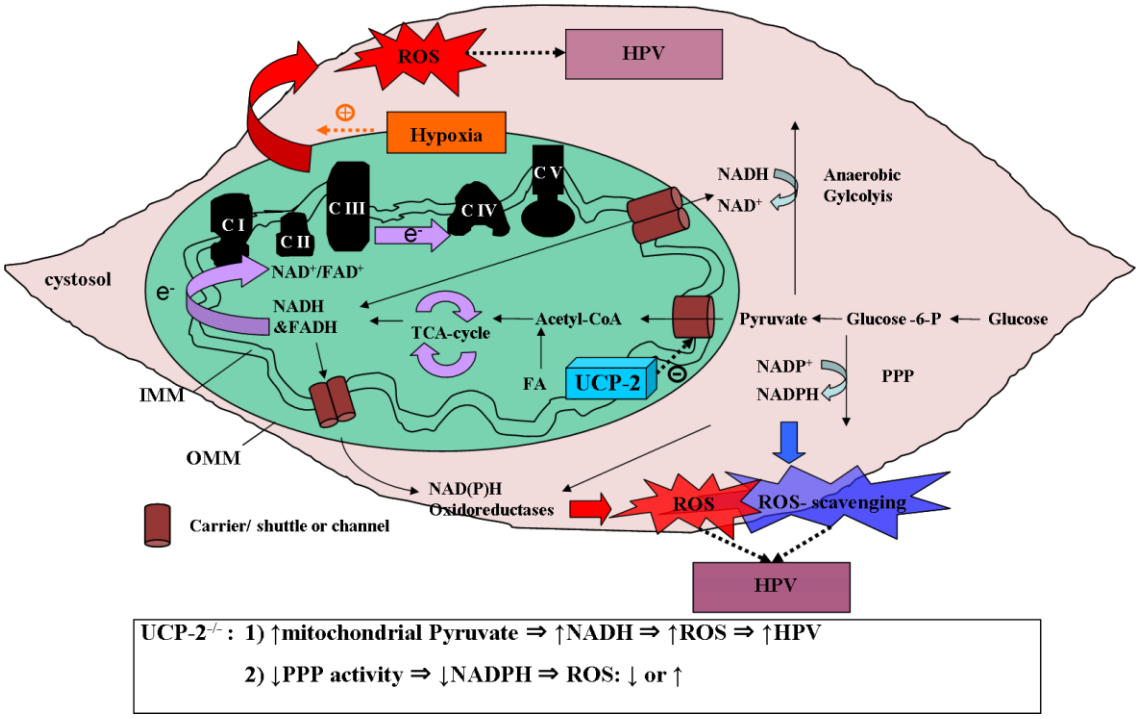

Fig. 4-3: Possible Model of UCP-2 acting as negative regulator of mitochondria pyruvate uptake. CI – CIV: respiratory chain complexes I – IV, CV: ATP synthase, Δp: mitochondrial protonmotive force, e$^-$: electron, H$^+$: hydrogen ion, FA: fatty acid, Glucose-6-P: glucose-6-phosphat, HPV: hypoxic pulmonary vasoconstriction, IMM: inner mitochondrial membrane, m-Ca^{2+}: mitochondrial calcium, m-Na$^+$: mitochondrial sodium, NAD+/NADH: oxidized/reduced nicotinamide adenine dinucleotide, NADP+/NADPH: oxidized/reduced nicotinamide adenine dinucleotide phosphate, OMM: outer mitochondrial membrane, PPP: pentose phosphate pathway ROS: reactive oxygen species, TCA-cycle: tricarboxylic acid- cycle.

The metabolic theory itself is based on experiments addressing the influence of UCP-2 on pyruvate and FA utilization in mouse embryonic fibroblasts [24]. However, there is not much direct experimental evidence to support a function as suggested by the authors and the theory so far lacks a precise mechanism that may explain how the novel UCPs might perform their assumed role. It has been additionally pointed out that the metabolic and uncoupling activities might both be functions of the novel UCPs. According to this hypothesis the frequently described uncoupling phenotype might then either occur during non-physiological conditions, or could be assigned to a proton co-transport as part of the actual physiological function [24].

4.4 Effect of UCP-2 on sustained HPV

To investigate the effect of UCP-2 on the process of sustained HPV, response of WT and UCP-$2^{-/-}$ mice to prolonged hypoxia in an isolated, artificially ventilated and buffer-perfused mouse lung model were compared. Both strains of mice exhibited a biphasic vasoconstrictor response pattern in a comparable sequence, but whereas the acute phase seemed enhanced (cf. 3.1.1 and 3.1.3: the first and second hypoxic maneuver had only a tendency towards higher Δ-PAP but HPV becomes significantly enhanced at the third maneuver), the sustained phase was attenuated in the UCP-$2^{-/-}$ mice. A statistically significant difference was present for a certain time period during the sustained phase and diminished towards the end of the experiment. The PAP values after restoring normoxic ventilation were not altered significantly in the UCP-$2^{-/-}$ mice compared to those of WT mice. In reference experiments applying continuous normoxic ventilation both mouse strains exhibited a small but steady PAP increase, which was found pronounced in UCP-$2^{-/-}$ mice, compared to the increase in WT mice. Comparable to the before mentioned use of short-time thromboxane infusions, in these experiments examining sustained vasoconstriction, a continuous U46619 infusion was intended to demonstrate the impact of genotypes on non-hypoxia-induced vasoconstriction. This should allow conclusions on the specificity of function of UCP-2 in HPV, as discussed before. During sustained infusion of U46619 both strains of mice developed an increased PAP which undulated on a certain level over time. Even though a tendency towards higher PAP responses could be registered in UCP-$2^{-/-}$ mice, there was no significant difference between both strains. UCP-$2^{-/-}$ mice had a particularly high intra-group variability in these U46619

experiments. There was a non-significant trend towards higher weight gain in WT mice during the experiments involving sustained hypoxia, normoxia and U46619 infusion. Thus in contrast to acute hypoxia, where an increase in the strength of HPV was found, sustained HPV was diminished in UCP-$2^{-/-}$ mice. These effects seem specific for hypoxia-induced vasoconstriction as the U46619-induced vasoconstriction was found unchanged and therefore the data argues against an unspecific effect of UCP-2 on the general mechanisms of vasoconstriction. Taken together with the results from the acute hypoxia experiments, a hypothesis able to explain the impact of UCP-2 knock-out on acute and sustained HPV needs to imply differential regulation of these two interdependent phases. There are several physiological variables and processes found particularly important for sustained HPV. Some of them are potential candidates involved in the altered pressure response to sustained hypoxia in the UCP-$2^{-/-}$ mice:

- Cellular glucose metabolism
- Calcium sensitization via the RhoA pathway (cf. chapter 1.3.1.1)
- Modulation of vasoconstriction via changes in calcium homeostasis
- NO signalling (cf. chapter 1.3.2.2)
- AMP/ATP – AMPK and cADPR signalling (cf. chapter 1.3.2.2)

4.4.1 Glucose metabolism

It has been reported that the strength of sustained HPV depends on the availability of glucose and that an amplification of glucose uptake and (anaerobic) glycolysis is required to enable contraction and maintain the cellular energy state during hypoxia [102]. Lowering glucose levels lead to a decreased pressure response after one hour of sustained hypoxia, without affecting the acute phase or the tension during normoxic conditions [101,103]. Vice versa, exposure to high glucose levels enabled a greater vasoconstriction during sustained hypoxia [101,213]. Considered analogous, in this study the effect of UCP-2 knock-out mimicked a state of reduced glucose availability during sustained hypoxia, as it specifically attenuated the second phase of HPV. Referring to the previ-

ously mentioned metabolic theory [24], it is plausible that in the absence of UCP-2 the shift towards anaerobic glycolysis following exposure to hypoxia might be less effective. If UCP-2 works as a negative regulator of pyruvate uptake into the mitochondrion the aerobic pathway is preferred in UCP-$2^{-/-}$ mice. Subsequently, if the aerobic pathway becomes inhibited during hypoxia, the decreased activity of the anaerobic glycolytic pathway in the UCP-$2^{-/-}$ mice could be responsible for the attenuation of sustained HPV, resembling a state of reduced glucose availability. An important interface between the two pathways of pyruvate utilization might be the concentration of NADH. Oxidized NAD^+ is needed for glycerinaldehyd-3-phosphat dehydrogenase activity of glycolysis and is regenerated either during oxidative phosphorylation or by lactate dehydrogenase (LDH) activity [109].

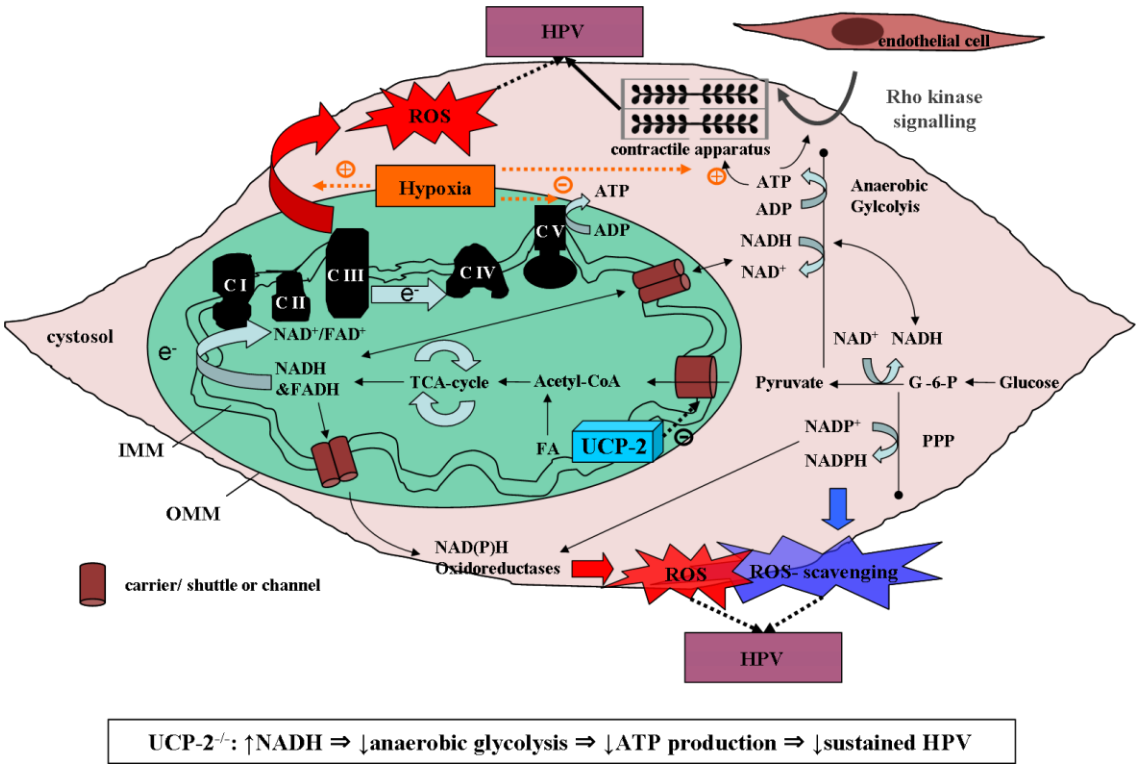

Fig. 4-4: Possible Model of UCP-2 acting as a negative regulator of mitochondrial pyruvate uptake during sustained hypoxia. ADP: adenosine diphosphate, ATP: adenosine triphosphate, CI – CIV: respiratory chain complexes I – IV, CV: ATP synthase, Δp: mitochondrial protonmotive force, e^-: electron, H^+: hydrogen ion, FA: fatty acid, G-6-P: glucose-6-phosphat, HPV: hypoxic pulmonary vasoconstriction, IMM: inner mitochondrial membrane, m-Ca^{2+}: mitochondrial calcium, m-Na^+: mitochondrial sodium, NAD+/NADH: oxidized/reduced nicotinamide adenine dinucleotide, NADP+/NADPH: oxidized/reduced nicotinamide adenine dinucleotide phosphate, OMM: outer mitochondrial membrane, PPP: pentose phosphate pathway, ROS: reactive oxygen species, TCA-cycle: tricarboxylic acid- cycle.

If in UCP-$2^{-/-}$ mice pyruvate is to a greater extend directed towards the TCA cycle and oxidative phosphorylation, glycolysis is more inhibited due to decreased activity of LDH and the higher levels of NADH. Glycolysis is a central element of the cellular metabolism and connected to several other pathways including the PPP which regenerates NADPH from $NADP^+$ and is involved in ROS generation via NAD(P)H – oxidases as well as ROS scavenging. Elevated levels of NAD(P)H have been reported [101,212], but were mostly interpreted under the assumption of a reduced cytosolic redox state serving as hypoxic signal [7]. The metabolic theory offers certain advantages in explaining the findings of this thesis: 1) SMC fit the described profile of cells that maintain anaerobic glycolysis during aerobic conditions [24,102]. 2) Taken together with the assumption that contraction during sustained HPV is specifically dependent on anaerobic glycolysis [102,213], the theory fits well the finding of an attenuated pressure response during hypoxia, the unchanged response to U46619 and the former observations and theories by Leach et al. These authors further suggested a concept of compartmentalized energy production and that ATP derived from glycolysis is needed to support contraction via the RhoA/Rho kinase pathway [102]. Even though the growing evidence pointing towards a fundamental difference in regulation and energy supply between acute and sustained hypoxia it remains unclear how hypoxia induces the changes in the cellular metabolism that leads to activation of anaerobic glycolysis. It still needs to be clarified how the mitochondrial metabolism changes under hypoxic conditions and what are the key enzymes and substrates affected by these changes.

4.4.2 Calcium sensitization

The RhoA pathway itself is thought to mediate or at least modulate smooth muscle contraction via regulation of Ca^{2+} - sensitivity and suggested to be triggered by different mechanisms, among others hypoxia [53,146,187] as well as G protein coupled ET-1 and thromboxane receptors [114,129]. The connection between hypoxia and RhoA/Rho kinase activity is not clear but it has been suggested that ROS might be involved and enhance Ca^{2+} sensitivity [37]. The new findings in this thesis, interpreted under the assumption of an uncoupling activity leading to an attenuation of ROS production, do not support the view of a major importance for ROS enhanced Rho axis mediated vascular contraction during sustained hypoxia.

4.4.3 Adenosine monophosphate activated protein kinase signalling

The involvement of the AMPK as a potential mediator of sustained hypoxia-induced metabolic signals needs to be addressed as well. Inhibitors of AMPK are able to prevent sustained HPV exclusively [151] and the enzyme has been suggested to be regulated by increasing AMP/ATP ratio and activate cADPR dependent SR- calcium release under hypoxia [51]. Furthermore the activity of this signalling pathway was found enhanced by ROS [50,130,191]. According to this theory and to integrate the own findings, either the intensity of the trigger signal "AMP/ATP ratio", or one of the other steps along this pathway need to be negatively affected by the ablation of the UCP-2 gene. To account for a lower vasoconstrictor response, there might be less AMP build up or less ROS generation in UCP-$2^{-/-}$ mice during sustained hypoxia. If uncoupling is the primary role of UCP-2, a higher Δp in the knock-out mice might theoretically help to preserve mitochondrial ATP generation, but unlikely reduce ROS formation (as discussed before for acute HPV). UCP-2 was found to be a negative regulator of Δp, ATP level [226] and to reduce ROS production [26] in most of the studies. If UCP-2 acts as a metabolic switch inhibiting pyruvate utilization by the mitochondria, metabolism in UCP-$2^{-/-}$ deficient mice might provide less fuel for the anaerobic glycolysis [24]. Assuming that mitochondrial ATP production becomes inhibited during hypoxia and this may lead to an overall deficiency in ATP, UCP-$2^{-/-}$ mitochondria could have a higher Δp and an increased ATP production. Again, ROS generation would also rather be enhanced by this mechanism.

4.4.4 Calcium homeostasis

Assuming a direct interdependency of calcium buffering by the mitochondria, as well as of $[Ca^{2+}]_c$ and the extend of PASMC contraction, the suggested function of UCP-2 as an essential part of the calcium uniporter is not in line with the result of a reduction in the strength of sustained HPV. Instead an overall lower amount of $[Ca^{2+}]_c$ during sustained contraction is expected in the UCP-$2^{-/-}$ mice to explain the observed difference. A direct correlation between Δp and calcium uptake has been described [62], the assumed higher Δp in UCP-$2^{-/-}$ mice may serve as an explanation. Still it leaves the problem of a reverse effect of UCP-2 knock-out on the acute and sustained HPV unsolved. Only a complex mode of action for UCP-2 and mitochondrial calcium metabolism could explain these results. During excitation of chromaffin cells, for example, mitochondria take up cyto-

solic calcium quickly, but also produce a prolonged low plateau phase of calcium elevation [62,77], a mechanism that, when translated to smooth muscle contraction, would allow the combination of a higher acute HPV and a lower plateau phase in UCP-2$^{-/-}$ mice, if UCP-2 is at all part of a calcium uptake and efflux system.

4.4.5 Nitric oxide generation

NO is an important mediator of systemic and pulmonary vascular tone [22]. Manipulations of the cellular NO level alter both acute and sustained vasoconstrictor responses to hypoxia [202,210]. As it has been demonstrated that endothelial NO generation is Ca^{2+} dependent [98,197], attenuation of sustained HPV in UCP-2$^{-/-}$ mice via increase in endothelial $[Ca^{2+}]_c$ and subsequent NO generation is a possible mechanism, if UCP-2 is a regulator of intracellular calcium [180]. Hence the enhancement of the acute phase might be a direct effect of intracellular calcium in PASMC and the attenuation of the second phase an effect of increased NO production in endothelial cells. Due to the problems in reliably detecting UCP-2 on the protein level [138] it is currently not possible to predict its abundance or activity in the different cell types, like endothelial cells or the PASMC, involved in the different phases HPV. Solving this problem would help to better understand the influence of UCP-2 on acute and sustained HPV.

4.4.6 Secondary effects of the insulin level

The effect of insulin on both phases of HPV has been addressed before and is of special interest as insulin levels are altered in UCP-2$^{-/-}$ mice [226] and insulin regulates cellular energy balance and many other processes. It has been shown that insulin pre-incubation increases the pressure response in isolated PA due to sustained hypoxia between 15 and 55 minutes, but had no effect on acute HPV or PAP after 60 minutes [101]. Comparing the time dependent effects of insulin pre-incubation in this study with the own findings, as well as in consideration of the experimental circumstances, the data does not support the view that the pressure response in the experiments described here is altered through short-time effects of an increased insulin concentration. It is feasible but also highly speculative that either the higher insulin level or the lower plasma glucose levels in the UCP-2$^{-/-}$ mice induced long-term adaptation processes in lung vessels, affecting glucose

uptake and utilization and may be responsible for the observed differences in the two mouse strains.

4.4.7 Analogy between glucose sensing and oxygen sensing

It has been demonstrated that UCP-2 is able to negatively impact insulin secretion [226] and it is interesting to note certain analogies, not only between the effect of UCP-2 knock-out on insulin secretion and the effect of UCP-2 knock-out on HPV characteristics in this study, but also between the process of glucose sensing and insulin secretion in pancreatic β-cells and oxygen sensing in HPV. Insulin release from β-cells is a biphasic response following glucose stimulation, the first phase peaks around 4min, is followed by a decline for several minutes and a subsequent increase in secretion [173]. This reaction, especially the time course under experimental conditions is strikingly similar to the biphasic response of HPV (cf. chapter 1.1.2), as is the effect of the UCP-2 knock-out on both phases of insulin secretion and HPV. While UCP-2 knock-out caused enhanced insulin levels 15 minutes after glucose stimulation in obese mice, insulin levels were significantly lower at the 60 and 90 minute time-points [226]. However, as in this situation, a negative feedback loop is established and as the higher insulin secretion in phase 1 seems to influence blood glucose levels [226] this could likely be responsible for the lower insulin level during phase 2. It is still interesting that, while it is well established that insulin secretion is essentially based on enhancement of mitochondrial ATP production during high glucose conditions, subsequent closure of cellular K_{ATP} –channels, membrane depolarization and calcium influx, other mediators seem to modulate the process and especially the second phase is controlled by a glucose dependent, non-electrogenic and yet uncharacterized amplifying pathway [76].

Even though it is only an observation of an analogy it is conceivable that these two physiological responses to changes in essential metabolic compounds (glucose and oxygen) share a common principle of signal transduction. An increased Δp in UCP-$2^{-/-}$ mice could cause a rise in ATP production from mitochondria, as pointed out before, but the HPV sensor mechanism is unlikely based on a rise in ATP production from mitochondria, closure of cellular K_{ATP} –channels and membrane depolarization during hypoxia as this was described for glucose sensing. Most studies investigating the influence of K_{ATP}

–channels using the unspecific blocker glibenclamide did not find an influence on PASMC membrane potential or PA tone [46,72]. It has already been suggested that ROS signalling is part of glucose sensing and insulin secretion in pancreatic β-cells, as glucose stimulation leads to increase in ROS generation and exogenous H_2O_2 was able to induce insulin secretion [141]. There are both mitochondrial K_{ATP} –as well as cellular membrane K_{ATP} –channels but the specificity of the pharmacological effects of the currently known K_{ATP} –channel modulators is unclear. Regarding HPV both the unspecific inhibitors glibenclamide and the specific mitochondrial K_{ATP} inhibitor 5-hydroxydecanoate suppressed HPV and the specific mitochondrial K_{ATP} activator substance diazoxide as well as the unselective substance pinacidil suppressed HPV and induced vasodilation [132].

4.5 Concept of mitochondrial oxygen sensing

The results of this study in connection with the current concepts of UCP-2 function and signalling in HPV are most consistent with the theory of oxygen sensing and signal transduction via amplification of mitochondrial ROS. It has been suggested that during hypoxia mitochondrial complex IV and mitochondrial respiration become inhibited and an elevated Δp leads to increases in ROS formation [169]. From this point of view it can be speculated that UCP-2 impacts both the glucose and the oxygen sensor systems in the same way, because both mechanisms may rely on Δp and ROS signalling, parameters of the activity of the respiratory chain. During glucose sensing a high metabolic turnover rate leads to increasing electron supply into the respiratory chain, while the principle of oxygen sensing might be enabled by hyperpolarisation due to lack of the final electron acceptor -oxygen.

4.6 Effect of UCP-2 on the adaptation to chronic hypoxia

RVSP measurement, evaluation of heart ratio and morphometric analysis of the lungs' vasculature of both WT and UCP-$2^{-/-}$ mice were performed in animals held under normoxic conditions as well as in those exposed to a reduced normobaric FiO_2. Under normoxic conditions the UCP-$2^{-/-}$ mice displayed no statistically significant differences in RVSP or heart ratio compared to WT mice. However significant differences in the morphometry of pulmonary vessels of UCP-$2^{-/-}$ mice compared to WT mice were found:

UCP-2$^{-/-}$ mice have a lower rate of non-muscularized arteries and a higher amount of partially and fully-muscularized vessels. After exposure to chronic hypoxia both mouse strains developed a similar degree of vascular remodelling and right ventricular hypertrophy. Interestingly in the chronic hypoxic mice the RVSP was found to be significantly higher in UCP-2$^{-/-}$ mice compared to WT mice. Differences comparing the two mouse strains regarding their hematocrit under normoxic conditions or in the degree of polycythemia induced by hypoxia could not be observed.

Both concepts, those involving protonophoric activity of UCP-2 and the metabolic theory, might explain an intensified muscularization of vessels during normoxic conditions, as ablation of UCP-2 could promote proliferation of PASMC through mitochondrial hyperpolarisation and increase of ROS as demonstrated for murine embryonic fibroblasts [139]. Still the results from this part of the study are not overall conclusive. The three main target parameters of this experiment (RVSP, heart ratio and the vascular morphometric analysis) should basically reflect the same process but do not show the expected consistency, as RVSP and heart ratio were not increased despite an increased vascular remodelling. A similar discrepancy was found in chronic hypoxia.

As the RVSP was found significantly enhanced in UCP-2$^{-/-}$ mice compared to WT mice under hypoxic conditions, the heart ratio is expected to be increased as well, as this would reflect the known physiological adaptation of right ventricular tissue to the higher afterload. Moreover the muscularization of pulmonary vessels determines its resistance and following Ohm`s law, and under the assumption of a constant cardiac output, also determines the RVSP. Therefore it would have been expected to find the source of a higher RVSP in a marked remodelling of the pulmonary vessels, but this was not the case. In contrast to the above reasoning an interesting study performed in rats exposed to chronic hypoxia gives a good explanation for separating results from vessels wall thickness measurement and vascular lumen. In this study the fixed pulmonary vasculature indeed did not show overall narrowing of the vessel lumen while the other signs of hypoxia-induced PH like right ventricular hypertrophy and proliferation of all three parts of the pulmonary vessels could be demonstrated as expected [81]. A possible explanation may be that the vessels measured by morphometry do not depict the critical anatomical regions responsible for regulation of pulmonary resistance or that there may

be marked differences between the measured lumen in fixed and in vivo tissue [81]. As not the difference in the vascular lumen but the differences in wall thickness between UCP-$2^{-/-}$ and WT mice were compared it can not be excluded that the found wall thickening is mainly directed outwards without lumen encroachment [81]. A higher RVSP in the UCP-$2^{-/-}$ mice following chronic exposure to hypoxia, in absence of a more pronounced vascular remodelling and lacking a resulting intensified right ventricular hypertrophy, may also be explained by differences in another cardiovascular characteristic. One possibility is an increased cardiac output at a constant vascular resistance in the UCP-$2^{-/-}$ mice during the in vivo measurements. An influence of UCP-2 on ventricular contractility is conceivable as this was demonstrated for rat cardiomyocytes [181]. Another possibility is that despite the similar degree of vascular muscularization in both mouse strains the actual resistance of the vascular bed is higher in the UCP-$2^{-/-}$ mice. This might be due to an amplified basal tone of pulmonary vessels which cannot be observed in the morphometric analysis of embedded lung tissue. In the experiments of acute and sustained hypoxia baseline PAP in a buffer- perfused mouse lung system with a fixed flow rate were compared, which allows conclusions on the pulmonary vascular resistance in living tissue. No significant difference in the baseline PAP at the start of the experiments but significant difference in the course of PAP during three hours of normoxic ventilation between UCP-$2^{-/-}$ and WT mice could be observed.

To explain the similar degree of right ventricular hypertrophy at different levels of RVSP it can be assumed that the RV of UCP-$2^{-/-}$ mice is less prone to hypertrophy under hypoxia. Alternatively it is possible that the observed pressure difference between WT and UCP-$2^{-/-}$ mice is not appropriate in size or time of influence to induce a significant alteration in heart ratio. Concerning this an interesting observation was made in hemoxygenase-1 (HO-1) knock-out mice, where a similar amount of pulmonary remodelling led to a significantly greater change in ventricular hypertrophy, which was interpreted as an effect of HO-1 on cardiomyocytes adaption to the increase in PAP [219]. In UCP-$2^{-/-}$ mice a higher RVSP might be established, but due to an additional effect on ventricular adaptation, hypertrophy could be attenuated. The experiments for RVSP measurement themselves were performed under normoxic conditions even in the group of mice previously exposed to hypoxia (cf. chapter 2.3.2), so finally re-exposure to oxygen might have a distinct effect on WT and UCP-$2^{-/-}$ mice.

Time dependency of the adaptation processes to chronic hypoxia might have major importance for the understanding of the effects of UCP-2 on pulmonary hypertension, but cannot be monitored due to the study limitation offering only two reading points: animals under normoxic conditions and animals after the exposure to hypoxia. For example in a study investigating the effect of a partial HIF-1α deficiency on the development of right ventricular hypertrophy in response to chronic hypoxia, the target values were monitored at intervals between one week and six weeks [220]. This enabled the observation that in HIF-1α deficient animals the response to chronic hypoxia becomes significantly delayed but not eliminated [220]. These differences between WT and knock-out animals were most pronounced in the third week, but no significant difference was seen after six weeks [220].

However the results of this thesis demonstrate that the mechanisms of adaptation to chronic hypoxia, that is pulmonary vessel remodelling, PH and right ventricular hypertrophy, were maintained in the UCP-$2^{-/-}$ animals. In this context the equivalent changes of hematocrit indicates that both mouse strains do not differ in this aspect of adaptation to hypoxia. This finding furthermore stands against an important direct or indirect influence of UCP-$2^{-/-}$ on the activation of the HIF pathways that is in control of the red blood cell mass via secretion of erythropoietin under hypoxic conditions [105].

Taken together, during normoxia the UCP-$2^{-/-}$ strain exhibits a phenotype of increased muscularization of the pulmonary vasculature compared to the wild type mouse strain. This effect is not mirrored by an increase in hematocrit and established as a trend towards higher RVSP and heart ratio. Furthermore the difference in muscularization is not detectable after exposure to hypoxia, a finding that can be interpreted as a loss of function of UCP-2 during hypoxia, for example via downregulation of the UCP-2 gene in WT mice.

Proceeding from the results and to overcome limitations of this study, additional experiments, including advanced hemodynamics, morphometry and echocardiography were meanwhile conducted in the same laboratory as was this thesis. The results were very recently published and actually indicate a slight but statistically significant higher RVSP and heart ratio in UCP-$2^{-/-}$ mice compared to WT mice under normoxic condi-

tions [134]. Additionally it was shown that under normoxia UCP-2$^{-/-}$ mice have an increased right ventricular wall thickness and an impaired function of the right ventricle compared to WT animals [134]. Furthermore PASMC isolated from UCP-2$^{-/-}$ mice have a higher $\Delta\Psi m$, an increased proliferation and a higher ROS production [134]. The increased proliferation of PASMC from UCP-2$^{-/-}$ mice could then again be reduced by FCCP as well as ROS scavengers [134]. Therefore it was suggested that UCP-2$^{-/-}$ mice exhibit a phenotype of increased pulmonary vascular remodelling during normoxia based on mitochondrial hyperpolarisation and increased ROS production [134].

Summary

Hypoxic pulmonary vasoconstriction (HPV) is a specific physiological reaction of the pulmonary circulation which optimizes pulmonary gas exchange. Due to selective vasoconstriction of precapillary pulmonary vessels, systemic oxygen availability is preserved in case of a localized reduction of ventilation or a lack of local alveolar oxygen. Additional interdependent mechanisms lead to vascular remodelling during adaptation to chronic hypoxia. Similar changes are also part of the pathogenesis of certain severe pulmonary vascular diseases. Despite intensive research, the sub-cellular and molecular nature of the mechanisms enabling HPV and vascular remodelling due to hypoxia remain unclear. Uncoupling protein 2 (UCP-2) is a mitochondrial protein and a more recently identified homologue of the protein thermogenin (UCP-1). Recent studies suggest important interaction between UCP-2 and the signalling pathways of HPV.

Against this background, the aim of this study was to investigate the role of UCP-2 in the lungs' adaptation to acute, sustained and chronic hypoxia. Therefore important characteristics of HPV in wild-type (WT) and UCP-2 deficient (UCP-$2^{-/-}$) mice were compared. It could be demonstrated that while acute HPV was enhanced in UCP-$2^{-/-}$ mice, sustained HPV was attenuated. This difference was found to be specific for hypoxia as a vasoconstrictor stimulus. The muscularization of pulmonary vessels was increased under normoxic conditions in UCP-$2^{-/-}$ mice and following exposure to chronic hypoxia the right ventricular systolic pressure was found elevated in UCP-$2^{-/-}$ mice compared to WT mice.

The results depict that ablation of UCP-2 divergently impacts the consecutive phases of HPV by a yet incompletely understood mechanism. This requires differences in the sensor or mediator systems of acute and sustained HPV. UCP-2 is able to directly or indirectly control the muscularization of pulmonary vessels under normoxic conditions and likely the pulmonary vascular tone under chronic hypoxia.

Zusammenfassung

Die Hypoxische Pulmonale Vasokonstriktion (HPV) ist eine spezifische physiologische Reaktion des Lungenkreislaufes zur Optimierung des pulmonalen Gasaustausches. Durch selektive Engstellung von präkapillären Gefäßen wird die systemische Sauerstoffversorgung im Fall lokal begrenzter Belüftungsstörung oder einer lokalen alveolären Hypoxie aufrechterhalten. Zusätzliche, mit dieser Reaktion überlappende Mechanismen führen zum Gefäßumbau während chronischen Sauerstoffmangels. Diese strukturellen Veränderungen sind auch Bestandteil der Pathogenese einiger schwerwiegender Lungengefäßerkrankungen. Trotz intensiver Forschung auf diesem Gebiet sind die subzellulären und molekularen Grundlagen der HPV und des Gefäßumbaues unter Hypoxie weiterhin unklar. Das Uncoupling Protein 2 (UCP-2) ist ein mitochondriales Protein, welches Homologien zu dem länger bekannten Protein Thermogenin (UCP-1) besitzt. Aktuelle Untersuchungen weisen auf wichtige Wechselbeziehungen zwischen UCP-2 und den Signalwegen der HPV hin.

Davon ausgehend war das Ziel dieser Arbeit die Bedeutung von UCP-2 für die Reaktionen des Lungenkreislaufes auf akute, anhaltende und chronische Hypoxie zu untersuchen. Daher wurde die Ausprägung wichtiger Merkmale der HPV von Wildtyp- (WT) und UCP-2 defizienten (UCP-$2^{-/-}$) Mäusen verglichen. Es zeigte sich, dass die akute HPV in UCP-$2^{-/-}$ Mäusen verstärkt abläuft, während die anhaltende HPV abgeschwächt ist. Dieser Unterschied war nur für eine durch Hypoxie ausgelöste Gefäßkontraktion nachweisbar. Unter Normoxie ist der Muskularisierungsgrad der pulmonalen Gefäße in den UCP-$2^{-/-}$ Mäusen erhöht und nach Exposition gegenüber chronischer Hypoxie zeigten UCP-$2^{-/-}$, verglichen mit WT Mäusen einen erhöhten rechtsventrikulären systolischen Druck. Die Ergebnisse verdeutlichen, dass die Ausschaltung von UCP-2 die aufeinanderfolgenden Phasen der HPV über einen bisher nicht aufgeklärten Mechanismus in gegensätzlicher Weise beeinflusst. Voraussetzung dafür sind Unterschiede in den Sensor- oder Mediatorsystemen der akuten und anhaltenden HPV. UCP-2 reguliert unter normoxischen Bedingungen direkt oder indirekt den Muskularisierungsgrad von pulmonalen Gefäßen und wahrscheinlich auch den pulmonalen Gefäßtonus unter chronischer Hypoxie.

Abbreviations

%	-	percentage
ABC	-	avidin/biotinylated enzyme complex
ADP	-	adenosine diphosphate
AMP	-	adenosine monophosphate
AMPK	-	adenosine monophosphate activated protein kinase
ANOVA	-	analysis of variance model
anti- α-SMA	-	anti- α- smooth muscle actin
anti- vWF	-	anti- von Willebrand factor
ATP	-	adenosine triphosphate
BAT	-	brown adipose tissue
body wt.	-	body weight
BSA	-	bovine serum albumin
Ca^{2+}	-	calcium ion
$[Ca^{2+}]_c$	-	cytosolic calcium concentration
$[Ca^{2+}]_m$	-	mitochondrial calcium concentration
$CaCl_2$	-	calcium chloride
cADPR	-	cyclic adenosine diphosphate ribose
CCE	-	capacitative calcium entry
cf.	-	confer
cGMP	-	cyclic guanosine monophosphate
CH_2O	-	formaldehyde
CICR	-	calcium-induced calcium release
cm	-	centimetre
CN^-	-	cyanide
CO_2	-	carbon dioxide
DAB	-	3,3-diaminobenzidine
DAG	-	diacylglycerol
°C	-	degree Celsius
DNA	-	deoxyribonucleic acid
DNP	-	2,4-dinitrophenol
Δp	-	mitochondrial protonmotive force
Δ-PAP	-	change in pulmonary artery pressure
ΔpH	-	mitochondrial chemical/ osmotic proton gradient

$\Delta\Psi m$	-	mitochondrial membrane potential
e^-	-	electron
e.g.	-	exempli gratia (for example)
E_M	-	cellular membrane potential
ER	-	endoplasmic reticulum
ET-1	-	endothelin-1
ETC	-	electron transport chain
FA	-	fatty acid
FAD	-	flavin adenine dinucleotide – oxidised
FADH	-	flavin adenine dinucleotide – reduced
FCCP	-	carbonyl– cyanide-p–triflouromethoxyphenylhydrazone
FiO_2	-	fraction of inspired oxygen
g	-	gram
G-6-P	-	glucose-6-phosphat
GSH	-	glutathione – reduced
GSSG	-	glutathione – oxidised
h	-	hour
H^+	-	hydrogen ion
H_2O	-	water
H_2O_2	-	hydrogen peroxide
HIF-1	-	hypoxia-inducible factor-1
HO	-	hemoxygenase
HO-1	-	hemoxygenase-1
HO-2	-	hemoxygenase-2
HOX	-	hypoxic group
HPV	-	hypoxic pulmonary vasoconstriction
Ig	-	immunoglobulin
IgG	-	immunoglobulin G
IHC	-	immunohistochemistry
i.p.	-	intraperitoneal
IPAH	-	idiopathic pulmonary arterial hypertension
IP_3	-	inositol-1,4,5-trisphosphate
I_K	-	conductance of potassium
IMAC	-	inner membrane anion channel
i.v.	-	intravenous
IU	-	international unit

K^+	-	potassium ion
$[K^+]$	-	potassium concentration
KCl	-	potassium chloride
kg	-	kilogram
KH_2PO_4	-	potassium dihydrogen phosphate
Kv channel	-	voltage-gated potassium channel
l	-	litre
LV	-	left ventricle
LVP	-	left ventricular pressure
µ	-	micro
M	-	molar
MCU	-	mitochondrial calcium uniporter
µg	-	microgram
mg	-	milligram
$MgCl_2$	-	magnesium chloride
min	-	minute
µl	-	microlitre
ml	-	millilitre
MLC	-	myosin light chain
mRNA	-	messenger- ribonucleic acid
µm	-	micrometre
µM	-	micromolar
mmHg	-	millimetre of mercury
M.O.M	-	mouse on mouse
n	-	number of experiments
N_2	-	molecular nitrogen
Na^+	-	sodium ion
NaCl	-	sodium chloride
NAD	-	nicotinamide adenine dinucleotide – oxidised
NADH	-	nicotinamide adenine dinucleotide – reduced
NADP	-	nicotinamide adenine dinucleotide phosphate – oxidised
NADPH	-	nicotinamide adenine dinucleotide phosphate – reduced
ng	-	nanogram
$NaHCO_3$	-	sodium bicarbonate
Na_2HPO_4	-	disodium hydrogen phosphate
NaH_2PO_4	-	sodium dihydrogen phosphate

NaN3	-	sodium azide
NO	-	nitric oxide
NOS	-	nitric oxide synthase
NOX	-	normoxic group
NSCC	-	non-specific cation channel
O_2	-	oxygen
O_2^-	-	superoxide
PA	-	pulmonary artery
PAH	-	pulmonary arterial hypertension
PAP	-	pulmonary artery pressure
PASMC	-	pulmonary artery smooth muscle cell
PaO_2	-	alveolar partial pressure of oxygen
PBS	-	phosphate buffered saline
PC	-	personal computer
PEEP	-	positive end-expiratory pressure
pH	-	negative decadal logarithm of hydrogen-ion activity in solution
PH	-	pulmonary hypertension
PLC	-	phospholipase C
PPP	-	pentose phosphate pathway
PvO_2	-	mixed venous oxygen tension
Q	-	ubiquinone
Q•	-	ubisemiquinone
QH_2	-	ubiquinol
Qo	-	quinol oxidase site of respiratory chain complex III
RA	-	right atrium
ROCC	-	receptor operated calcium channel
ROS	-	reactive oxygen species
RV	-	right ventricle
RVP	-	right ventricular pressure
RVSP	-	right ventricular systolic pressure
RYR	-	ryanodine receptor
s	-	second
SEM	-	standard error of the mean
SMA	-	smooth muscle actin
SMC	-	smooth muscle cell
SOCC	-	store operated calcium channel

SOCR	-	store operated calcium release
SR	-	sarcoplasmic reticulum
TRPC	-	transient receptor potential channel
$TRPC6^{-/-}$	-	transient receptor potential channel 6 deficient
TCA	-	tricarboxylic acid
U46619	-	a thromboxane A2 mimetic
UCP-1	-	uncoupling protein 1 or thermogenin
UCP-2	-	uncoupling protein 2
$UCP\text{-}2^{-/-}$	-	uncoupling protein 2 deficient
VDAC	-	voltage-dependent anion channel
VEGF	-	vascular endothelial growth factor
VOCC	-	voltage-operated calcium channel
VOCE	-	voltage-operated calcium entry
vol.	-	volume
VP	-	ventilation pressure
V/Q	-	ventilation to perfusion
vWF	-	von-Willebrand factor
WF	-	weight force
WT	-	wild type

Reference

1. Aaronson PI, Robertson TP, Knock GA, et al: Hypoxic pulmonary vasoconstriction: mechanisms and controversies. J Physiol 570:53-58, 2006
2. Aaronson PI, Robertson TP, Ward JP: Endothelium-derived mediators and hypoxic pulmonary vasoconstriction. Respir Physiol Neurobiol 132:107-120, 2002
3. al-Tinawi A, Krenz GS, Rickaby DA, et al: Influence of hypoxia and serotonin on small pulmonary vessels. J Appl Physiol 76:56-64, 1994
4. Andreyev AY, Kushnareva YE, Starkov AA: Mitochondrial metabolism of reactive oxygen species. Biochemistry (Mosc) 70:200-214, 2005
5. Andrukhiv A, Costa AD, West IC, et al: Opening mitoKATP increases superoxide generation from complex I of the electron transport chain. Am J Physiol Heart Circ Physiol 291:H2067-2074, 2006
6. Aon MA, Cortassa S, O'Rourke B: Redox-optimized ROS balance: a unifying hypothesis. Biochim Biophys Acta 1797:865-877, 2010
7. Archer SL, Huang J, Henry T, et al: A redox-based O2 sensor in rat pulmonary vasculature. Circ Res 73:1100-1112, 1993
8. Archer SL, London B, Hampl V, et al: Impairment of hypoxic pulmonary vasoconstriction in mice lacking the voltage-gated potassium channel Kv1.5. Faseb J 15:1801-1803, 2001
9. Archer SL, Nelson DP, Weir EK: Simultaneous measurement of O2 radicals and pulmonary vascular reactivity in rat lung. J Appl Physiol 67:1903-1911, 1989
10. Archer SL, Souil E, Dinh-Xuan AT, et al: Molecular identification of the role of voltage-gated K+ channels, Kv1.5 and Kv2.1, in hypoxic pulmonary vasoconstriction and control of resting membrane potential in rat pulmonary artery myocytes. J Clin Invest 101:2319-2330, 1998
11. Archer SL, Weir EK, Wilkins MR: Basic Science of Pulmonary Arterial Hypertension for Clinicians: New Concepts and Experimental Therapies. Circulation 121:2045-2066, 2010
12. Archer SL, Wu XC, Thebaud B, et al: Preferential expression and function of voltage-gated, O2-sensitive K+ channels in resistance pulmonary arteries explains regional heterogeneity in hypoxic pulmonary vasoconstriction: ionic diversity in smooth muscle cells. Circ Res 95:308-318, 2004
13. Arsenijevic D, Onuma H, Pecqueur C, et al: Disruption of the uncoupling protein-2 gene in mice reveals a role in immunity and reactive oxygen species production. Nat Genet 26:435-439, 2000
14. Aviado DM, Jr., Cerletti A, Alanis J, et al: Effects of anoxia on pressure, resistance and blood (P32) volume of pulmonary vessels. Am J Physiol 169:460-470, 1952
15. Barja G: Mitochondrial oxygen radical generation and leak: sites of production in states 4 and 3, organ specificity, and relation to aging and longevity. J Bioenerg Biomembr 31:347-366, 1999

16. Bartsch P, Maggiorini M, Ritter M, et al: Prevention of high-altitude pulmonary edema by nifedipine. N Engl J Med 325:1284-1289, 1991

17. Beech DJ: Emerging functions of 10 types of TRP cationic channel in vascular smooth muscle. Clin Exp Pharmacol Physiol 32:597-603, 2005

18. Bell EL, Emerling BM, Chandel NS: Mitochondrial regulation of oxygen sensing. Mitochondrion 5:322-332, 2005

19. Bennie RE, Packer CS, Powell DR, et al: Biphasic contractile response of pulmonary artery to hypoxia. Am J Physiol 261:L156-163, 1991

20. Bergofsky EH, Bass BG, Ferretti R, et al: Pulmonary Vasoconstriction in Response to Precapillary Hypoxemia. J Clin Invest 42:1201-1215, 1963

21. Bindslev L, Jolin A, Hedenstierna G, et al: Hypoxic pulmonary vasoconstriction in the human lung: effect of repeated hypoxic challenges during anesthesia. Anesthesiology 62:621-625, 1985

22. Blitzer ML, Loh E, Roddy MA, et al: Endothelium-derived nitric oxide regulates systemic and pulmonary vascular resistance during acute hypoxia in humans. J Am Coll Cardiol 28:591-596, 1996

23. Bootman MD, Berridge MJ: The elemental principles of calcium signaling. Cell 83:675-678, 1995

24. Bouillaud F: UCP2, not a physiologically relevant uncoupler but a glucose sparing switch impacting ROS production and glucose sensing. Biochimica et Biophysica Acta (BBA) - Bioenergetics 1787:377-383, 2009

25. Bradford JR, Dean HP: The Pulmonary Circulation. J Physiol 16:34-158 125, 1894

26. Brand MD, Affourtit C, Esteves TC, et al: Mitochondrial superoxide: production, biological effects, and activation of uncoupling proteins. Free Radic Biol Med 37:755-767, 2004

27. Brandt U: Redoxreaktionen, Sauerstoff und oxidative Phosphorylierung, in Biochemie & Pathobiochemie. Berlin Heidelberg New York: Löffler, G. und Petrides, P.E., 2003, pp 532-555

28. Brookes PS, Parker N, Buckingham JA, et al: UCPs--unlikely calcium porters. Nat Cell Biol 10:1235-1237; author reply 1237-1240, 2008

29. Brookes PS, Yoon Y, Robotham JL, et al: Calcium, ATP, and ROS: a mitochondrial love-hate triangle. Am J Physiol Cell Physiol 287:C817-833, 2004

30. Budowick M: Terminale Luftwege - Grafik, in Lehrbuch Histologie. Jena: Welsch, U., 2003, p 295

31. Bunn HF, Poyton RO: Oxygen sensing and molecular adaptation to hypoxia. Physiol Rev 76:839-885, 1996

32. Burton RR, Besch EL, Smith AH: Effect of chronic hypoxia on the pulmonary arterial blood pressure of the chicken. Am J Physiol 214:1438-1442, 1968

33. Cannon B, Nedergaard J: Brown adipose tissue: function and physiological significance. Physiol Rev 84:277-359, 2004

34. Chandel NS, McClintock DS, Feliciano CE, et al: Reactive oxygen species generated at mitochondrial complex III stabilize hypoxia-inducible factor-1alpha during hypoxia: a mechanism of O2 sensing. J Biol Chem 275:25130-25138, 2000

35. Chandel NS, Schumacker PT: Cells depleted of mitochondrial DNA (rho0) yield insight into physiological mechanisms. FEBS Lett 454:173-176, 1999

36. Chen Q, Vazquez EJ, Moghaddas S, et al: Production of reactive oxygen species by mitochondria: central role of complex III. J Biol Chem 278:36027-36031, 2003

37. Chi AY, Waypa GB, Mungai PT, et al: Prolonged hypoxia increases ROS signaling and RhoA activation in pulmonary artery smooth muscle and endothelial cells. Antioxid Redox Signal 12:603-610, 2010

38. Coppock EA, Martens JR, Tamkun MM: Molecular basis of hypoxia-induced pulmonary vasoconstriction: role of voltage-gated K+ channels. Am J Physiol Lung Cell Mol Physiol 281:L1-12, 2001

39. Cornfield DN, Reeve HL, Tolarova S, et al: Oxygen causes fetal pulmonary vasodilation through activation of a calcium-dependent potassium channel. Proc Natl Acad Sci U S A 93:8089-8094, 1996

40. Cornfield DN, Stevens T, McMurtry IF, et al: Acute hypoxia causes membrane depolarization and calcium influx in fetal pulmonary artery smooth muscle cells. Am J Physiol 266:L469-475, 1994

41. Crosswhite P, Sun Z: Nitric oxide, oxidative stress and inflammation in pulmonary arterial hypertension. J Hypertens 28:201-212, 2010

42. Dias-Junior CA, Cau SB, Tanus-Santos JE: [Role of nitric oxide in the control of the pulmonary circulation: physiological, pathophysiological, and therapeutic implications]. J Bras Pneumol 34:412-419, 2008

43. Dipp M, Nye PC, Evans AM: Hypoxic release of calcium from the sarcoplasmic reticulum of pulmonary artery smooth muscle. Am J Physiol Lung Cell Mol Physiol 281:L318-325, 2001

44. Drummond RM, Tuft RA: Release of Ca2+ from the sarcoplasmic reticulum increases mitochondrial [Ca2+] in rat pulmonary artery smooth muscle cells. J Physiol 516:139-147, 1999

45. Du W, Frazier M, McMahon TJ, et al: Redox activation of intracellular calcium release channels (ryanodine receptors) in the sustained phase of hypoxia-induced pulmonary vasoconstriction. Chest 128:556S-558S, 2005

46. Dumas JP, Dumas M, Sgro C, et al: Effects of two K+ channel openers, aprikalim and pinacidil, on hypoxic pulmonary vasoconstriction. Eur J Pharmacol 263:17-23, 1994

47. Dumitrascu R, Weissmann N, Ghofrani HA, et al: Activation of soluble guanylate cyclase reverses experimental pulmonary hypertension and vascular remodeling. Circulation 113:286-295, 2006

48. Durmowicz AG, Stenmark KR: Mechanisms of structural remodeling in chronic pulmonary hypertension. Pediatr Rev 20:e91-e102, 1999

49. Echtay KS, Roussel D, St-Pierre J, et al: Superoxide activates mitochondrial uncoupling proteins. Nature 415:96-99, 2002

50. Emerling BM, Weinberg F, Snyder C, et al: Hypoxic activation of AMPK is dependent on mitochondrial ROS but independent of an increase in AMP/ATP ratio. Free Radic Biol Med 46:1386-1391, 2009

51. Evans AM: AMP-activated protein kinase and the regulation of Ca2+ signalling in O2-sensing cells. J Physiol 574:113-123, 2006

52. Evans AM, Mustard KJ, Wyatt CN, et al: Does AMP-activated protein kinase couple inhibition of mitochondrial oxidative phosphorylation by hypoxia to calcium signaling in O2-sensing cells? J Biol Chem 280:41504-41511, 2005

53. Fagan KA, Oka M, Bauer NR, et al: Attenuation of acute hypoxic pulmonary vasoconstriction and hypoxic pulmonary hypertension in mice by inhibition of Rho-kinase. Am J Physiol Lung Cell Mol Physiol 287:L656-664, 2004

54. Fink L, Kohlhoff S, Stein MM, et al: cDNA array hybridization after laser-assisted microdissection from nonneoplastic tissue. Am J Pathol 160:81-90, 2002

55. Firth AL, Mandel J, Yuan JX: Idiopathic pulmonary arterial hypertension. Dis Model Mech 3:268-273, 2010

56. Fishman AP: Hypoxia on the pulmonary circulation. How and where it acts. Circ Res 38:221-231, 1976

57. Fishman AP: Respiratory gases in the regulation of the pulmonary circulation. Physiol Rev 41:214-280, 1961

58. Fleury C, Neverova M, Collins S, et al: Uncoupling protein-2: a novel gene linked to obesity and hyperinsulinemia. Nat Genet 15:269-272, 1997

59. Frostell C, Fratacci MD, Wain JC, et al: Inhaled nitric oxide. A selective pulmonary vasodilator reversing hypoxic pulmonary vasoconstriction. Circulation 83:2038-2047, 1991

60. Fuchs B, Rupp M, Ghofrani HA, et al: Diacylglycerol regulates acute hypoxic pulmonary vasoconstriction via TRPC6. Respir Res 12:20, 2011

61. Ghofrani HA, Voswinckel R, Reichenberger F, et al: Hypoxia- and non-hypoxia-related pulmonary hypertension - established and new therapies. Cardiovasc Res 72:30-40, 2006

62. Graier WF, Frieden M, Malli R: Mitochondria and Ca(2+) signaling: old guests, new functions. Pflugers Arch 455:375-396, 2007

63. Graier WF, Trenker M, Malli R: Mitochondrial Ca2+, the secret behind the function of uncoupling proteins 2 and 3? Cell Calcium 44:36-50, 2008

64. Grimminger F, Spriestersbach R, Weissmann N, et al: Nitric oxide generation and hypoxic vasoconstriction in buffer-perfused rabbit lungs. J Appl Physiol 78:1509-1515, 1995

65. Grover RF: Pulmonary circulation in animals and man at high altitude. Ann N Y Acad Sci 127:632-639, 1965

66. Gunter TE, Sheu SS: Characteristics and possible functions of mitochondrial Ca(2+) transport mechanisms. Biochim Biophys Acta 1787:1291-1308, 2009

67. Gunther A, Walmrath D, Grimminger F, et al: Pathophysiology of acute lung injury. Semin Respir Crit Care Med 22:247-258, 2001

68. Hall J, Jones TH, Channer KS, et al: Mechanisms of agonist-induced constriction in isolated human mesenteric arteries. Vascul Pharmacol 44:427-433, 2006

69. Hambraeus-Jonzon K, Bindslev L, Mellgard AJ, et al: Hypoxic pulmonary vasoconstriction in human lungs. A stimulus-response study. Anesthesiology 86:308-315, 1997

70. Han D, Antunes F, Canali R, et al: Voltage-dependent anion channels control the release of the superoxide anion from mitochondria to cytosol. J Biol Chem 278:5557-5563, 2003

71. Harder DR, Madden JA, Dawson C: Hypoxic induction of Ca2+-dependent action potentials in small pulmonary arteries of the cat. J Appl Physiol 59:1389-1393, 1985

72. Hasunuma K, Rodman DM, McMurtry IF: Effects of K+ channel blockers on vascular tone in the perfused rat lung. Am Rev Respir Dis 144:884-887, 1991

73. Hauge A: Conditions governing the pressor response to ventilation hypoxia in isolated perfused rat lungs. Acta Physiol Scand 72:33-44, 1968

74. Hauge A: Role of histamine in hypoxic pulmonary hypertension in the rat. I. Blockade or potentiation of endogenous amines, kinins, and ATP. Circ Res 22:371-383, 1968

75. Heaton GM, Wagenvoord RJ, Kemp A, Jr., et al: Brown-adipose-tissue mitochondria: photoaffinity labelling of the regulatory site of energy dissipation. Eur J Biochem 82:515-521, 1978

76. Henquin J: Regulation of insulin secretion: a matter of phase control and amplitude modulation. Diabetologia 52:739-751, 2009

77. Herrington J, Park YB, Babcock DF, et al: Dominant role of mitochondria in clearance of large Ca2+ loads from rat adrenal chromaffin cells. Neuron 16:219-228, 1996

78. Hoeper MM, Krowka MJ, Strassburg CP: Portopulmonary hypertension and hepatopulmonary syndrome. Lancet 363:1461-1468, 2004

79. Hofmann T, Obukhov AG, Schaefer M, et al: Direct activation of human TRPC6 and TRPC3 channels by diacylglycerol. Nature 397:259-263, 1999

80. Hoshi T, Lahiri S: Cell biology. Oxygen sensing: it's a gas! Science 306:2050-2051, 2004

81. Howell K, Preston RJ, McLoughlin P: Chronic hypoxia causes angiogenesis in addition to remodelling in the adult rat pulmonary circulation. J Physiol 547:133-145, 2003

82. Huang JS, Ramamurthy SK, Lin X, et al: Cell signalling through thromboxane A2 receptors. Cell Signal 16:521-533, 2004

83. Hulme JT, Coppock EA, Felipe A, et al: Oxygen sensitivity of cloned voltage-gated K(+) channels expressed in the pulmonary vasculature. Circ Res 85:489-497, 1999

84. Ide H, Nakano H, Ogasa T, et al: Regulation of pulmonary circulation by alveolar oxygen tension via airway nitric oxide. J Appl Physiol 87:1629-1636, 1999

85. Jacobs ER, Zeldin DC: The lung HETEs (and EETs) up. Am J Physiol Heart Circ Physiol 280:H1-H10, 2001

86. Janssen LJ, Lu-Chao H, Netherton S: Excitation-contraction coupling in pulmonary vascular smooth muscle involves tyrosine kinase and Rho kinase. Am J Physiol Lung Cell Mol Physiol 280:L666-674, 2001

87. Jeffery TK, Morrell NW: Molecular and cellular basis of pulmonary vascular remodeling in pulmonary hypertension. Prog Cardiovasc Dis 45:173-202, 2002

88. Jensen KS, Micco AJ, Czartolomna J, et al: Rapid onset of hypoxic vasoconstriction in isolated lungs. J Appl Physiol 72:2018-2023, 1992

89. Jin N, Packer CS, Rhoades RA: Pulmonary arterial hypoxic contraction: signal transduction. Am J Physiol 263:L73-78, 1992

90. Kang TM, Park MK, Uhm DY: Characterization of hypoxia-induced [Ca2+]i rise in rabbit pulmonary arterial smooth muscle cells. Life Sci 70:2321-2333, 2002

91. Kang TM, Park MK, Uhm DY: Effects of hypoxia and mitochondrial inhibition on the capacitative calcium entry in rabbit pulmonary arterial smooth muscle cells. Life Sci 72:1467-1479, 2003

92. Kazemi H, Bruecke PE, Parsons EF: Role of the autonomic nervous system in the hypoxic response of the pulmonary vascular bed. Respir Physiol 15:245-254, 1972

93. Korshunov SS, Skulachev VP, Starkov AA: High protonic potential actuates a mechanism of production of reactive oxygen species in mitochondria. FEBS Lett 416:15-18, 1997

94. Kourembanas S, Marsden PA, McQuillan LP, et al: Hypoxia induces endothelin gene expression and secretion in cultured human endothelium. J Clin Invest 88:1054-1057, 1991

95. Kovitz KL, Aleskowitch TD, Sylvester JT, et al: Endothelium-derived contracting and relaxing factors contribute to hypoxic responses of pulmonary arteries. Am J Physiol 265:H1139-1148, 1993

96. Krauss S, Zhang CY, Lowell BB: The mitochondrial uncoupling-protein homologues. Nat Rev Mol Cell Biol 6:248-261, 2005

97. Krauss S, Zhang CY, Lowell BB: A significant portion of mitochondrial proton leak in intact thymocytes depends on expression of UCP2. Proc Natl Acad Sci U S A 99:118-122, 2002

98. Kuchan MJ, Frangos JA: Role of calcium and calmodulin in flow-induced nitric oxide production in endothelial cells. Am J Physiol 266:C628-636, 1994

99. Lambert AJ, Brand MD: Superoxide production by NADH:ubiquinone oxidoreductase (complex I) depends on the pH gradient across the mitochondrial inner membrane. Biochem J 382:511-517, 2004

100. Le Cras TD, McMurtry IF: Nitric oxide production in the hypoxic lung. Am J Physiol Lung Cell Mol Physiol 280:L575-582, 2001

101. Leach RM, Hill HM, Snetkov VA, et al: Divergent roles of glycolysis and the mitochondrial electron transport chain in hypoxic pulmonary vasoconstriction of the rat: identity of the hypoxic sensor. J Physiol 536:211-224, 2001

102. Leach RM, Hill HS, Snetkov VA, et al: Hypoxia, energy state and pulmonary vasomotor tone. Respir Physiol Neurobiol 132:55-67, 2002

103. Leach RM, Sheehan DW, Chacko VP, et al: Energy state, pH, and vasomotor tone during hypoxia in precontracted pulmonary and femoral arteries. Am J Physiol Lung Cell Mol Physiol 278:L294-304, 2000

104. Ledesma A, de Lacoba MG, Rial E: The mitochondrial uncoupling proteins. Genome Biol 3:3015.3011-3015.3019, 2002

105. Lee FS, Percy MJ: The HIF pathway and erythrocytosis. Annu Rev Pathol 6:165-192, 2011

106. Liu Q, Sham JS, Shimoda LA, et al: Hypoxic constriction of porcine distal pulmonary arteries: endothelium and endothelin dependence. Am J Physiol Lung Cell Mol Physiol 280:L856-865, 2001

107. Lloyd TC, Jr.: Effect of Alveolar Hypoxia on Pulmonary Vascular Resistance. J Appl Physiol 19:1086-1094, 1964

108. Lloyd TC, Jr.: Pulmonary vasoconstriction during histotoxic hypoxia. J Appl Physiol 20:488-490, 1965

109. Löffler G: Stoffwechsel von Glucose und Glykogen, in Biochemie und Pathobiochemie. Berlin: Petrides PE, 2003

110. Madden JA, Dawson CA, Harder DR: Hypoxia-induced activation in small isolated pulmonary arteries from the cat. J Appl Physiol 59:113-118, 1985

111. Madden JA, Vadula MS, Kurup VP: Effects of hypoxia and other vasoactive agents on pulmonary and cerebral artery smooth muscle cells. Am J Physiol 263:L384-393, 1992

112. Marshall BE, Marshall C: Continuity of response to hypoxic pulmonary vasoconstriction. J Appl Physiol 49:189-196, 1980

113. Marshall C, Marshall BE: Hypoxic pulmonary vasoconstriction is not endothelium dependent. Proc Soc Exp Biol Med 201:267-270, 1992

114. Martin C, Goggel R, Ressmeyer AR, et al: Pressor responses to platelet-activating factor and thromboxane are mediated by Rho-kinase. Am J Physiol Lung Cell Mol Physiol 287:L250-257, 2004

115. Mathews L: Paradigm Shift in Hemodynamic Monitoring. The Internet Journal of Anesthesiology 11, 2007

116. McMurtry IF: BAY K 8644 potentiates and A23187 inhibits hypoxic vasoconstriction in rat lungs. Am J Physiol 249:H741-746, 1985

117. McMurtry IF, Davidson AB, Reeves JT, et al: Inhibition of hypoxic pulmonary vasoconstriction by calcium antagonists in isolated rat lungs. Circ Res 38:99-104, 1976

118. Michelakis ED, Hampl V, Nsair A, et al: Diversity in mitochondrial function explains differences in vascular oxygen sensing. Circ Res 90:1307-1315, 2002

119. Michelakis ED, Thébaud B, Weir EK, et al: Hypoxic pulmonary vasoconstriction: redox regulation of O2-sensitive K+ channels by a mitochondrial O2-sensor in resistance artery smooth muscle cells. Journal of Molecular and Cellular Cardiology 37:1119-1136, 2004

120. Morio Y, McMurtry IF: Ca(2+) release from ryanodine-sensitive store contributes to mechanism of hypoxic vasoconstriction in rat lungs. J Appl Physiol 92:527-534, 2002

121. Motley HL, Cournand A, et al.: The influence of short periods of induced acute anoxia upon pulmonary artery pressures in man. Am J Physiol 150:315-320, 1947

122. Moudgil R, Michelakis ED, Archer SL: Hypoxic pulmonary vasoconstriction. J Appl Physiol 98:390-403, 2005

123. Murphy MP: How mitochondria produce reactive oxygen species. Biochem J 417:1-13, 2009

124. Murphy MP, Echtay KS, Blaikie FH, et al: Superoxide activates uncoupling proteins by generating carbon-centered radicals and initiating lipid peroxidation: studies using a mitochondria-targeted spin trap derived from alpha-phenyl-N-tert-butylnitrone. J Biol Chem 278:48534-48545, 2003

125. Naeije R, Brimioulle S: Physiology in medicine: importance of hypoxic pulmonary vasoconstriction in maintaining arterial oxygenation during acute respiratory failure. Crit Care 5:67-71, 2001

126. Naeije R, Hallemans R, Melot C, et al: Eicosanoids and hypoxic pulmonary vasoconstriction in normal man. Bull Eur Physiopathol Respir 23:613-617, 1987

127. Nagendran J, Stewart K, Hoskinson M, et al: An anesthesiologist's guide to hypoxic pulmonary vasoconstriction: implications for managing single-lung anesthesia and atelectasis. Curr Opin Anaesthesiol 19:34-43, 2006

128. Negre-Salvayre A, Hirtz C, Carrera G, et al: A role for uncoupling protein-2 as a regulator of mitochondrial hydrogen peroxide generation. Faseb J 11:809-815, 1997

129. Nossaman BD, Nossaman VE, Murthy SN, et al: Role of the RhoA/Rho-kinase pathway in the regulation of pulmonary vasoconstrictor function. Can J Physiol Pharmacol 88:1-8, 2010

130. Okabe E, Tsujimoto Y, Kobayashi Y: Calmodulin and cyclic ADP-ribose interaction in Ca2+ signaling related to cardiac sarcoplasmic reticulum: superoxide anion radical-triggered Ca2+ release. Antioxid Redox Signal 2:47-54, 2000

131. Olschewski A, Hong Z, Peterson DA, et al: Opposite effects of redox status on membrane potential, cytosolic calcium, and tone in pulmonary arteries and ductus arteriosus. Am J Physiol Lung Cell Mol Physiol 286:L15-22, 2004

132. Paddenberg R, Faulhammer P, Goldenberg A, et al: Impact of modulators of mitochondrial ATP-sensitive potassium channel (mitoK(ATP)) on hypoxic pulmonary vasoconstriction. Adv Exp Med Biol 648:361-368, 2009

133. Pak O, Aldashev A, Welsh D, et al: The effects of hypoxia on the cells of the pulmonary vasculature. Eur Respir J 30:364-372, 2007

134. Pak O, Sommer N, Hoeres T, et al: Mitochondrial Hyperpolarization in Pulmonary Vascular Remodeling - UCP2 Deficiency as Disease Model. Am J Respir Cell Mol Biol, 2013 [Epub ahead of print]

135. Panos RJ, Eschenbacher W: Exertional Desaturation in Patients with Chronic Obstructive Pulmonary Disease. COPD 6:478-487, 2009

136. Parker N, Vidal-Puig AJ, Azzu V, et al: Dysregulation of glucose homeostasis in nicotinamide nucleotide transhydrogenase knockout mice is independent of uncoupling protein 2. Biochim Biophys Acta 1787:1451-1457, 2009

137. Peake MD, Harabin AL, Brennan NJ, et al: Steady-state vascular responses to graded hypoxia in isolated lungs of five species. J Appl Physiol 51:1214-1219, 1981

138. Pecqueur C, Alves-Guerra MC, Gelly C, et al: Uncoupling protein 2, in vivo distribution, induction upon oxidative stress, and evidence for translational regulation. J Biol Chem 276:8705-8712, 2001

139. Pecqueur C, Bui T, Gelly C, et al: Uncoupling protein-2 controls proliferation by promoting fatty acid oxidation and limiting glycolysis-derived pyruvate utilization. Faseb J 22:9-18, 2008

140. Peiper U: Lehrbuch der Physiologie. Stuttgart: Rainer Klinke und Stefan Silbernagel, 1996

141. Pi J, Bai Y, Zhang Q, et al: Reactive oxygen species as a signal in glucose-stimulated insulin secretion. Diabetes 56:1783-1791, 2007

142. Plumier L: La circulation pulmonaire chez le chien. Arch Int Physiol 1:176-213, 1904

143. Post JM, Gelband CH, Hume JR: [Ca2+]i inhibition of K+ channels in canine pulmonary artery. Novel mechanism for hypoxia-induced membrane depolarization. Circ Res 77:131-139, 1995

144. Post JM, Hume JR, Archer SL, et al: Direct role for potassium channel inhibition in hypoxic pulmonary vasoconstriction. Am J Physiol 262:C882-890, 1992

145. Quinlan TR, Li D, Laubach VE, et al: eNOS-deficient mice show reduced pulmonary vascular proliferation and remodeling to chronic hypoxia. Am J Physiol Lung Cell Mol Physiol 279:L641-650, 2000

146. Robertson TP: Point: release of an endothelium-derived vasoconstrictor and RhoA/Rho kinase-mediated calcium sensitization of smooth muscle cell contraction are/are not the main effectors for full and sustained hypoxic pulmonary vasoconstriction. J Appl Physiol 102:2071-2072; discussion 2075-2076, 2007

147. Robertson TP, Aaronson PI, Ward JP: Ca2+ sensitization during sustained hypoxic pulmonary vasoconstriction is endothelium dependent. Am J Physiol Lung Cell Mol Physiol 284:L1121-1126, 2003

148. Robertson TP, Aaronson PI, Ward JP: Hypoxic vasoconstriction and intracellular Ca2+ in pulmonary arteries: evidence for PKC-independent Ca2+ sensitization. Am J Physiol 268:H301-307, 1995

149. Robertson TP, Dipp M, Ward JP, et al: Inhibition of sustained hypoxic vasoconstriction by Y-27632 in isolated intrapulmonary arteries and perfused lung of the rat. Br J Pharmacol 131:5-9, 2000

150. Robertson TP, Hague D, Aaronson PI, et al: Voltage-independent calcium entry in hypoxic pulmonary vasoconstriction of intrapulmonary arteries of the rat. J Physiol 525 Pt 3:669-680, 2000

151. Robertson TP, Mustard KJ, Lewis TH, et al: AMP-activated protein kinase and hypoxic pulmonary vasoconstriction. Eur J Pharmacol 595:39-43, 2008

152. Roth M, Rupp M, Hofmann S, et al: Heme oxygenase-2 and large-conductance Ca2+-activated K+ channels: lung vascular effects of hypoxia. Am J Respir Crit Care Med 180:353-364, 2009

153. Rudolph AM, Yuan S: Response of the pulmonary vasculature to hypoxia and H+ ion concentration changes. J Clin Invest 45:399-411, 1966

154. Sakurada S, Okamoto H, Takuwa N, et al: Rho activation in excitatory agonist-stimulated vascular smooth muscle. Am J Physiol Cell Physiol 281:C571-578, 2001

155. Salvaterra CG, Goldman WF: Acute hypoxia increases cytosolic calcium in cultured pulmonary arterial myocytes. Am J Physiol 264:L323-328, 1993

156. Sander M, Welling KL, Ravn JB, et al: Endogenous NO does not regulate baseline pulmonary pressure, but reduces acute pulmonary hypertension in dogs. Acta Physiol Scand 178:269-277, 2003

157. Schermuly RT, Dony E, Ghofrani HA, et al: Reversal of experimental pulmonary hypertension by PDGF inhibition. J Clin Invest 115:2811-2821, 2005

158. Semenza GL: HIF-1: mediator of physiological and pathophysiological responses to hypoxia. J Appl Physiol 88:1474-1480, 2000

159. Sham JS: Hypoxic pulmonary vasoconstriction: ups and downs of reactive oxygen species. Circ Res 91:649-651, 2002

160. Sheehan DW, Giese EC, Gugino SF, et al: Characterization and mechanisms of H2O2-induced contractions of pulmonary arteries. Am J Physiol 264:H1542-1547, 1993

161. Shigemori K, Ishizaki T, Matsukawa S, et al: Adenine nucleotides via activation of ATP-sensitive K+ channels modulate hypoxic response in rat pulmonary artery. Am J Physiol 270:L803-809, 1996

162. Shirai M, Sada K, Ninomiya I: Effects of regional alveolar hypoxia and hypercapnia on small pulmonary vessels in cats. J Appl Physiol 61:440-448, 1986

163. Silove ED, Inoue T, Grover RF: Comparison of hypoxia, pH, and sympathomimetic drugs on bovine pulmonary vasculature. J Appl Physiol 24:355-365, 1968

164. Simonneau G, Galie N, Rubin LJ, et al: Clinical classification of pulmonary hypertension. J Am Coll Cardiol 43:5S-12S, 2004

165. Simonneau G, Robbins IM, Beghetti M, et al: Updated clinical classification of pulmonary hypertension. J Am Coll Cardiol 54:S43-54, 2009

166. Skovgaard N, Abe AS, Andrade DV, et al: Hypoxic pulmonary vasoconstriction in reptiles: a comparative study of four species with different lung structures and pulmonary blood pressures. Am J Physiol Regul Integr Comp Physiol 289:R1280-1288, 2005

167. Somlyo AV: Cyclic GMP Regulation of Myosin Phosphatase: A New Piece for the Puzzle? Circ Res 101:645-647, 2007

168. Sommer N, Dietrich A, Schermuly RT, et al: Regulation of hypoxic pulmonary vasoconstriction: basic mechanisms. Eur Respir J 32:1639-1651, 2008

169. Sommer N, Pak O, Schorner S, et al: Mitochondrial cytochrome redox states and respiration in acute pulmonary oxygen sensing. Eur Respir J, 2010

170. Staub NC: Site of hypoxic pulmonary vasoconstriction. Chest 88:240S-245S, 1985

171. Stenmark KR, Meyrick B, Galie N, et al: Animal models of pulmonary arterial hypertension: the hope for etiological discovery and pharmacological cure. Am J Physiol Lung Cell Mol Physiol 297:L1013-1032, 2009

172. Steudel W, Scherrer-Crosbie M, Bloch KD, et al: Sustained pulmonary hypertension and right ventricular hypertrophy after chronic hypoxia in mice with congenital deficiency of nitric oxide synthase 3. J Clin Invest 101:2468-2477, 1998

173. Straub SG, Sharp GWG: Hypothesis: one rate-limiting step controls the magnitude of both phases of glucose-stimulated insulin secretion. Am J Physiol Cell Physiol 287:C565-C571, 2004

174. Sylvester JT: Hypoxic pulmonary vasoconstriction: a radical view. Circ Res 88:1228-1230, 2001

175. Takeda S, Nakanishi K, Inoue T, et al: Delayed elevation of plasma endothelin-1 during unilateral alveolar hypoxia without systemic hypoxemia in humans. Acta Anaesthesiol Scand 41:274-280, 1997

176. Tang C, To WK, Meng F, et al: A role for receptor operated Ca(2+) entry in human pulmonary artery smooth muscle cells in response to hypoxia. Physiol Res, 2010

177. Terada H: Uncouplers of oxidative phosphorylation. Environ Health Perspect 87:213-218, 1990

178. Thilenius OG, Candiolo BM, Beug JL: Effect of adrenergic blockade on hypoxia-induced pulmonary vasoconstriction in awake dogs. Am J Physiol 213:990-998, 1967

179. Trenker M, Fertschai I, Malli R, et al: UCP2/3 [mdash] likely to be fundamental for mitochondrial Ca2+ uniport. Nat Cell Biol 10:1237-1240, 2008

180. Trenker M, Malli R, Fertschai I, et al: Uncoupling proteins 2 and 3 are fundamental for mitochondrial Ca2+ uniport. Nat Cell Biol 9:445-452, 2007

181. Turner JD, Gaspers LD, Wang G, et al: Uncoupling protein-2 modulates myocardial excitation-contraction coupling. Circ Res 106:730-738

182. Turrens JF: Mitochondrial formation of reactive oxygen species. J Physiol 552:335-344, 2003

183. v. Euler US LG: Observations on the Pulmonary Arterial Blood Pressure in the Cat. Acta Physiol Scand 12:301-320, 1946

184. Vejlstrup NG, Dorrington KL: Intense slow hypoxic pulmonary vasoconstriction in gas-filled and liquid-filled lungs: an in vivo study in the rabbit. Acta Physiol Scand 148:305-313, 1993

185. Wang J, Shimoda LA, Weigand L, et al: Acute hypoxia increases intracellular [Ca2+] in pulmonary arterial smooth muscle by enhancing capacitative Ca2+ entry. Am J Physiol Lung Cell Mol Physiol 288:L1059-1069, 2005

186. Wang QS, Zheng YM, Dong L, et al: Role of mitochondrial reactive oxygen species in hypoxia-dependent increase in intracellular calcium in pulmonary artery myocytes. Free Radic Biol Med 42:642-653, 2007

187. Wang Z, Lanner MC, Jin N, et al: Hypoxia inhibits myosin phosphatase in pulmonary arterial smooth muscle cells: role of Rho-kinase. Am J Respir Cell Mol Biol 29:465-471, 2003

188. Ward JP, Aaronson PI: Mechanisms of hypoxic pulmonary vasoconstriction: can anyone be right? Respir Physiol 115:261-271, 1999

189. Ward JP, Robertson TP: The role of the endothelium in hypoxic pulmonary vasoconstriction. Exp Physiol 80:793-801, 1995

190. Ward JP, Robertson TP, Aaronson PI: Capacitative calcium entry: a central role in hypoxic pulmonary vasoconstriction? Am J Physiol Lung Cell Mol Physiol 289:L2-4, 2005

191. Ward JP, Snetkov VA, Aaronson PI: Calcium, mitochondria and oxygen sensing in the pulmonary circulation. Cell Calcium 36:209-220, 2004

192. Waypa GB, Chandel NS, Schumacker PT: Model for hypoxic pulmonary vasoconstriction involving mitochondrial oxygen sensing. Circ Res 88:1259-1266, 2001

193. Waypa GB, Guzy R, Mungai PT, et al: Increases in mitochondrial reactive oxygen species trigger hypoxia-induced calcium responses in pulmonary artery smooth muscle cells. Circ Res 99:970-978, 2006

194. Waypa GB, Marks JD, Guzy R, et al: Hypoxia triggers subcellular compartmental redox signaling in vascular smooth muscle cells. Circ Res 106:526-535, 2010

195. Waypa GB, Marks JD, Mack MM, et al: Mitochondrial reactive oxygen species trigger calcium increases during hypoxia in pulmonary arterial myocytes. Circ Res 91:719-726, 2002

196. Waypa GB, Schumacker PT: Hypoxic pulmonary vasoconstriction: redox events in oxygen sensing. J Appl Physiol 98:404-414, 2005

197. Wei Z, Al-Mehdi AB, Fisher AB: Signaling pathway for nitric oxide generation with simulated ischemia in flow-adapted endothelial cells. Am J Physiol Heart Circ Physiol 281:H2226-2232, 2001

198. Weigand L, Foxson J, Wang J, et al: Inhibition of hypoxic pulmonary vasoconstriction by antagonists of store-operated Ca2+ and nonselective cation channels. Am J Physiol Lung Cell Mol Physiol 289:L5-L13, 2005

199. Weir EK: Does normoxic pulmonary vasodilatation rather than hypoxic vasoconstriction account for the pulmonary pressor response to hypoxia? The Lancet 311:476-477, 1978

200. Weir EK, Archer SL: The mechanism of acute hypoxic pulmonary vasoconstriction: the tale of two channels. Faseb J 9:183-189, 1995

201. Weir EK, Olschewski A: Role of ion channels in acute and chronic responses of the pulmonary vasculature to hypoxia. Cardiovasc Res 71:630-641, 2006

202. Weissmann N, Akkayagil E, Quanz K, et al: Basic features of hypoxic pulmonary vasoconstriction in mice. Respir Physiol Neurobiol 139:191-202, 2004

203. Weissmann N, Dietrich A, Fuchs B, et al: Classical transient receptor potential channel 6 (TRPC6) is essential for hypoxic pulmonary vasoconstriction and alveolar gas exchange. Proc Natl Acad Sci U S A 103:19093-19098, 2006

204. Weissmann N, Ebert N, Ahrens M, et al: Effects of mitochondrial inhibitors and uncouplers on hypoxic vasoconstriction in rabbit lungs. Am J Respir Cell Mol Biol 29:721-732, 2003

205. Weissmann N, Grimminger F, Voswinckel R, et al: Nitro blue tetrazolium inhibits but does not mimic hypoxic vasoconstriction in isolated rabbit lungs. Am J Physiol 274:L721-727, 1998

206. Weissmann N, Grimminger F, Walmrath D, et al: Hypoxic vasoconstriction in buffer-perfused rabbit lungs. Respir Physiol 100:159-169, 1995

207. Weissmann N, Manz D, Buchspies D, et al: Congenital erythropoietin overexpression causes "anti-pulmonary hypertensive" structural and functional changes in mice, both in normoxia and hypoxia. Thromb Haemost 94:630-638, 2005

208. Weissmann N, Nollen M, Gerigk B, et al: Downregulation of hypoxic vasoconstriction by chronic hypoxia in rabbits: effects of nitric oxide. Am J Physiol Heart Circ Physiol 284:H931-938, 2003

209. Weissmann N, Sommer N, Schermuly RT, et al: Oxygen sensors in hypoxic pulmonary vasoconstriction. Cardiovasc Res 71:620-629, 2006

210. Weissmann N, Winterhalder S, Nollen M, et al: NO and reactive oxygen species are involved in biphasic hypoxic vasoconstriction of isolated rabbit lungs. Am J Physiol Lung Cell Mol Physiol 280:L638-645, 2001

211. Weissmann N, Zeller S, Schafer RU, et al: Impact of mitochondria and NADPH oxidases on acute and sustained hypoxic pulmonary vasoconstriction. Am J Respir Cell Mol Biol 34:505-513, 2006

212. White CW, Jackson JH, McMurtry IF, et al: Hypoxia increases glutathione redox cycle and protects rat lungs against oxidants. J Appl Physiol 65:2607-2616, 1988

213. Wiener CM, Sylvester JT: Effects of glucose on hypoxic vasoconstriction in isolated ferret lungs. J Appl Physiol 70:439-446, 1991

214. Wilson HL, Dipp M, Thomas JM, et al: Adp-ribosyl cyclase and cyclic ADP-ribose hydrolase act as a redox sensor. a primary role for cyclic ADP-ribose in hypoxic pulmonary vasoconstriction. J Biol Chem 276:11180-11188, 2001

215. Wilson SM, Mason HS, Smith GD, et al: Comparative capacitative calcium entry mechanisms in canine pulmonary and renal arterial smooth muscle cells. J Physiol 543:917-931, 2002

216. Wolin MS, Ahmad M, Gupte SA: Oxidant and redox signaling in vascular oxygen sensing mechanisms: basic concepts, current controversies, and potential importance of cytosolic NADPH. Am J Physiol Lung Cell Mol Physiol 289:L159-173, 2005

217. Xu W, Kaneko FT, Zheng S, et al: Increased arginase II and decreased NO synthesis in endothelial cells of patients with pulmonary arterial hypertension. Faseb J 18:1746-1748, 2004

218. Xue C, Johns RA: Upregulation of Nitric Oxide Synthase Correlates Temporally With Onset of Pulmonary Vascular Remodeling in the Hypoxic Rat. Hypertension 28:743-753, 1996

219. Yet SF, Perrella MA, Layne MD, et al: Hypoxia induces severe right ventricular dilatation and infarction in heme oxygenase-1 null mice. J Clin Invest 103:R23-29, 1999

220. Yu AY, Shimoda LA, Iyer NV, et al: Impaired physiological responses to chronic hypoxia in mice partially deficient for hypoxia-inducible factor 1alpha. J Clin Invest 103:691-696, 1999

221. Yuan XJ: Voltage-gated K+ currents regulate resting membrane potential and [Ca2+]i in pulmonary arterial myocytes. Circ Res 77:370-378, 1995

222. Yuan XJ, Goldman WF, Tod ML, et al: Hypoxia reduces potassium currents in cultured rat pulmonary but not mesenteric arterial myocytes. Am J Physiol 264:L116-123, 1993

223. Yuan XJ, Sugiyama T, Goldman WF, et al: A mitochondrial uncoupler increases KCa currents but decreases KV currents in pulmonary artery myocytes. Am J Physiol 270:C321-331, 1996

224. Yuan XJ, Tod ML, Rubin LJ, et al: Contrasting effects of hypoxia on tension in rat pulmonary and mesenteric arteries. Am J Physiol 259:H281-289, 1990

225. Yuan XJ, Tod ML, Rubin LJ, et al: Hypoxic and metabolic regulation of voltage-gated K+ channels in rat pulmonary artery smooth muscle cells. Exp Physiol 80:803-813, 1995

226. Zhang CY, Baffy G, Perret P, et al: Uncoupling protein-2 negatively regulates insulin secretion and is a major link between obesity, beta cell dysfunction, and type 2 diabetes. Cell 105:745-755, 2001

227. Zhang F, Woodmansey PA, Morice AH: Acute hypoxic vasoconstriction in isolated rat small and large pulmonary arteries. Physiol Res 44:7-18, 1995

228. Zheng YM, Wang QS, Rathore R, et al: Type-3 ryanodine receptors mediate hypoxia-, but not neurotransmitter-induced calcium release and contraction in pulmonary artery smooth muscle cells. J Gen Physiol 125:427-440, 2005

Publikationsverzeichnis

Originalarbeiten:

O. Pak, N. Sommer, **T. Hoeres**, A. Bakr, S. Waisbrod, A. Sydykov, D. Haag, A. Esfandiary, B. Kojonazarov, F. Veit, B. Fuchs, F. C. Weisel, M. Hecker, R.T. Schermuly, F. Grimminger, H.A. Ghofrani, W. Seeger, N. Weissmann. Mitochondrial Hyperpolarization in Pulmonary Vascular Remodeling - UCP2 Deficiency as Disease Model. Am J Respir Cell Mol Biol. 2013 Apr 5. [Epub ahead of print]

Abstracts/Poster:

T. Höres, N. Sommer, H.A. Ghofrani, R.T. Schermuly, W. Seeger, F. Grimminger, N. Weissmann. Hypoxic pulmonary vasoconstriction in UCP-2 k/o mice during acute and sustained hypoxia. 49. Kongress der Deutschen Gesellschaft für Pneumologie und Beatmungsmedizin, 9. bis 12. April 2008 in Lübeck.

T. Höres, N. Sommer, H. A. Ghofrani, R.T. Schermuly, W. Seeger, F. Grimminger, N. Weissmann. Hypoxic pulmonary vasoconstriction is modulated in UCP-2 k/o mice during acute and sustained hypoxia. 15. European Bioenergetics Conference, 19 bis 24. Juli 2008 in Dublin.

Erklärung zur Dissertation

„Hiermit erkläre ich, dass ich die vorliegende Arbeit selbständig und ohne unzulässige Hilfe oder Benutzung anderer als der angegebenen Hilfsmittel angefertigt habe. Alle Textstellen, die wörtlich oder sinngemäß aus veröffentlichten oder nichtveröffentlichten Schriften entnommen sind, und alle Angaben, die auf mündlichen Auskünften beruhen, sind als solche kenntlich gemacht. Bei den von mir durchgeführten und in der Dissertation erwähnten Untersuchungen habe ich die Grundsätze guter wissenschaftlicher Praxis, wie sie in der „Satzung der Justus-Liebig-Universität Gießen zur Sicherung guter wissenschaftlicher Praxis“ niedergelegt sind, eingehalten sowie ethische, datenschutzrechtliche und tierschutzrechtliche Grundsätze befolgt. Ich versichere, dass Dritte von mir weder unmittelbar noch mittelbar geldwerte Leistungen für Arbeiten erhalten haben, die im Zusammenhang mit dem Inhalt der vorgelegten Dissertation stehen, oder habe diese nachstehend spezifiziert. Die vorgelegte Arbeit wurde weder im Inland noch im Ausland in gleicher oder ähnlicher Form einer anderen Prüfungsbehörde zum Zweck einer Promotion oder eines anderen Prüfungsverfahrens vorgelegt. Alles aus anderen Quellen und von anderen Personen übernommene Material, das in der Arbeit verwendet wurde oder auf das direkt Bezug genommen wird, wurde als solches kenntlich gemacht. Insbesondere wurden alle Personen genannt, die direkt und indirekt an der Entstehung der vorliegenden Arbeit beteiligt waren. Mit der Überprüfung meiner Arbeit durch eine Plagiatserkennungssoftware bzw. ein internetbasiertes Softwareprogramm erkläre ich mich einverstanden.“

_____ _____

Ort, Datum Unterschrift

Acknowledgement

I would like to thank my supervisor Dr. Natascha Sommer for providing the original idea and concept underlying this work. Thank you for your support, your willingness to discuss and solve problems during the experimental phase and the patience needed to help me write this thesis.

Many thanks go to my doctoral advisor Prof. Dr. Norbert Weißmann for his support and for providing me the opportunity to be part of the stimulating and supportive environment of his workgroup.

My deepest gratitude to all my former lab colleagues, the scientists and technicians, I had the honour to work with for their generous support and their dedication which enabled this work.

My special thanks go to Dr. Nirmal Parajuli, who sacrificed many hours for this project and if it wasn't for his commitment, the rather sophisticated closed chest RVSP measurement would not have been completed.

I'm also grateful to my fellow student Dr. Markus Rupp who helped me along with technical difficulties, was a great advisor and whose lab work and thesis set an example for my own efforts. I further like to acknowledge the help of Adel Bakr and Lisa Fröhlich with staining and performing morphometric analysis of the lung sections as well as the assistance of Anette Hanschke and Ewa Bieniek attempting IHC detection of UCP-2 even though it did not work out the way we hoped.

Der Lebenslauf wurde aus der elektronischen Version der Arbeit entfernt.

The curriculum vitae was removed from the electronic version of the paper.